

Search for Signatures of Large Extra Dimensions in High-Mass Diphoton Events from Proton-Proton Collisions at $\sqrt{s} = 13 \text{ TeV}$ with CMS

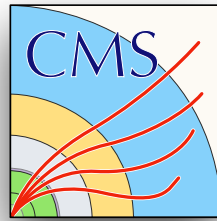
Dissertation Defense

Andrew Thomas Buccilli
Advisor: Prof. Conor Henderson

University of Alabama
07 November 2018



Dissertation committee members



Chair

- Prof. Conor Henderson (UA)

Members

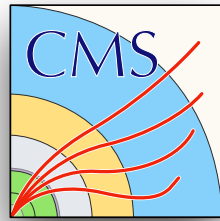
- Prof. Nobuchika Okada (UA)
- Prof. Toyoko Orimoto (NU)
- Prof. Andreas Piepke (UA)
- Prof. Paolo Rumerio (UA)
- Prof. Dawn R. Williams (UA)



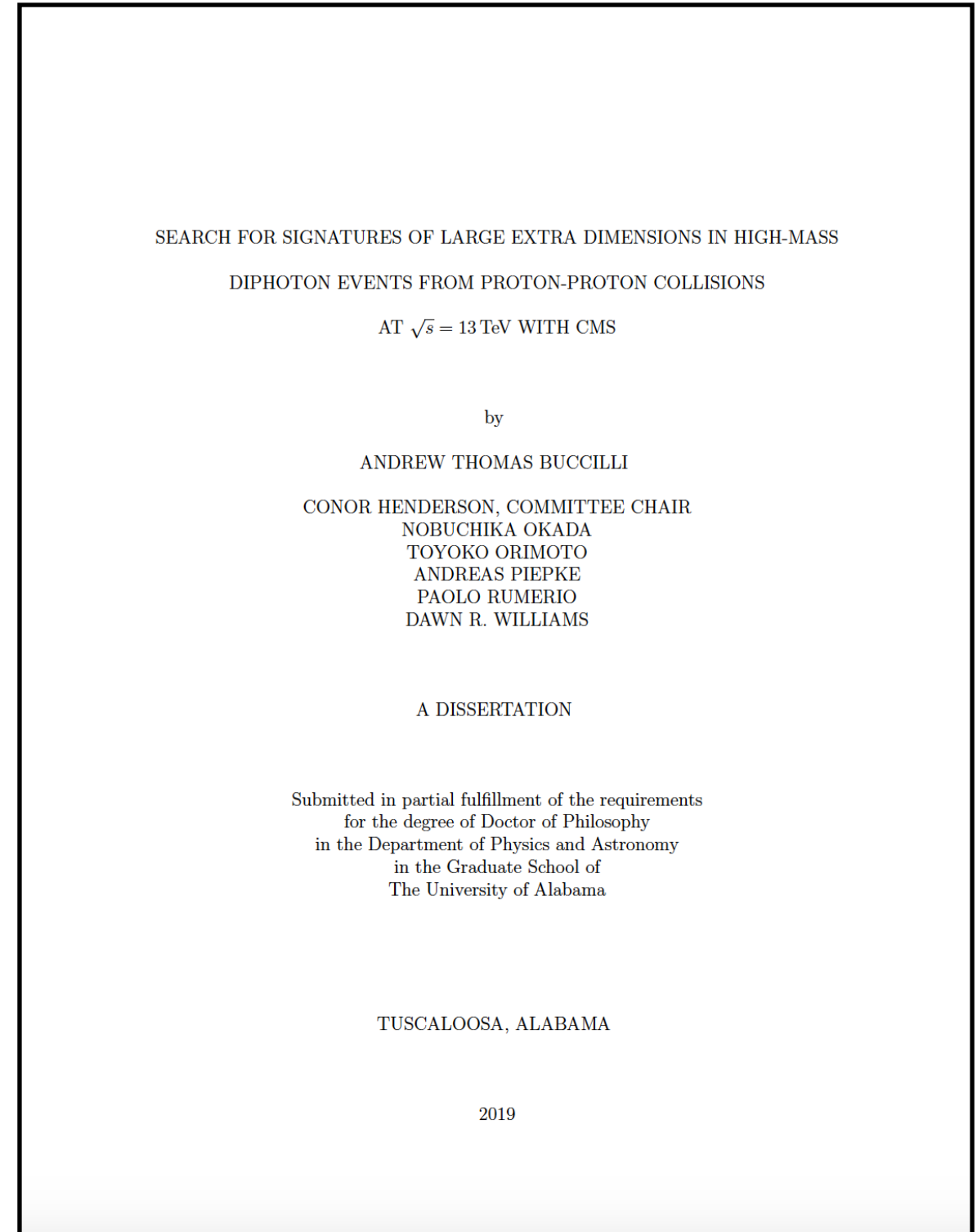
- Thank you for your 3 years of service since November 2015!



Introduction



- Dissertation research
 - 2015 - 2018
- CMS Collaboration
 - 2016 LHC data
 - **diphoton ($\gamma\gamma$) channel**
- Search for nonresonant excess of high-mass diphoton events over the Standard Model background prediction
 - large extra-dimensional signal

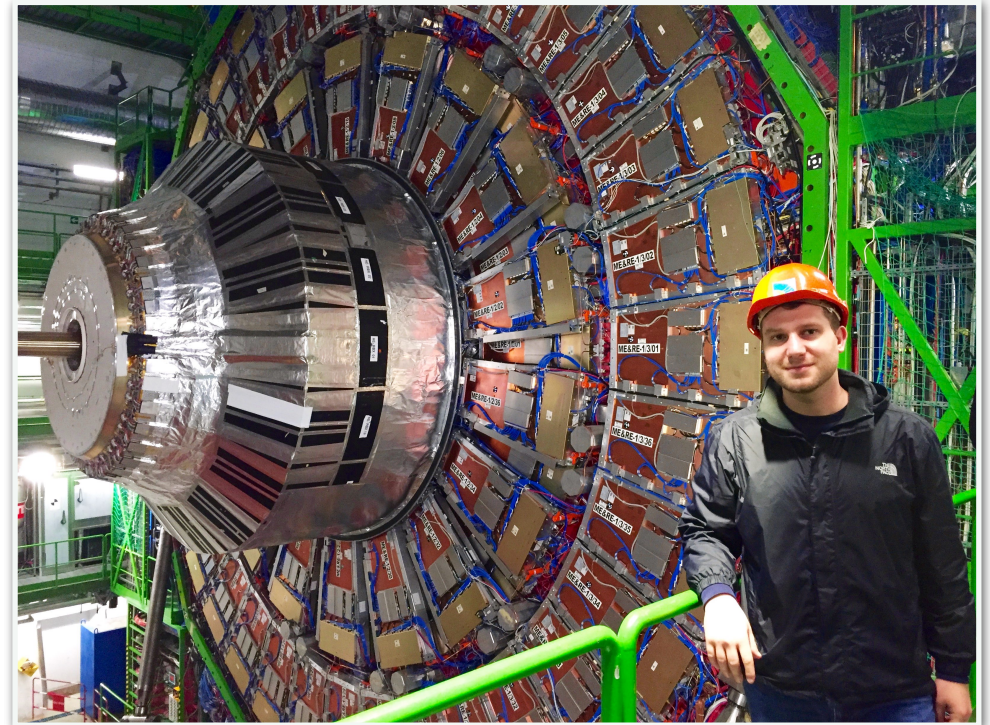




Outline

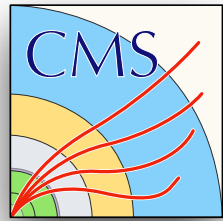


- Theoretical motivation
 - Standard Model
 - Beyond the Standard Model
- Experimental apparatus
 - Large Hadron Collider
 - CMS detector
- Photon reconstruction and diphoton selection
- High-mass diphoton search
 - Signal simulation
 - Background determination
- Sources of systematic uncertainty
- Results and limit setting





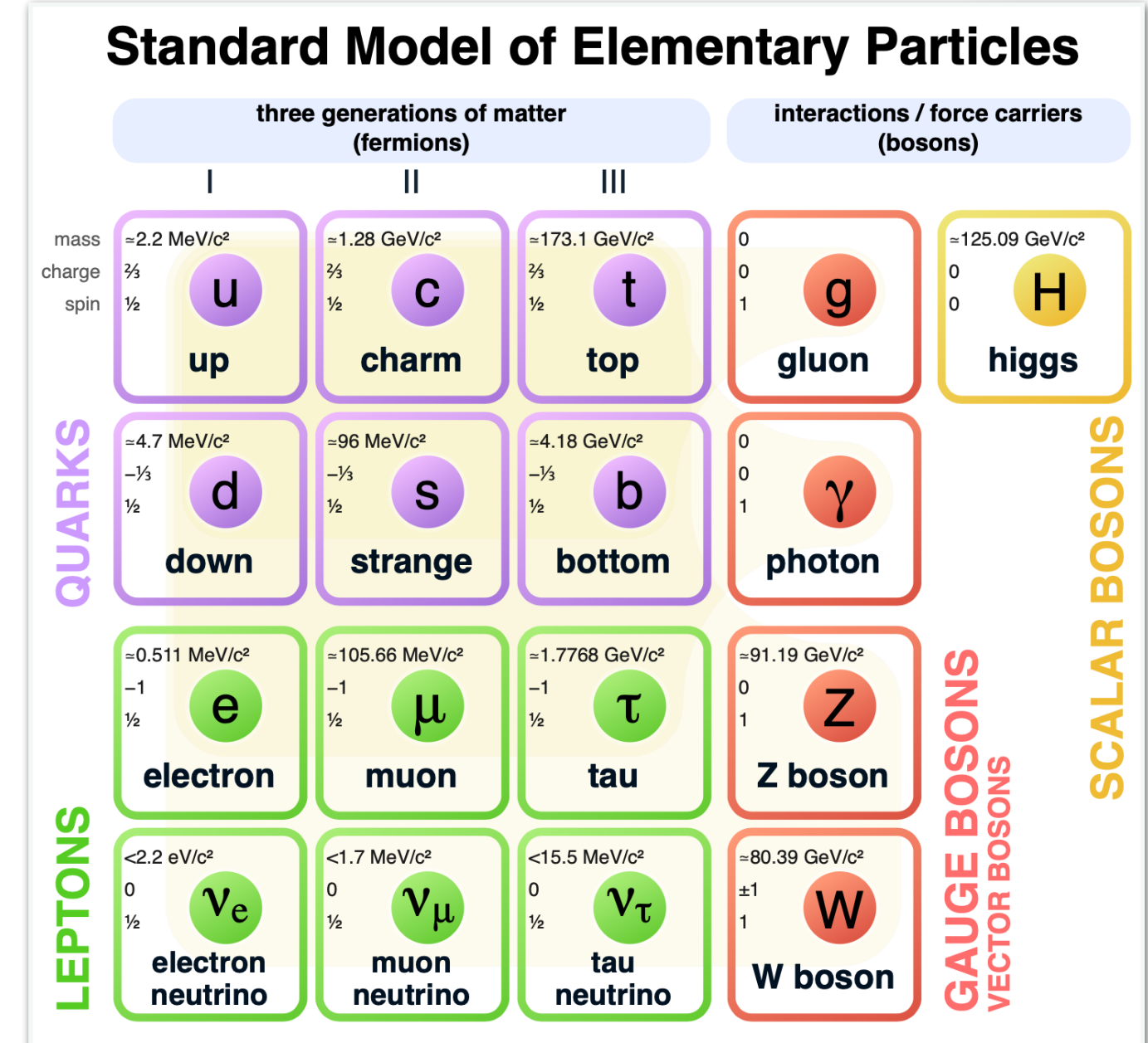
Standard Model



Gauge group

$$SU(3)_c \times SU(2)_L \times U(1)_Y$$

- Lagrangians invariant under local symmetry transformations
- Forces
 - strong $SU(3)_c$
 - electroweak $SU(2)_L \times U(1)_Y$
- Fermion representations
 - singlets not influenced by interaction

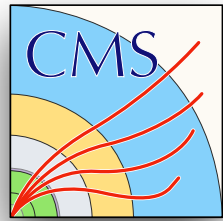


SM fermion $q_L = \begin{pmatrix} u_L \\ d_L \end{pmatrix}$ u_R d_R $\ell_L = \begin{pmatrix} \nu_L \\ e_L \end{pmatrix}$ e_R

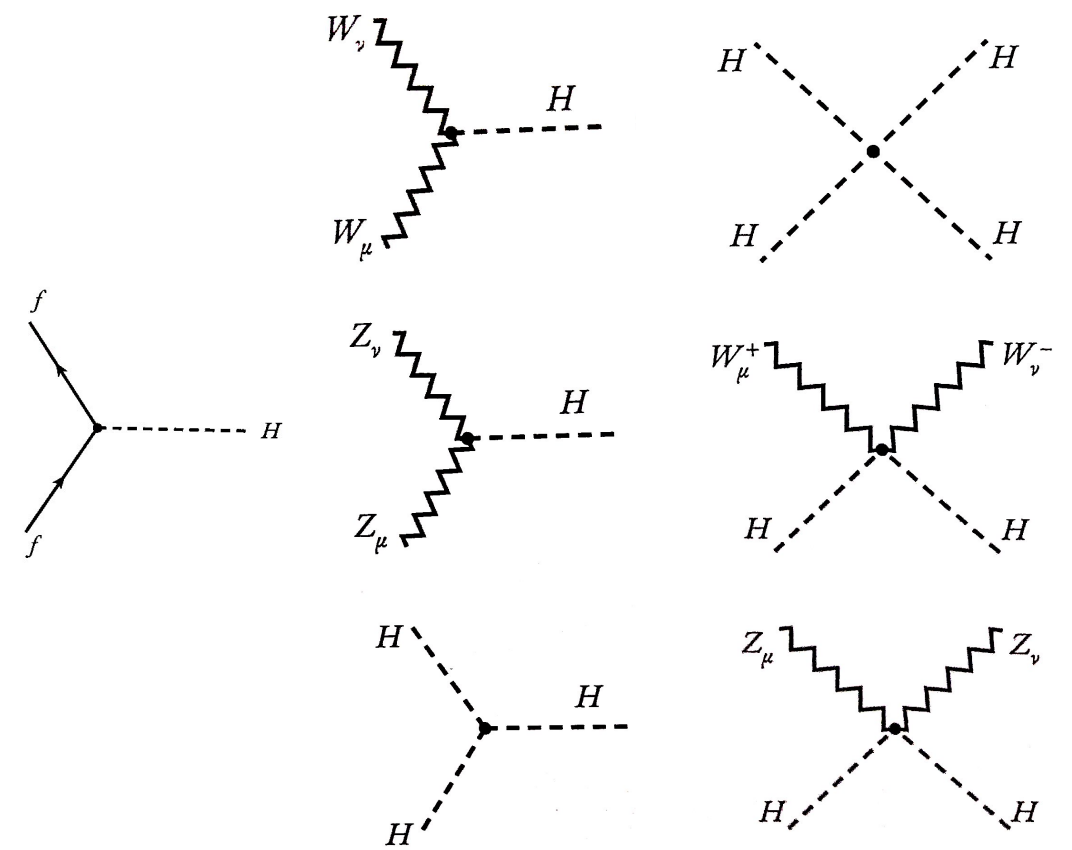
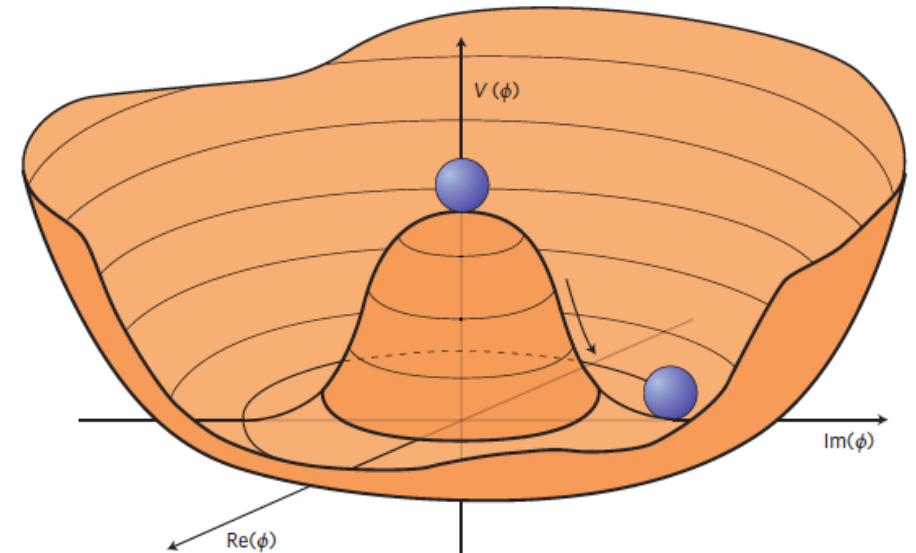
$(SU(3)_c, SU(2)_L, U(1)_Y)$
representation $(\mathbf{3}, \mathbf{2}, \frac{1}{6})$ $(\mathbf{3}, \mathbf{1}, \frac{2}{3})$ $(\mathbf{3}, \mathbf{1}, -\frac{1}{3})$ $(\mathbf{1}, \mathbf{2}, -\frac{1}{2})$ $(\mathbf{1}, \mathbf{1}, -1)$

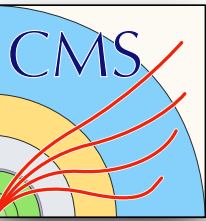


Electroweak symmetry breaking



- Higgs mechanism
 - spontaneous symmetry breaking of a local gauge symmetry
- Higgs field ϕ (**1,2,1/2**)
- $SU(2)_L \times U(1)_Y \rightarrow U(1)_{EM}$
- Massive, neutral scalar boson H
 - couples to mass
 - $m_H \approx 125$ GeV
- Responsible for generating masses
 - massive vector bosons
 - fermions (Yukawa interaction)
 - H boson



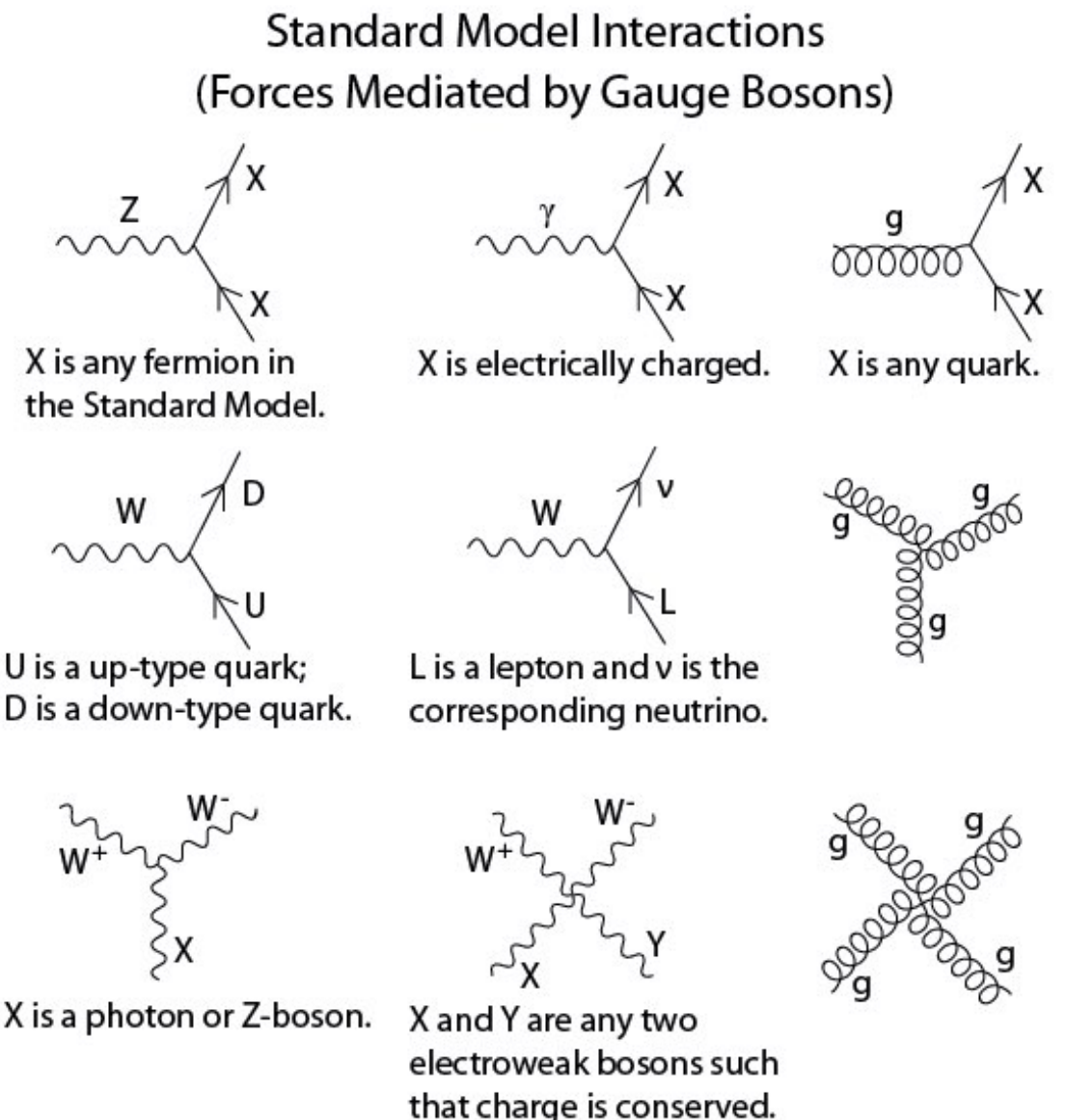


SM interactions

SM Lagrangian density

$$\begin{aligned} \mathcal{L} = & -\frac{1}{4}G_{\mu\nu}^\alpha G^{\alpha\mu\nu} - \frac{1}{4}W_{\mu\nu}^a W^{a\mu\nu} - \frac{1}{4}B_{\mu\nu} B^{\mu\nu} \\ & + \bar{q}_L i\cancel{D} q_L + \bar{u}_R i\cancel{D} u_R + \bar{d}_R i\cancel{D} d_R \\ & + \bar{\ell}_L i\cancel{D} \ell_L + \bar{e}_R i\cancel{D} e_R \\ & + (D_\mu \phi)^\dagger (D^\mu \phi) - V(\phi) \\ & - y_u \bar{q}_L \tilde{\phi} u_R - y_d \bar{q}_L \phi d_R - y_e \bar{\ell}_L \phi e_R \end{aligned}$$

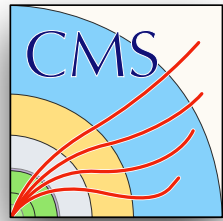
- Gauge invariance determines possible interactions and couplings
- gluons carry color and can self-interact



SM fermion	$q_L = \begin{pmatrix} u_L \\ d_L \end{pmatrix}$	u_R	d_R	$\ell_L = \begin{pmatrix} \nu_L \\ e_L \end{pmatrix}$	e_R
(SU(3) _c , SU(2) _L , U(1) _Y) representation	$(\mathbf{3}, \mathbf{2}, \frac{1}{6})$	$(\mathbf{3}, \mathbf{1}, \frac{2}{3})$	$(\mathbf{3}, \mathbf{1}, -\frac{1}{3})$	$(\mathbf{1}, \mathbf{2}, -\frac{1}{2})$	$(\mathbf{1}, \mathbf{1}, -1)$



Hierarchy problem



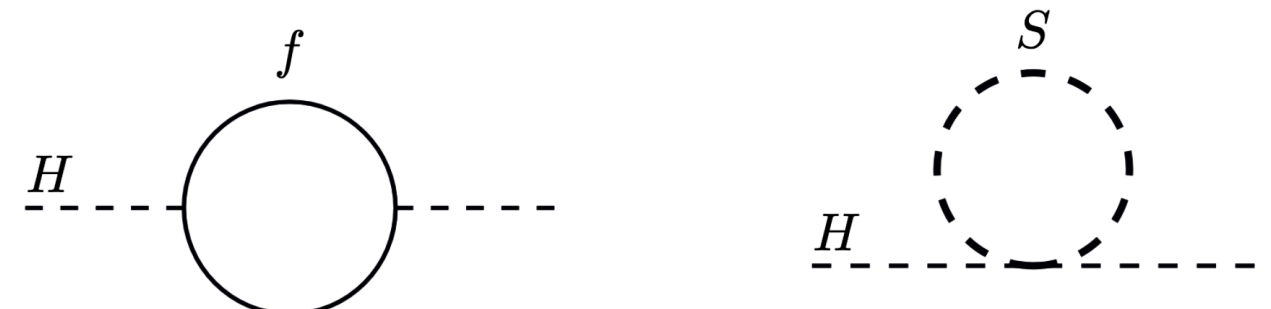
- Large difference between 2 fundamental scales
 - electroweak scale $M_{EW} \sim 10^2$ GeV
 - Planck scale $M_{Pl} = (\hbar c/G_N)^{1/2} \sim 10^{19}$ GeV
- Higgs boson (being a scalar) receives large quantum corrections proportional to the ultraviolet cutoff scale Λ^2

$$m_H^2 = m_0^2 + \Delta m_H^2$$

- Dominant one-loop corrections

$$\Delta m_H^2 = \frac{G_F \Lambda^2}{4\pi^2 \sqrt{2}} (6m_W^2 + 3m_Z^2 + m_H^2 - 12m_t^2)$$

- Only choice of cutoff is M_{Pl}
 - Fine-tuning $\mathcal{O}(10^{34})$ GeV required; seems unnatural

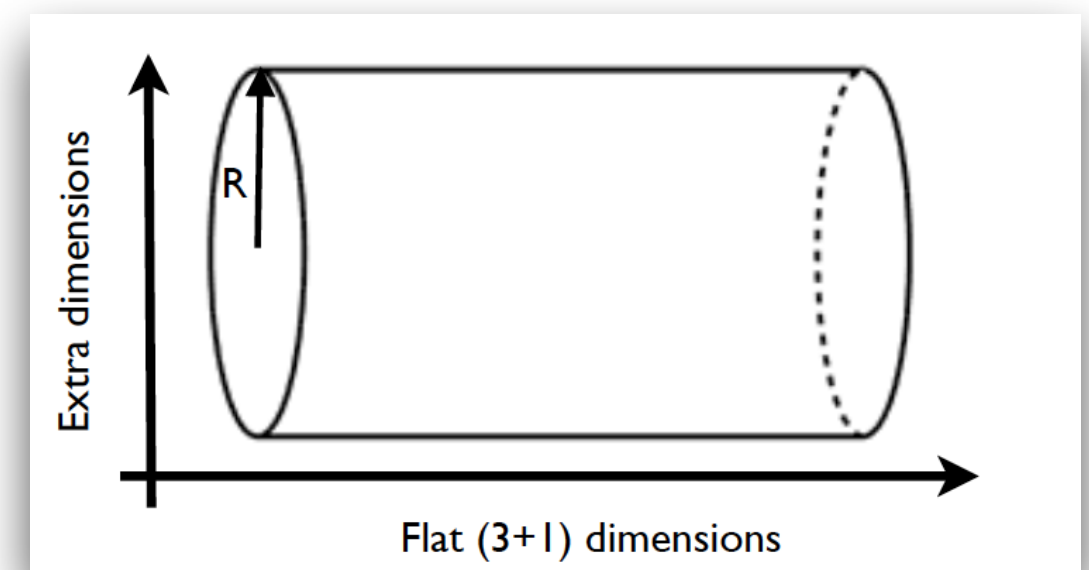




Extra dimensions



- The presence of extra spatial dimensions can modify the scale of gravity
 - fundamental Planck scale M_D in $(4+n_{ED})$ -dimensions is strong
 - observed Planck scale M_{Pl} in $(3+1)$ -dimensions appears weak
- Arkani-Hamed, Dimopoulos, and Dvali (ADD) model (*Phys. Lett. B* **429** (1998) 263)
- Proposes n_{ED} additional flat extra dimensions
- Gravity propagates through entire “bulk” space
- SM particles and gauge interactions are confined to $(3+1)$ -dimensional “brane” embedded in the bulk
- Extra dimensions are curled up and compactified in a sphere or torus of (average) radius R





Large extra dimensions



- Gravitational potential energy in $(4+n_{ED})$ -dimensions:

$$U(r) \sim \frac{m_1 m_2}{M_D^{n_{ED}+2}} \frac{1}{r^{n_{ED}+1}}, \text{ for } r \ll R$$

$$n_{ED} = 1, \quad R \sim 10^{11} \text{ m};$$

$$U(r) \sim \frac{m_1 m_2}{M_D^{n_{ED}+2} R^{n_{ED}}} \frac{1}{r}, \text{ for } r \gg R$$

$$n_{ED} = 2, \quad R \sim 0.1 \text{ mm};$$

- For $r \gg R$, we get the usual $1/r$ potential and

$$M_{Pl}^2 \sim M_D^{n_{ED}+2} R^{n_{ED}}$$

$$n_{ED} = 4, \quad R \sim 1 \text{ pm};$$

- If $M_D \sim M_{EW} \sim 1 \text{ TeV}$, we find

$$R \sim 10^{\frac{30}{n_{ED}} - 19} \text{ m}$$

$$n_{ED} = 5, \quad R \sim 100 \text{ fm};$$

- We get large extra dimensions

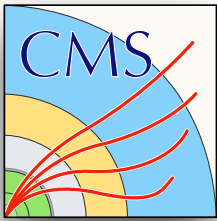
$$n_{ED} = 6, \quad R \sim 10 \text{ fm};$$

- $n_{ED} = 1$ ruled out as deviations from Newton's law of gravity would be observed

$$n_{ED} = 7, \quad R \sim 1 \text{ fm}$$



Phenomenology



- Graviton's momentum is quantized in $(4+n_{ED})$ -dimensions
 - appears as a tower of graviton excitations called Kaluza-Klein (KK) modes in $(3+1)$ -dimensions, contributing to its mass
- Ultraviolet cutoff scale Λ_G set to string mass scale M_s
 - Regularize cross section
 - Multiple cutoff conventions
- Cross section parameterized by η_G
 - interference between ADD signal and SM background can be large
- Energy spacing between adjacent modes $1/R$
 - 1 meV - 100 MeV ($n_{ED} = 2-7$)
 - effectively producing a nonresonant enhancement

$$\eta_G = \mathcal{F}/M_S^4$$
$$\mathcal{F} = \begin{cases} 1 & (\text{GRW}), \\ \log\left(\frac{M_S^2}{\hat{s}}\right), & \text{if } n_{ED} = 2 \\ \frac{2}{n_{ED}-2}, & \text{if } n_{ED} > 2 \\ \pm\frac{2}{\pi} & (\text{Hewett}), \end{cases} \quad (\text{HLZ}),$$

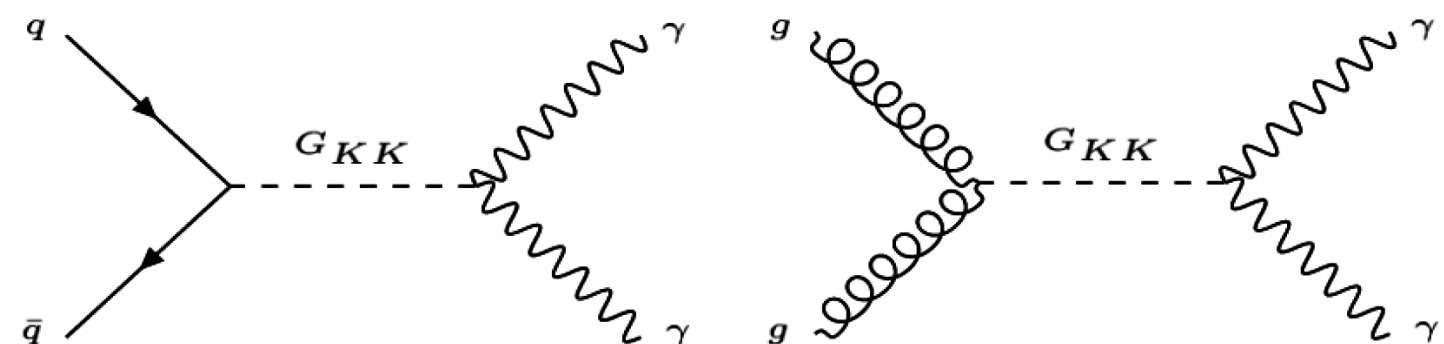
$$\sigma_{\text{total}} = \sigma_{\text{SM}} + \eta_G \sigma_{\text{int}} + \eta_G^2 \sigma_{\text{ADD}}$$



Diphoton channel

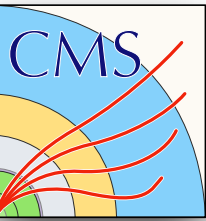


- $G_{KK} \rightarrow \gamma\gamma$
 - CMS detector provides excellent energy resolution for electromagnetic particles
 - Clean, isolated photon signature



- Dijet channel suffers from large background at the LHC
- Dilepton channel has a smaller branching ratio than diphoton
- Dilepton phase space is restricted since graviton G is spin-2
- Decay width for a KK Graviton is: $\Gamma_G \simeq \frac{293m_G^3}{960\pi\Lambda_G^2}$

G_{KK} decay mode	HH	gg	$\gamma\gamma$	W^+W^-	ZZ	$t\bar{t}$	$q\bar{q}$	l^+l^-
Branching ratio	2/293	96/293	12/293	24/293	12/293	16/293	90/293	12/293



Current limits

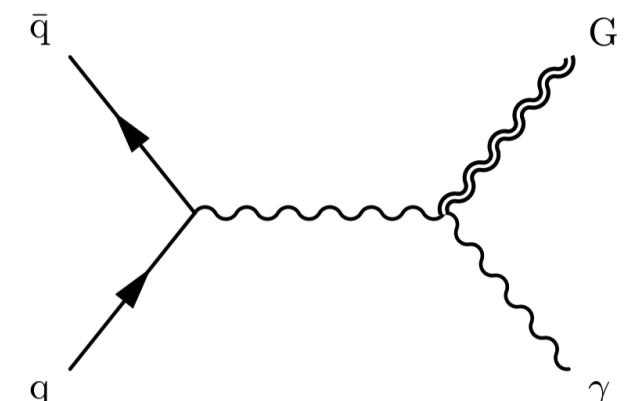
- Previous CMS nonresonant high-mass diphoton search used 2011 LHC data at $\sqrt{s} = 7 \text{ TeV}$

Search	\sqrt{s}	Data	Year	Limits on M_S
CMS-EXO-10-026	7 TeV	36 pb^{-1}	2010	1.31-2.23 TeV
CMS-EXO-11-038	7 TeV	2.2 fb^{-1}	2011	2.28-3.50 TeV

- CMS dijet angular search offers best limits on M_S to date ranging between 8.5-12 TeV depending on the model convention
 - using 35.9 fb^{-1} with $\sqrt{s} = 13 \text{ TeV}$
- ATLAS diphoton search sets limits on M_S from 5.7-8.1 TeV
 - using 37 fb^{-1} with $\sqrt{s} = 13 \text{ TeV}$
- Note: complementary searches for large extra dimensions
 - *direct graviton emission* $q\bar{q} \rightarrow \gamma G$
 - sets limits on M_D
 - *microscopic black hole production*
 - collision energy exceeds M_D

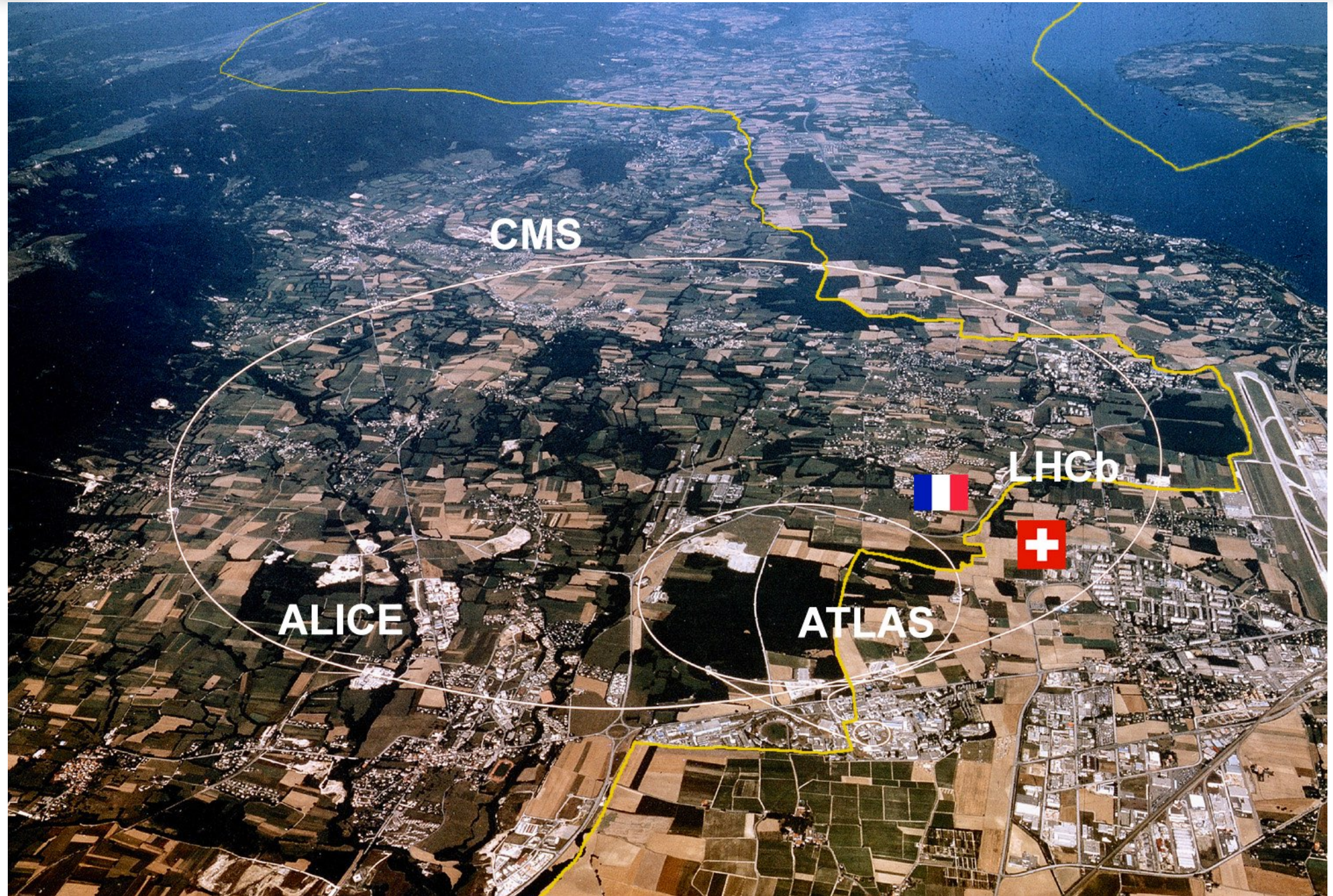
virtual graviton exchange

$$q\bar{q} \rightarrow \gamma G$$



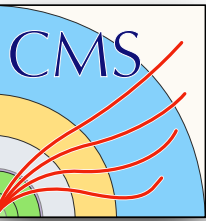


Large Hadron Collider

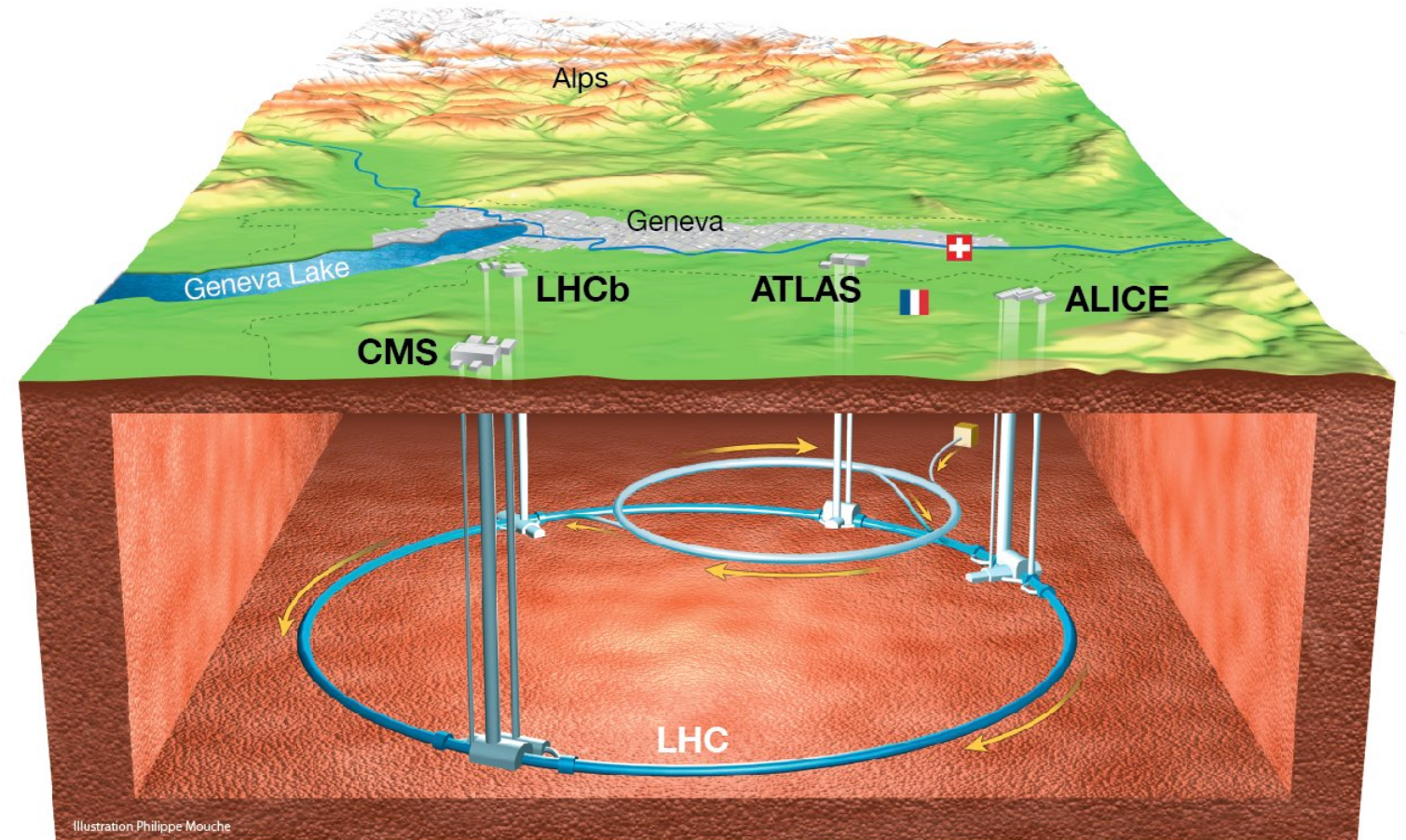




LHC overview

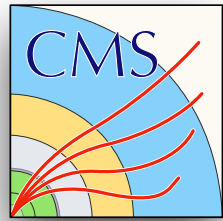


- Large Hadron Collider
 - 27 km circumference
 - ~ 100 m underground
- pp, pPb, PbPb, XeXe collisions
- 1232 superconducting magnets
 - 8.3 T
 - 15 m long
- proton bunches
 - 2808 bunches
 - 25 ns spacing
 - 10^{11} protons/bunch





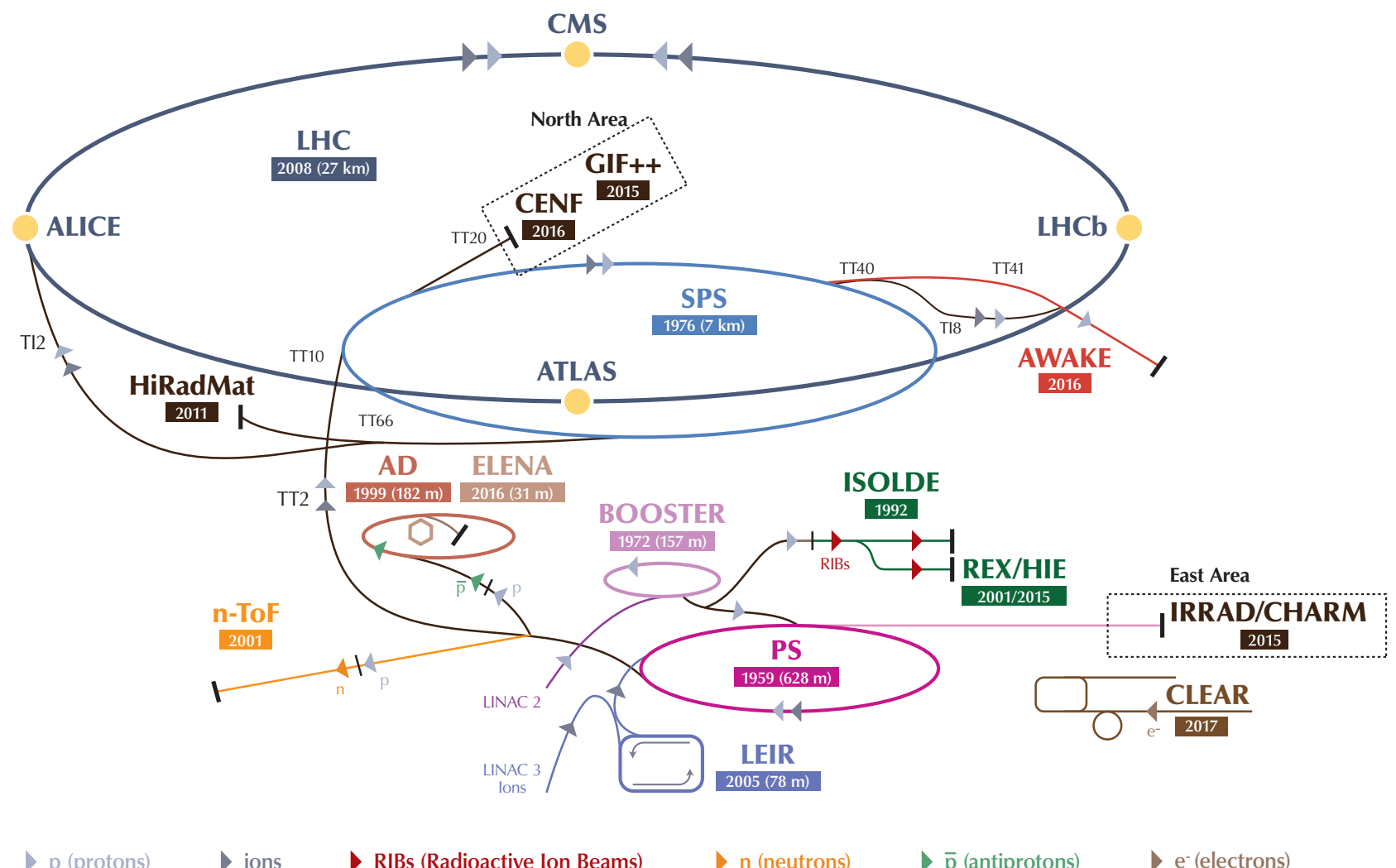
CERN accelerator complex



Proton acceleration chain:

1. Linac 2 (50 MeV)
2. PSB (1.4 GeV)
3. PS (25 GeV)
4. SPS (450 GeV)
5. LHC (14 TeV)

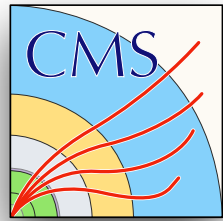
The CERN accelerator complex
Complexe des accélérateurs du CERN



LHC - Large Hadron Collider // SPS - Super Proton Synchrotron // PS - Proton Synchrotron // AD - Antiproton Decelerator // CLEAR - CERN Linear Electron Accelerator for Research // AWAKE - Advanced WAKEfield Experiment // ISOLDE - Isotope Separator OnLine // REX/HIE - Radioactive EXperiment/High Intensity and Energy ISOLDE // LEIR - Low Energy Ion Ring // LINAC - LINear ACcelerator // n-ToF - Neutrons Time Of Flight // HiRadMat - High-Radiation to Materials // CHARM - Cern High energy AcceleRator Mixed field facility // IRRAD - proton IRRADIation facility // GIF++ - Gamma Irradiation Facility // CENF - CErn Neutrino platForm



Luminosity



- Instantaneous luminosity

$$\mathcal{L} = \frac{N_b^2 f n_b}{4\pi \sigma_x^* \sigma_y^*} F$$

- Integrated luminosity

$$L = \int \mathcal{L} dt$$

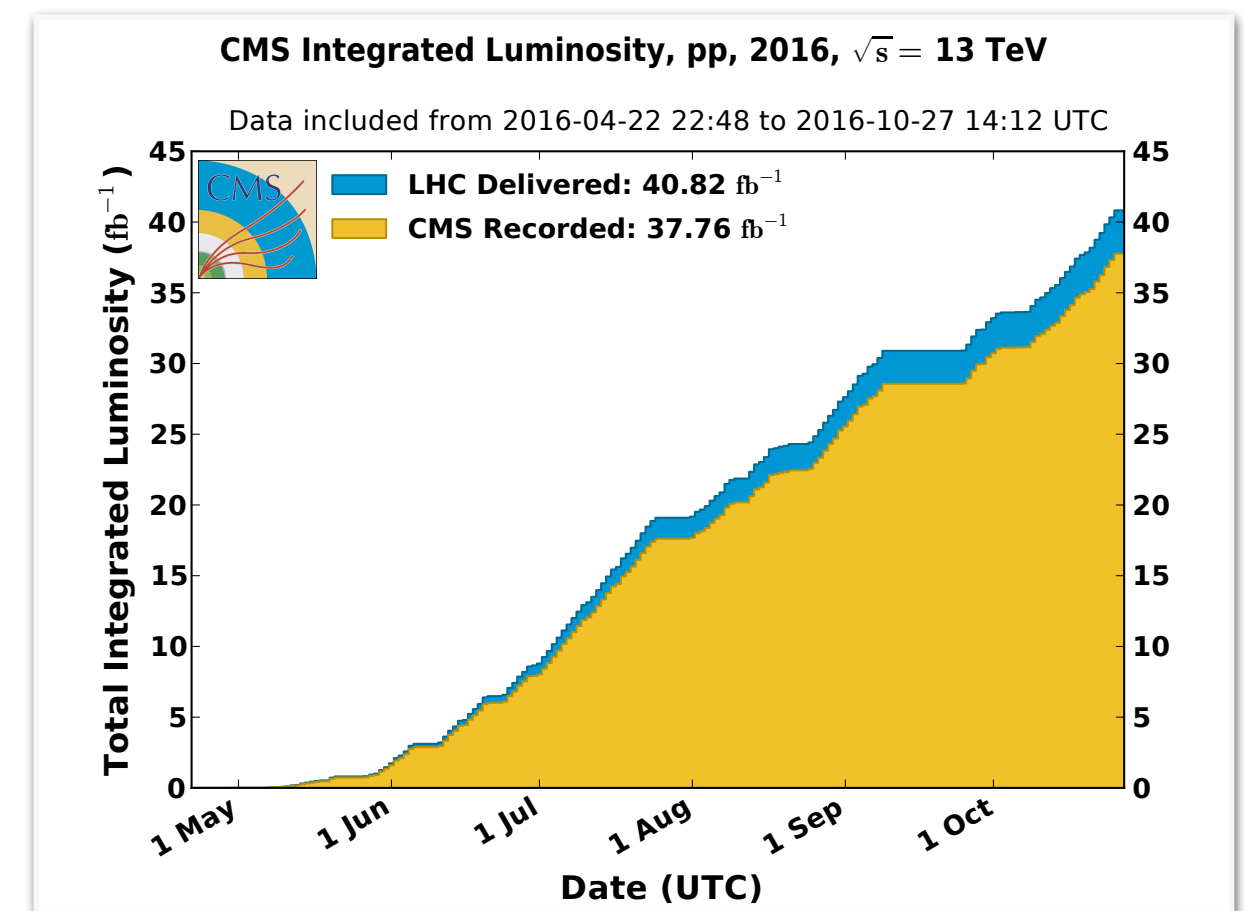
- Number of events N

$$L = N\sigma$$

- σ is pp interaction cross section
 - ~ 100 mb

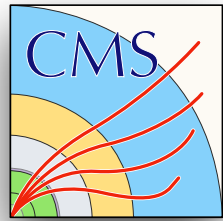
$$1 \text{ fb}^{-1} = 10^{39} \text{ cm}^{-2}$$

- N_b : number of protons/bunch
- n_b : number of bunches
- f : LHC revolution frequency
- F : geometric loss factor
- $\sigma_{x,y}^*$: transverse beam width at IP





LHC schedule

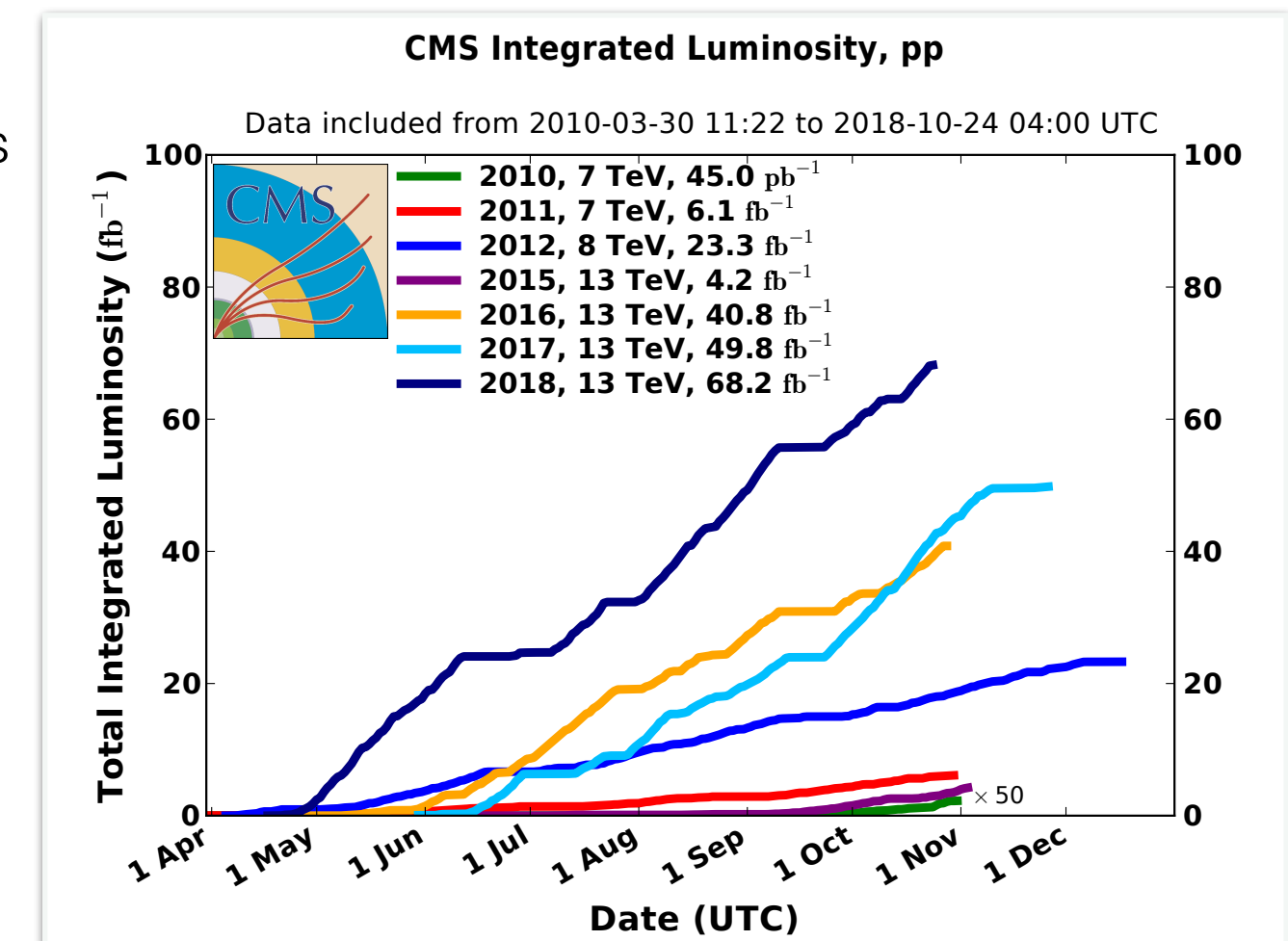


LHC physics production schedule for pp collisions with integrated luminosity recorded by CMS

- **Run 1:** 2010-2012
 - 2010: $\sqrt{s} = 7 \text{ TeV}$, 41.47 pb^{-1} , 50 ns
 - 2011: $\sqrt{s} = 7 \text{ TeV}$, 5.55 fb^{-1} , 50 ns
 - 2012: $\sqrt{s} = 8 \text{ TeV}$, 21.79 fb^{-1} , 50 ns
- **LS1:** 2013-2014
- **Run 2:** 2015-2018
 - 2015: $\sqrt{s} = 13 \text{ TeV}$, 3.81 fb^{-1} , 50 ns \rightarrow 25 ns
 - 2016: $\sqrt{s} = 13 \text{ TeV}$, 37.76 fb^{-1} , 25 ns
 - 2017: $\sqrt{s} = 13 \text{ TeV}$, 44.98 fb^{-1} , 25 ns
 - 2018: $\sqrt{s} = 13 \text{ TeV}$, 63.97 fb^{-1} , 25 ns
- **LS2:** 2019-2020
- **Run 3:** 2021-2023
 - $\sqrt{s} = 14 \text{ TeV}$
- **LS3:** 2024-?
 - High-Luminosity Large Hadron Collider

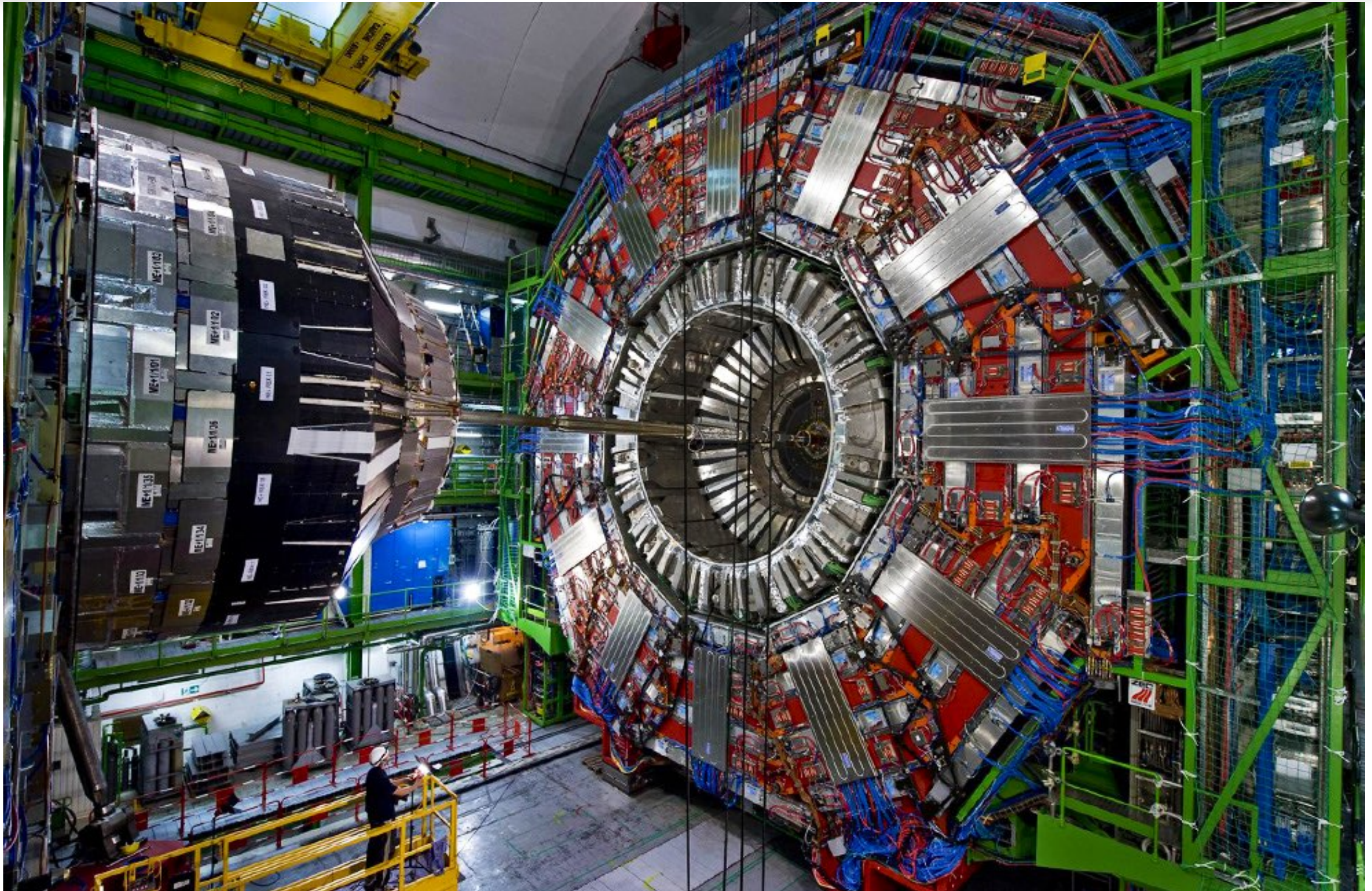
physics production run

long shutdown



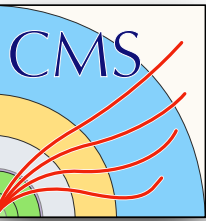


Compact Muon Solenoid





CMS detector



CMS DETECTOR

Total weight : 14,000 tonnes
Overall diameter : 15.0 m
Overall length : 28.7 m
Magnetic field : 3.8 T

STEEL RETURN YOKE
12,500 tonnes

SILICON TRACKERS
Pixel ($100 \times 150 \mu\text{m}$) $\sim 16\text{m}^2 \sim 66\text{M}$ channels
Microstrips ($80 \times 180 \mu\text{m}$) $\sim 200\text{m}^2 \sim 9.6\text{M}$ channels

SUPERCONDUCTING SOLENOID
Niobium titanium coil carrying $\sim 18,000\text{A}$

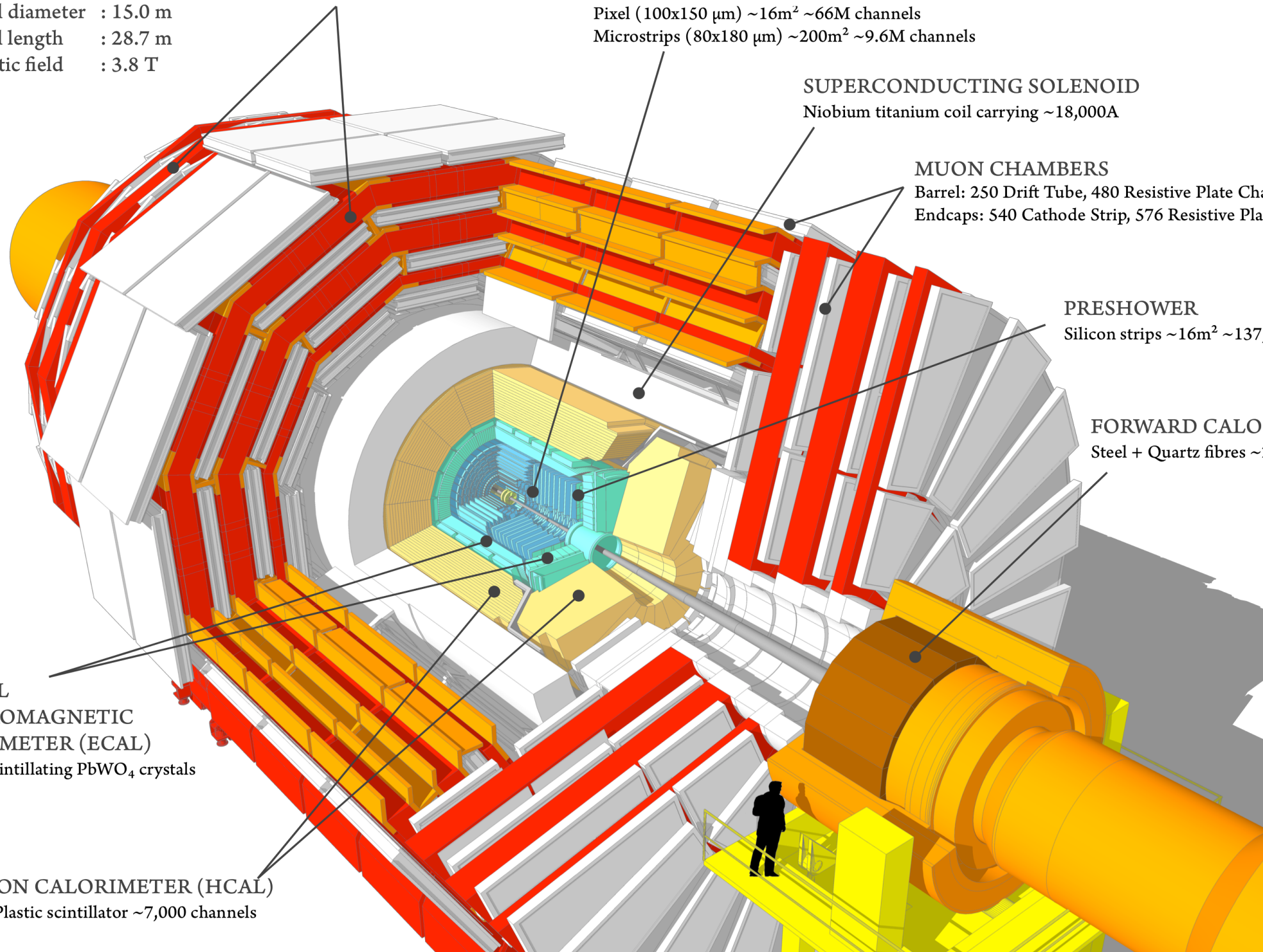
MUON CHAMBERS
Barrel: 250 Drift Tube, 480 Resistive Plate Chambers
Endcaps: 540 Cathode Strip, 576 Resistive Plate Chambers

PRESHOWER
Silicon strips $\sim 16\text{m}^2 \sim 137,000$ channels

FORWARD CALORIMETER
Steel + Quartz fibres $\sim 2,000$ Channels

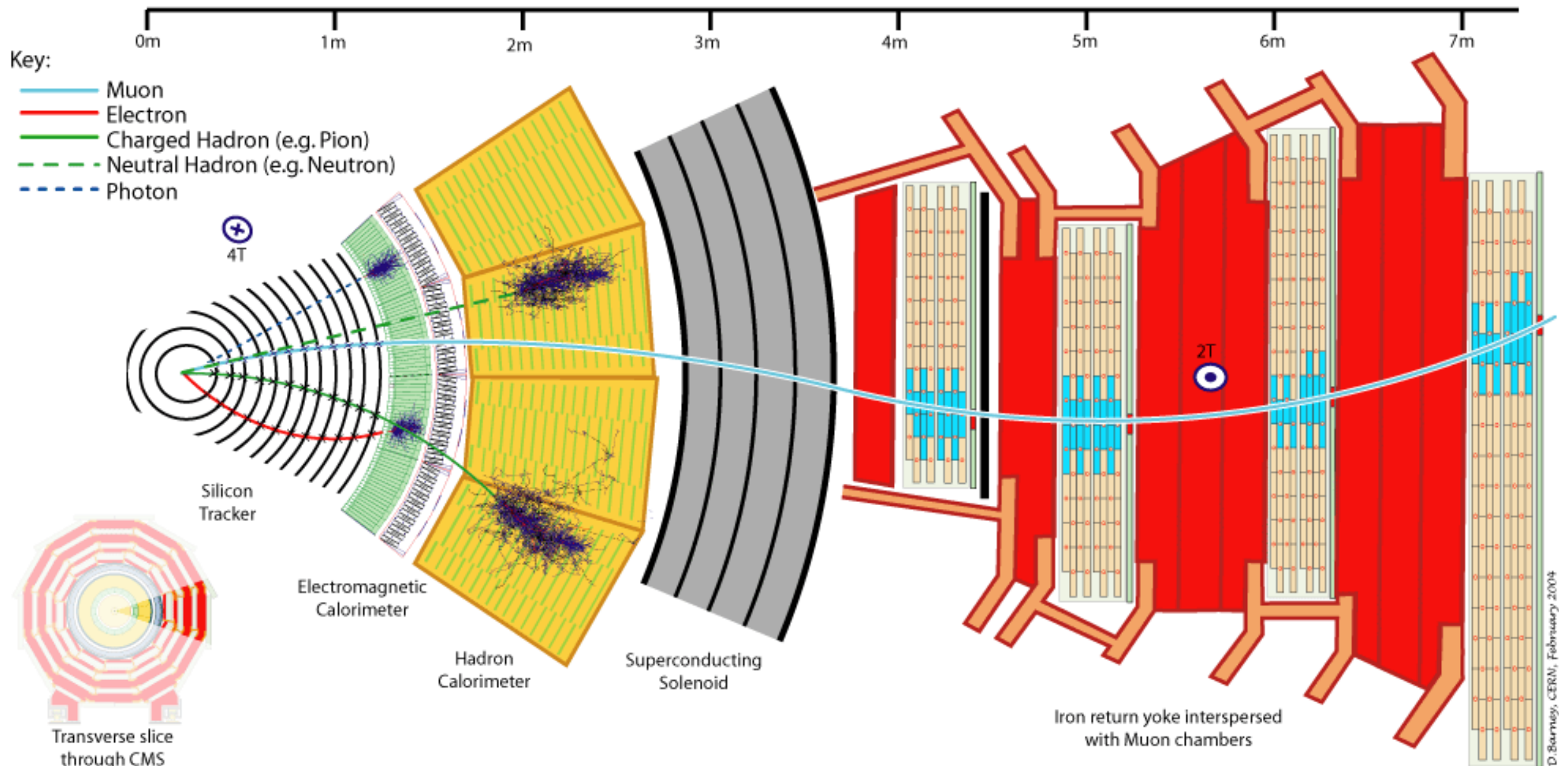
CRYSTAL
ELECTROMAGNETIC
CALORIMETER (ECAL)
 $\sim 76,000$ scintillating PbWO_4 crystals

HADRON CALORIMETER (HCAL)
Brass + Plastic scintillator $\sim 7,000$ channels





CMS particle identification

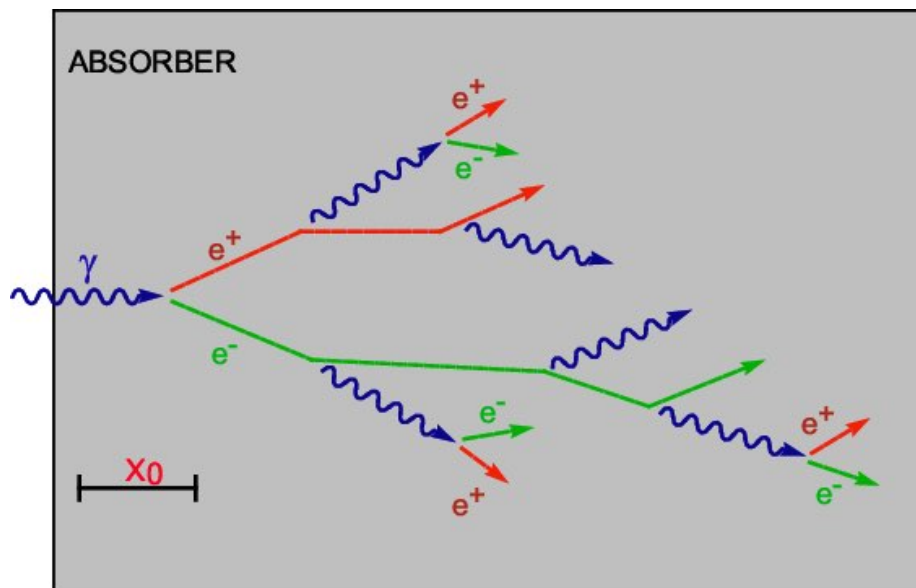
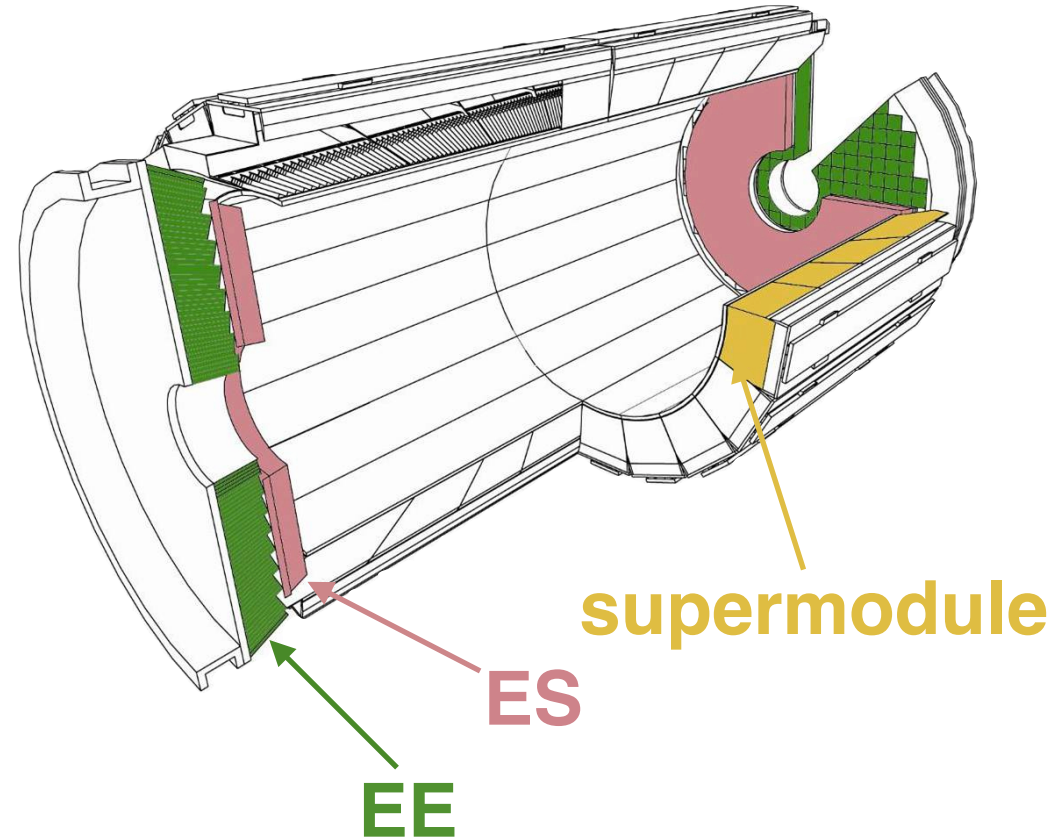




ECAL

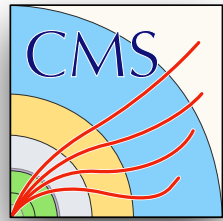


- Hermetic, homogeneous calorimeter comprising 75,000 PbWO₄ scintillating crystals
- ECAL barrel (**EB**) [$|\eta| < 1.48$]
 - 36 supermodules
 - $\Delta\eta \times \Delta\phi = 0.0174 \times 0.0174$
- ECAL endcap (**EE**) [$1.48 < |\eta| < 3.0$]
 - 2 endcap disks
 - crystals grouped into 5x5 arrays of supercrystals
 - $\Delta x \times \Delta y = 28.6 \times 28.6 \text{ mm}^2$
- ECAL preshower (ES) [$1.65 < |\eta| < 2.6$]
 - sampling calorimeter (lead and silicon strips)





ECAL energy resolution

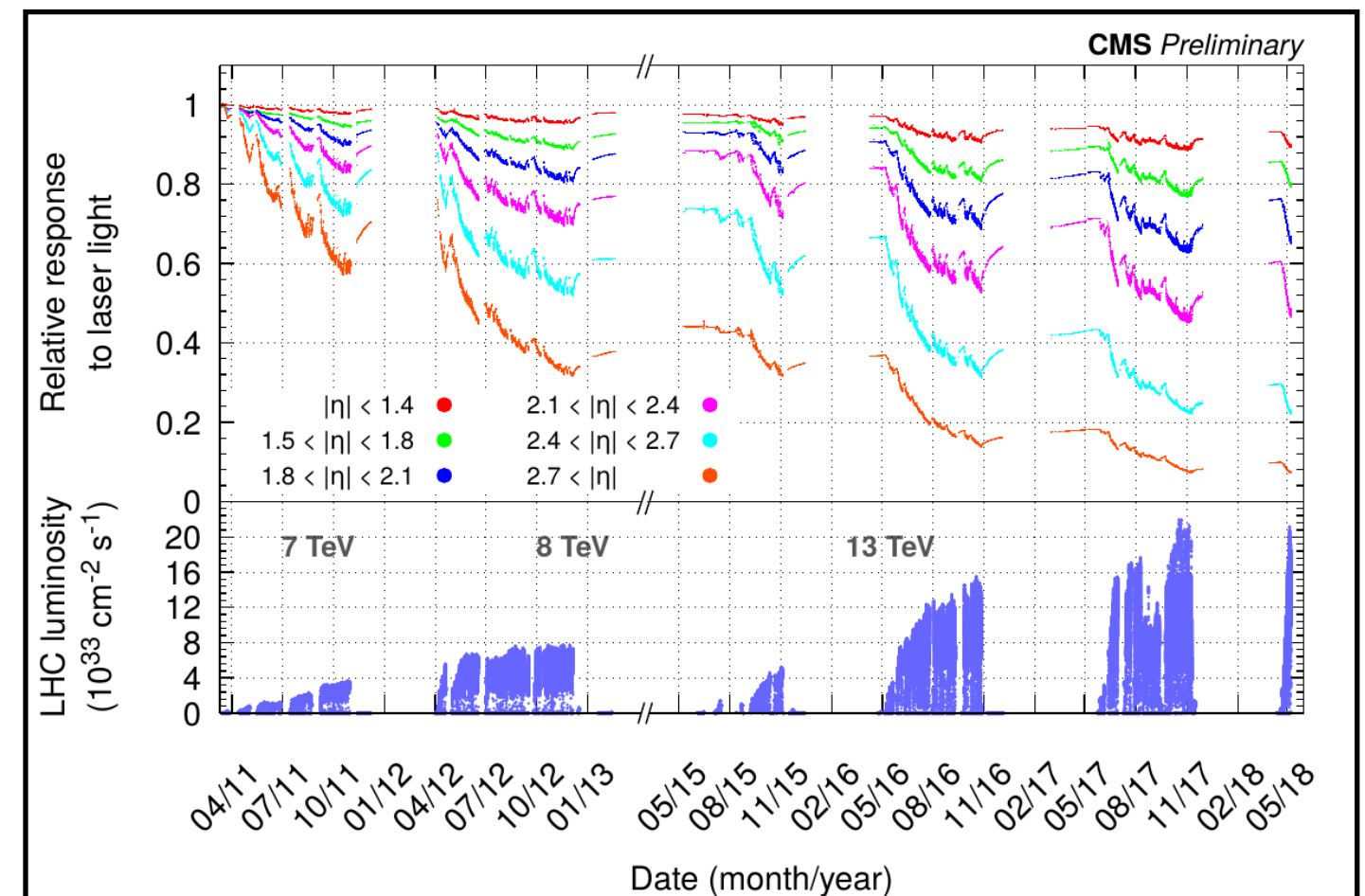


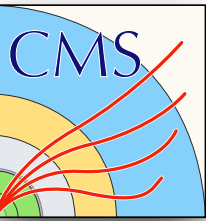
- Energy resolution
 - stochastic term $a = 2.8\%$
 - noise term $b = 12\%$
 - constant term $c = 0.3\%$

$$\frac{\sigma_E}{E} = \frac{a}{\sqrt{E}} \oplus \frac{b}{E} \oplus c$$

- Active laser monitoring system corrects the crystal response during collisions, reducing the dominant constant term

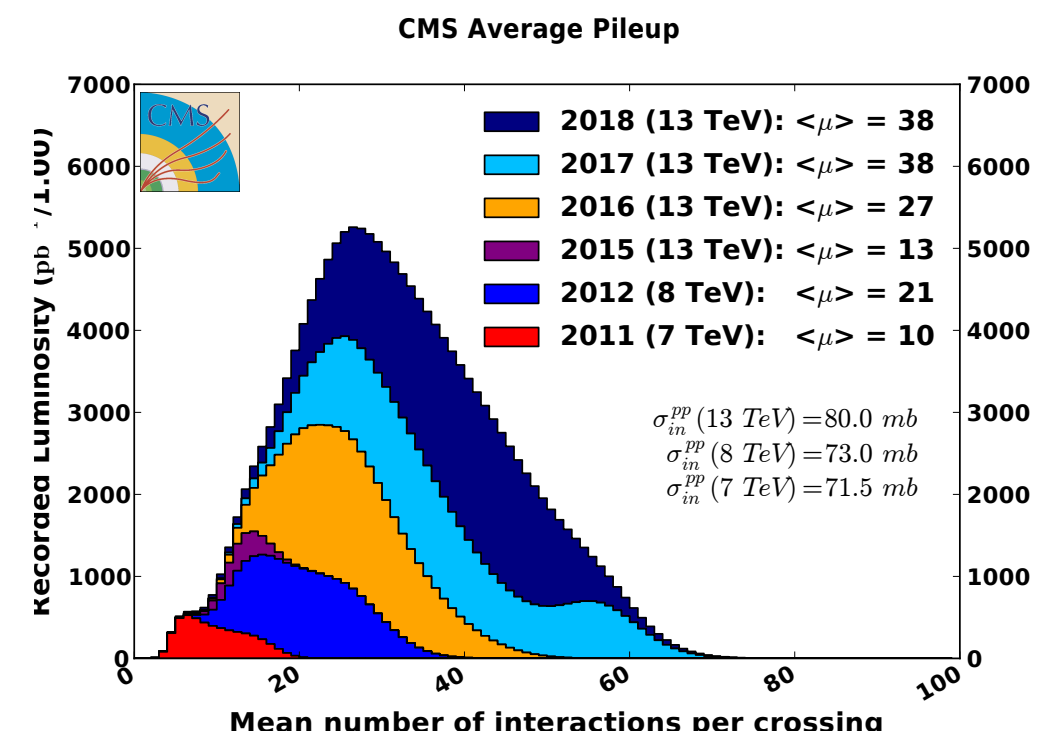
- High-energy photons have an energy resolution of about
 - 1.3-2.5% in the EB
 - 3-4% in the EEs





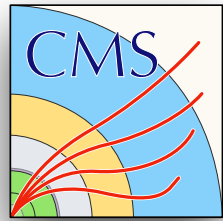
Trigger system

- pp collisions occur every 25 ns at 40 MHz
- Multiple pp interactions within a single bunch crossing, *pileup*
- 1 MB/event for full CMS info
- Two-tier trigger system:
 - L1 trigger and HLT
- L1 trigger
 - custom hardware
 - uses info from ECAL, HCAL, muon system
 - filters at 100 kHz (3.2 μ s latency)
- HLT
 - processor farm running CMS online reconstruction software
 - works with DAQ to reduce event rate to about 1 kHz





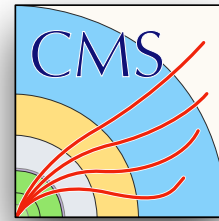
Event reconstruction



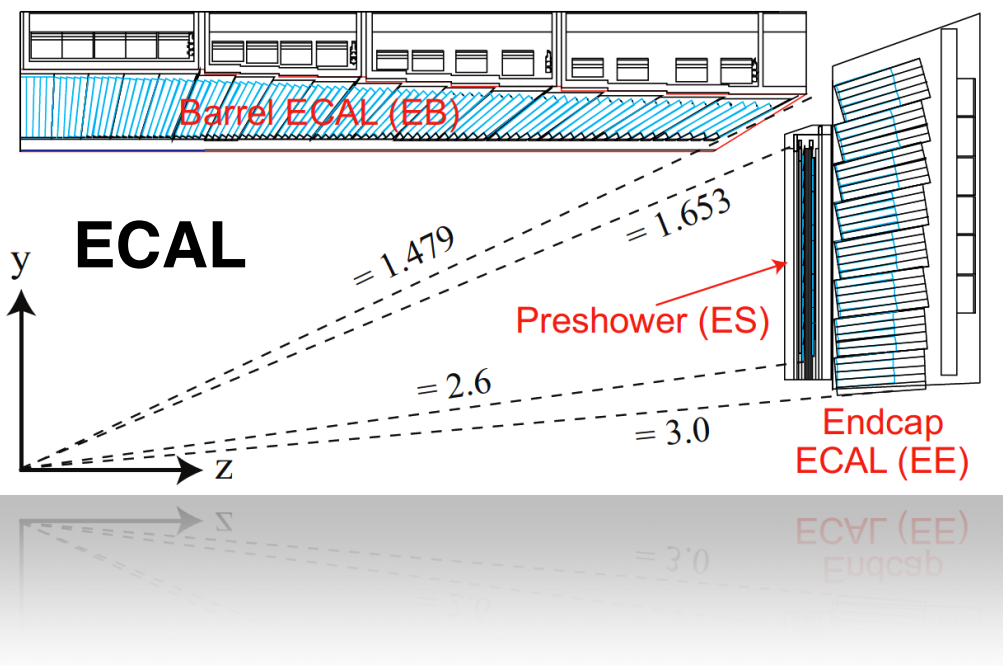
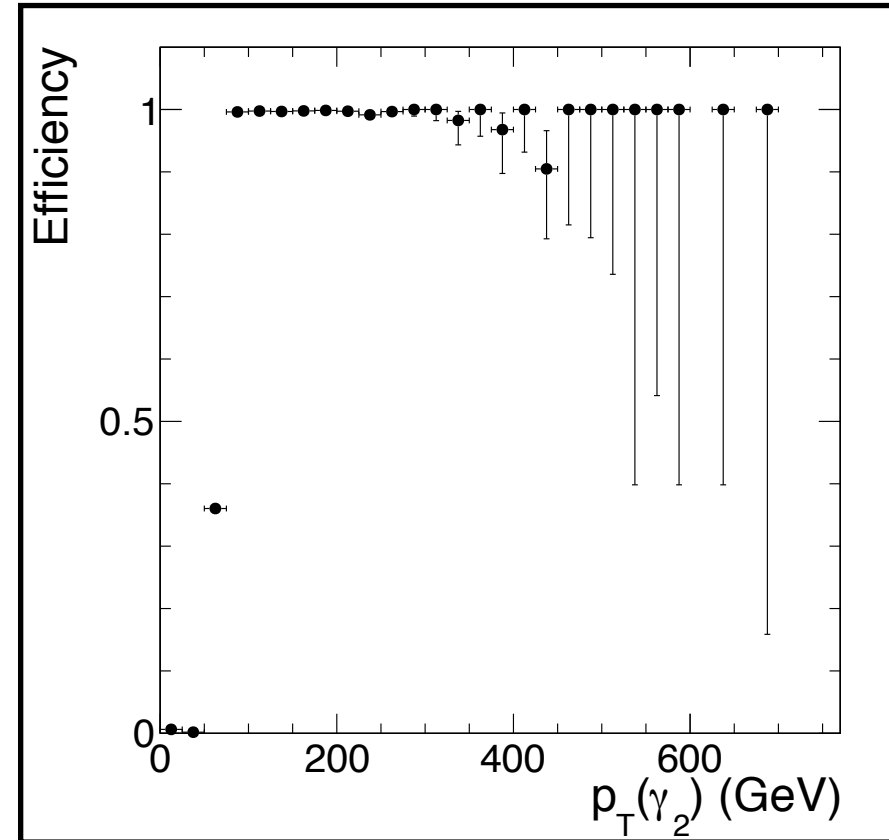
- Global event reconstruction uses the CMS particle-flow algorithm
- Tracks
 - hits in the silicon tracker are fit to form tracks
- Vertices
 - primary vertices have largest summed charged-particle track (p_T)²
- Photons
 - ECAL energy deposits are clustered into 5x5 arrays of crystals called superclusters centered on a seed
 - converted photons deposit energy extended along the ϕ direction
 - energy calibrated using $Z \rightarrow e^+e^-$ decays
 - ECAL electronics may saturate for high-energy photons depositing into a single crystal (~2 TeV)
 - scale factors derived from simulation are used to correct the energy scale and resolution
- Electrons
 - matching a track to an ECAL supercluster
- Muons
 - muon candidates in the muon system are fit to tracks in the inner tracking system
- Jets
 - quarks and gluons hadronize and are clustered into jets
- MET
 - missing energy in the transverse plane can be inferred given the initial transverse momentum is negligible



Diphoton event selection



- Trigger selection
 - events with 2 photon candidates each with $p_T > 60 \text{ GeV}$
- Kinematic preselection
 - photon $p_T > 75 \text{ GeV}$ (fully efficient trigger selection)
 - diphoton invariant mass $m_{\gamma\gamma} > 500 \text{ GeV}$
 - $\Delta R < 0.45$
 - EBEB: two photons in EB
 - EBEE: one photon in EB and one in either EE

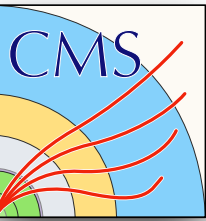


EB: ECAL barrel, $|\eta| < 1.44$
EE: ECAL endcap, $1.57 < |\eta| < 2.5$

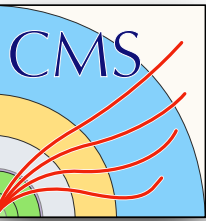
- Diphoton vertex selection
 - primary vertex algorithm suboptimal for photons
 - $H \rightarrow \gamma\gamma$ analysis algorithm
 - both methods coverage at high-mass



Photon identification



- Further criteria imposed to suppress misidentifications from jets and electrons
 - $\pi^0 \rightarrow \gamma\gamma$
- Custom high- p_T photon ID developed for this analysis
- Shower shape variables sensitive to multiple photon showers
 - $\sigma_{in\eta}$: shower shape along the η direction
 - **H/E**: ratio of HCAL over ECAL energy deposit
 - **R₉**: ratio of the energies of 3x3 crystal array over supercluster
- Isolation variables sensitive to extra activity around the photon
 - **Iso_γ**: p_T sum of other photons around photon candidate within $\Delta R = 0.3$
 - **Iso_{Ch}**: same for charged hadrons
$$\Delta R = \sqrt{(\eta - \eta_\gamma)^2 + (\phi - \phi_\gamma)^2}$$
- Electron veto to eliminate electron candidates with mis-assigned tracks
 - **CSEV**: further checks to ensure that tracks assigned to photon did not result from a photon conversion

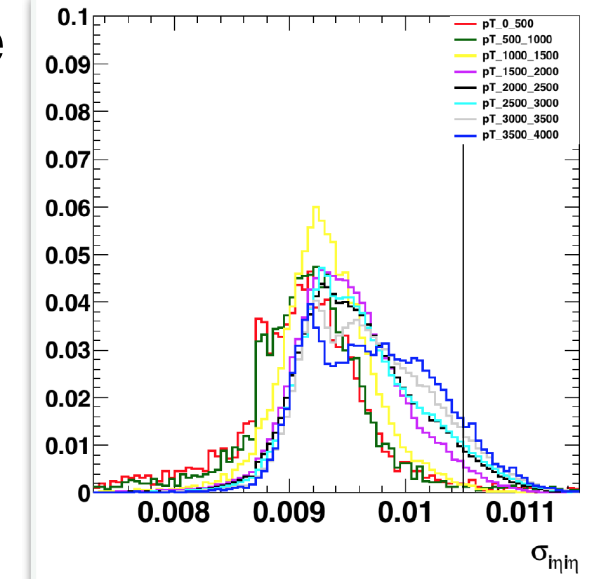


Photon ID

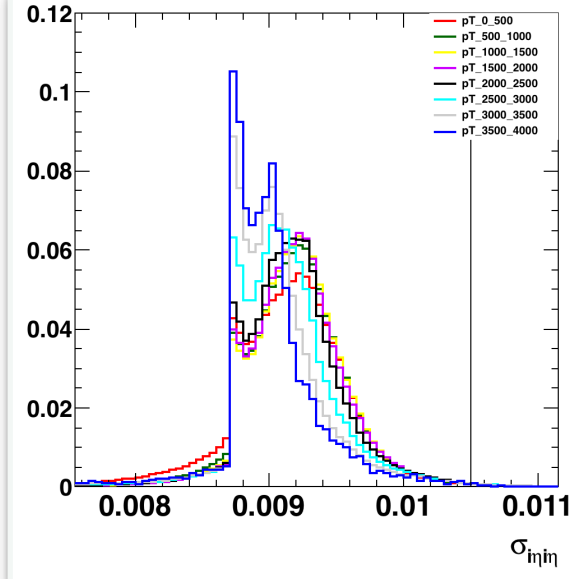
- Iso_γ is corrected for pileup and p_T dependence
- Saturation is accounted for in $\sigma_{inj\eta}$

$$\overline{\text{Iso}}_\gamma = \alpha + \text{Iso}_\gamma - \rho A - \kappa p_T$$

Detector region	α (GeV)	A	κ
$ \eta_{\text{SC}} < 0.9$	0.99	0.15	0.0016
$0.9 < \eta_{\text{SC}} < 1.4442$	0.99	0.13	0.0016
$1.566 < \eta_{\text{SC}} < 2.0$	0.77	0.093	0.00075
$2.0 < \eta_{\text{SC}} < 2.2$	0.77	0.15	0.00075
$2.2 < \eta_{\text{SC}} < 2.5$	0.77	0.21	0.00075



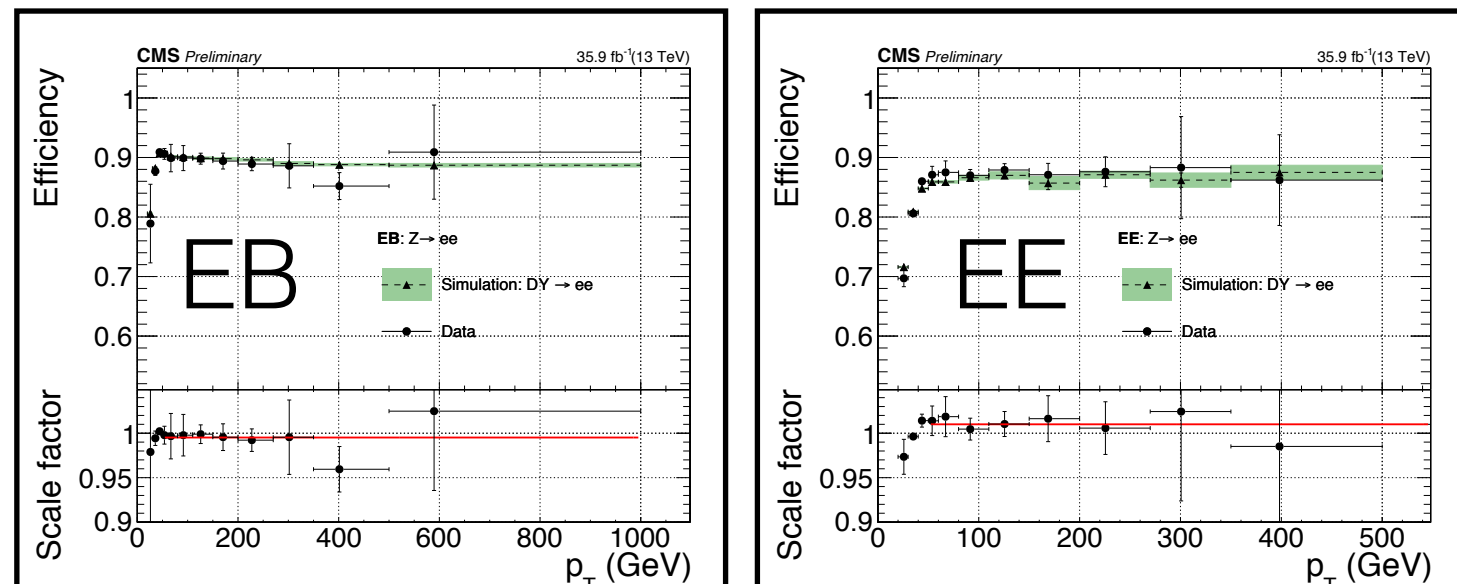
saturated



not saturated

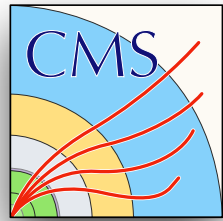
Photon category	Iso_{Ch} (GeV)	$\overline{\text{Iso}}_\gamma$ (GeV)	H/E	$\sigma_{inj\eta}$	R_9	CSEV
EB	5	2.75	0.05	0.0105 (0.0112)	0.8	applied
EE	5	2.0	0.05	0.028 (0.030)	0.8	applied

- Photon selection is 90 (87)% for single photons in the EB (EE) region





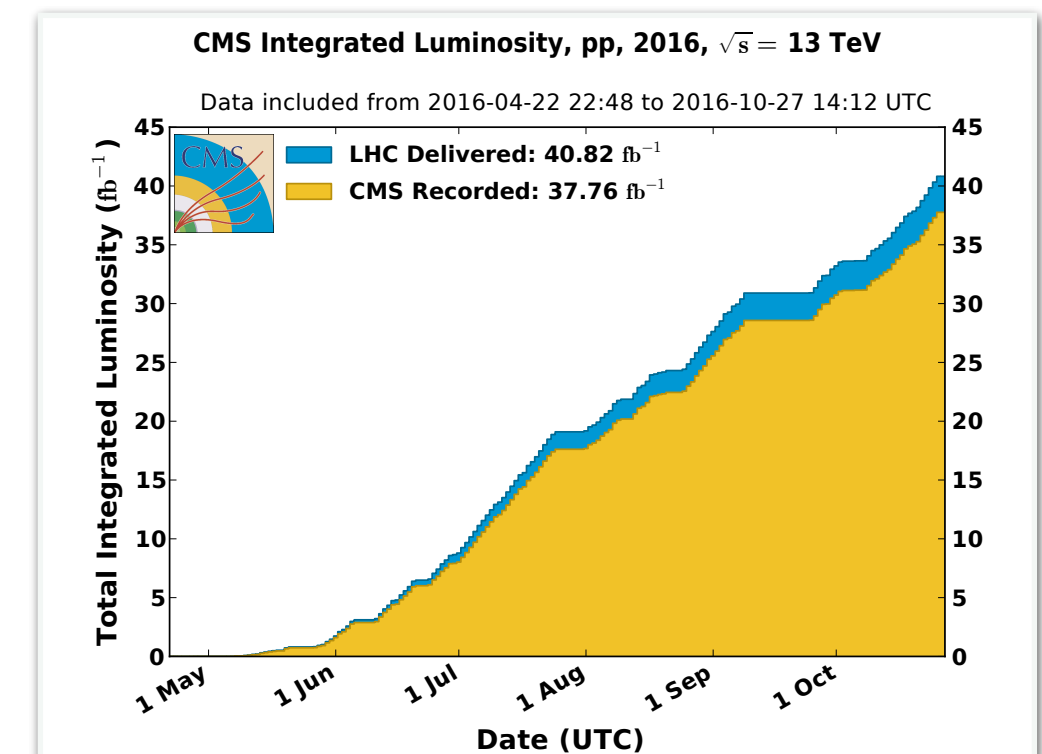
Analysis strategy

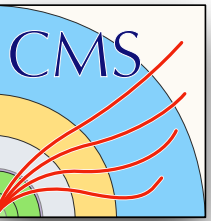


- Search for a nonresonant excess in the high-mass diphoton spectrum at $\sqrt{s} = 13$ TeV using the full 2016 dataset corresponding to an integrated luminosity of 35.9 fb^{-1}
- ADD signal modeled using Monte Carlo (MC) simulation

Full background prediction is made:

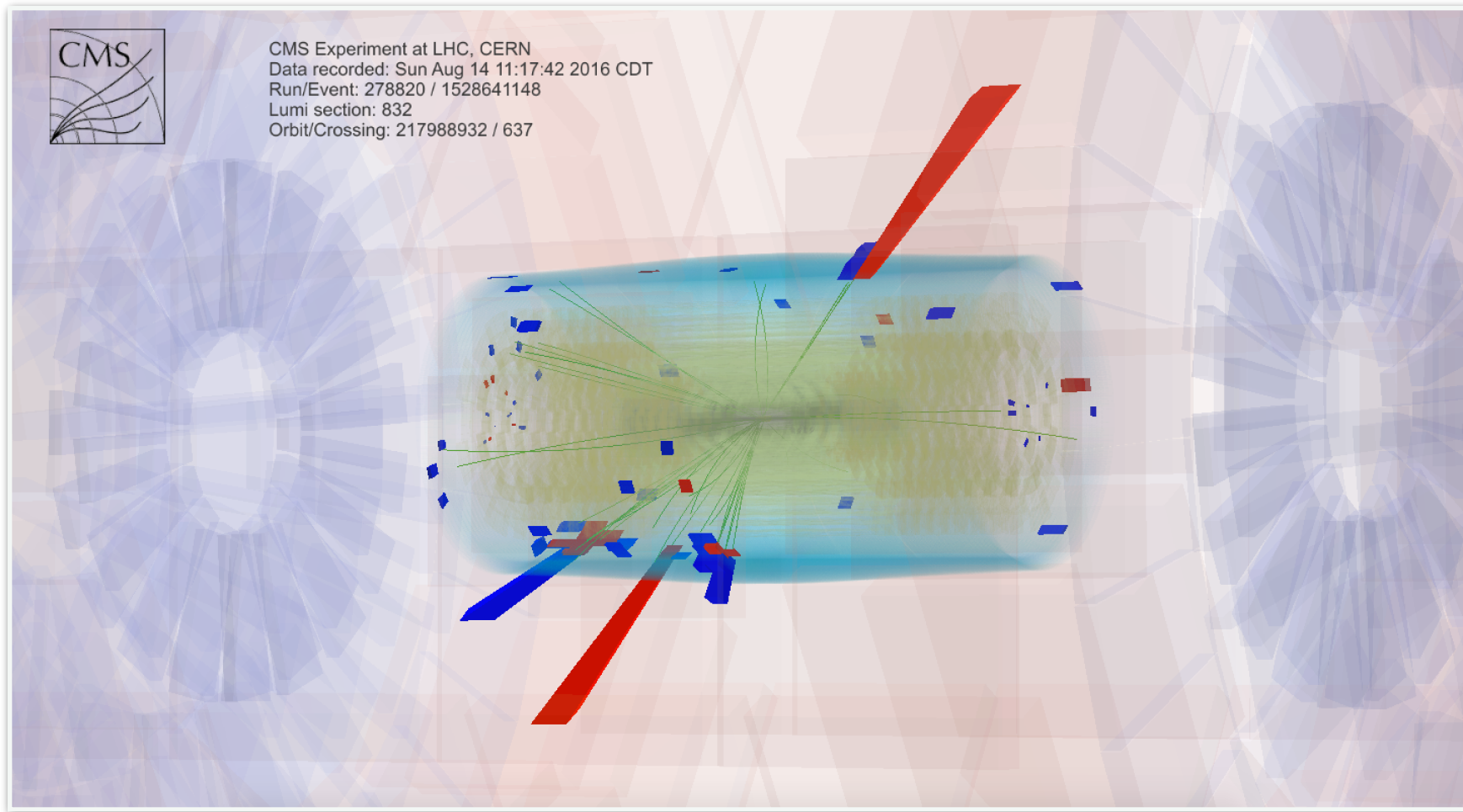
1. Dominant, irreducible prompt SM diphoton ($\gamma\gamma$) background
 - Next-to-next-to-leading order (NNLO) MC calculation
2. Sub-dominant, reducible jet-faking-photon ($\gamma j / jj$) background
 - Data-driven estimate using control samples





Event display

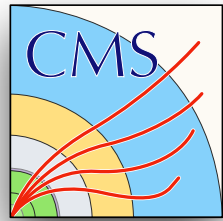
- Highest-mass diphoton event recorded on August 14, 2016 in EBEB at $m_{\gamma\gamma} = 1840$ GeV



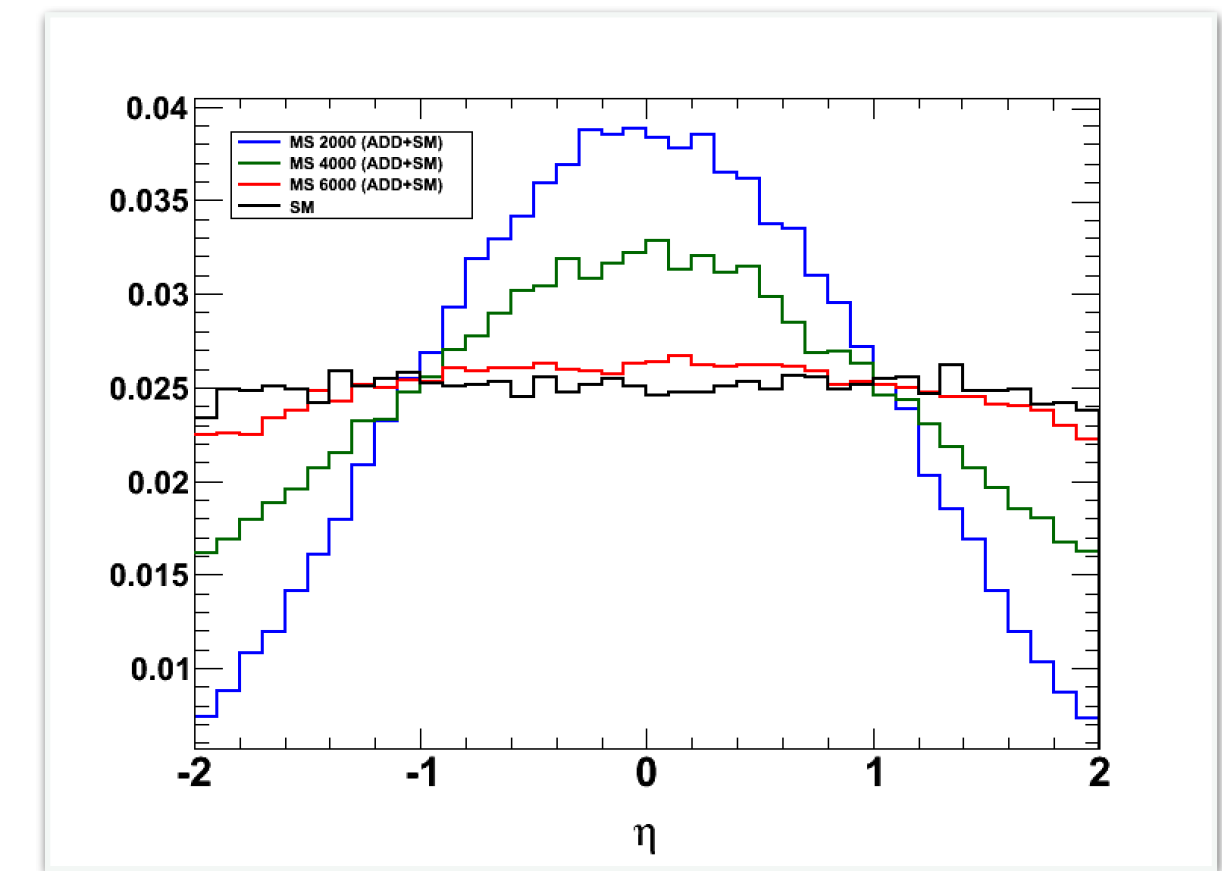
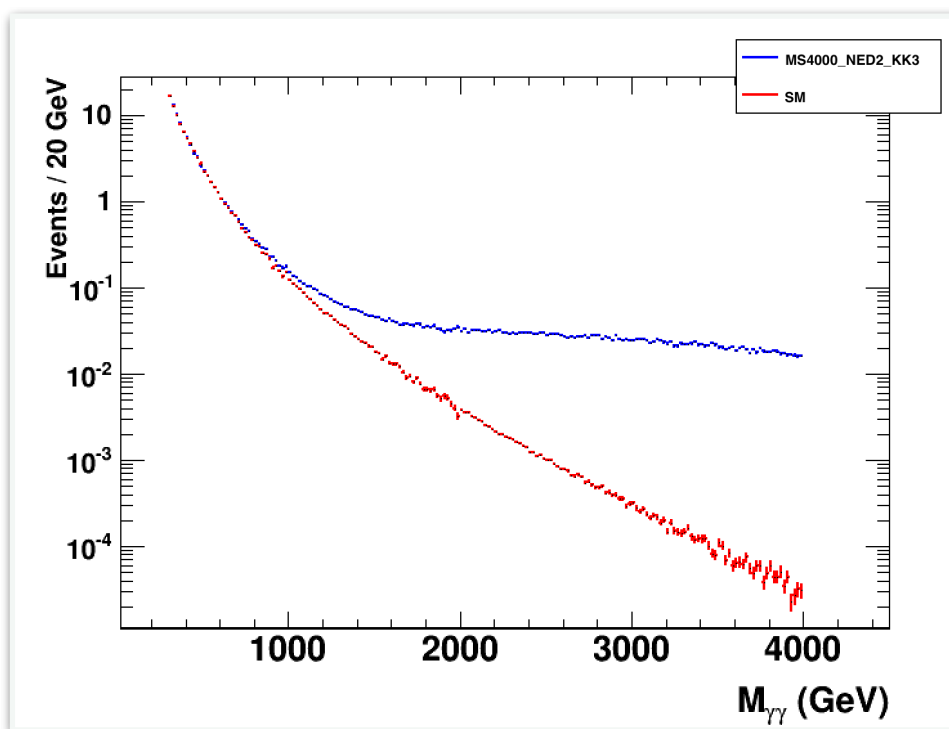
	$m_{\gamma\gamma}$ (GeV)	γ_1 (p_T , η_{SC})	γ_2 (p_T , η_{SC})	Run:LS:Event	Dataset path	Date
EBEB	1840.38	(964.15, -0.881)	(429.01, 0.916)	278820:832:1528641148	/Run2016G-X-v1	Aug 14
	1816.31	(833.60, -0.160)	(679.74, -1.424)	276810:249:448659898	/Run2016D-X-v1	Jul 14
	1777.39	(508.64, -1.053)	(451.83, 1.405)	276437:452:753595848	/Run2016D-X-v1	Jul 6
EBEE	2444.38	(415.88, -2.484)	(272.98, 1.442)	279794:445:700510844	/Run2016G-X-v1	Aug 30
	2134.42	(570.82, -0.695)	(515.46, 1.916)	284039:18:31148565	/Run2016H-X_ver3-v1	Oct 26
	1985.68	(577.69, -2.443)	(397.34, 0.273)	276585:21:32975214	/Run2016D-X-v1	Jul 10



ADD signal model

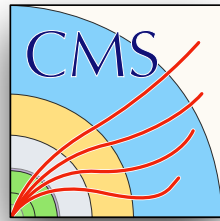


- ADD model is parameterized by n_{ED} and M_S
- Interference effects
 - signal generated with LO SM background using Sherpa v.2.1.1
 - samples generated with $m_{\gamma\gamma} \leq M_S$
- M_S cutoff conventions \mathcal{F}
 - consider **HLZ**, **GRW**, and **Hewett**
- Parameter space:
 - $M_S = 3\text{-}11 \text{ TeV}$
 - $n_{ED} = 2, 3, \dots, 7$

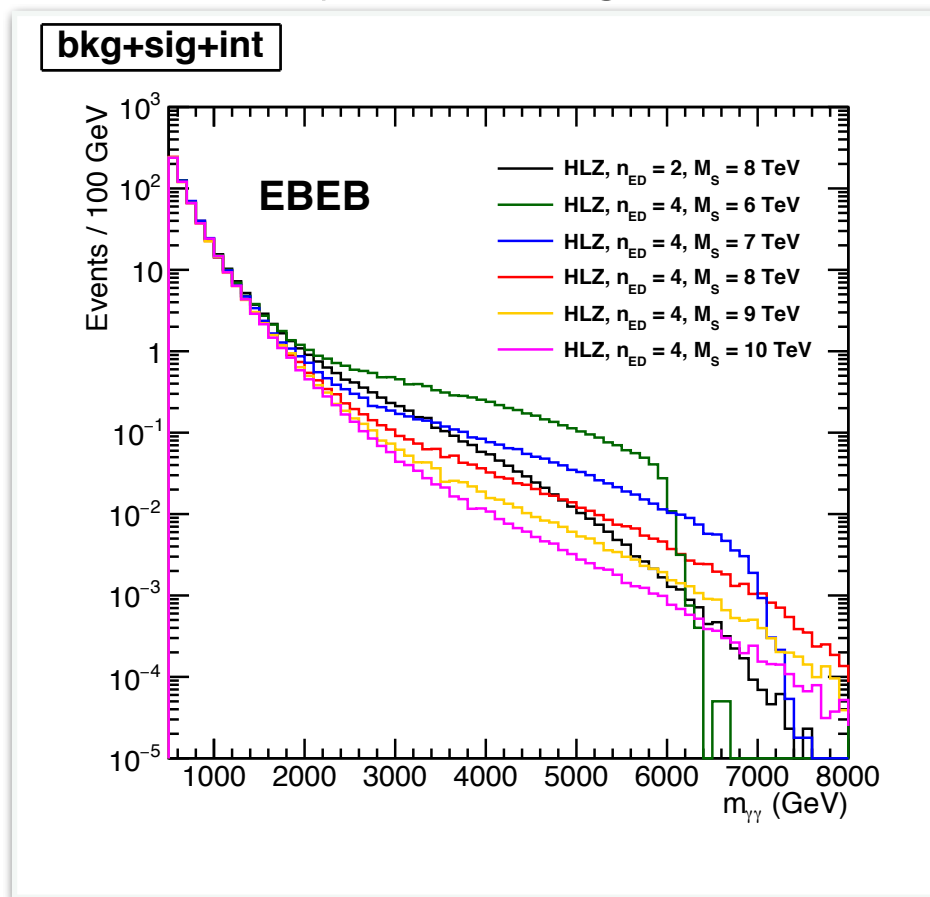




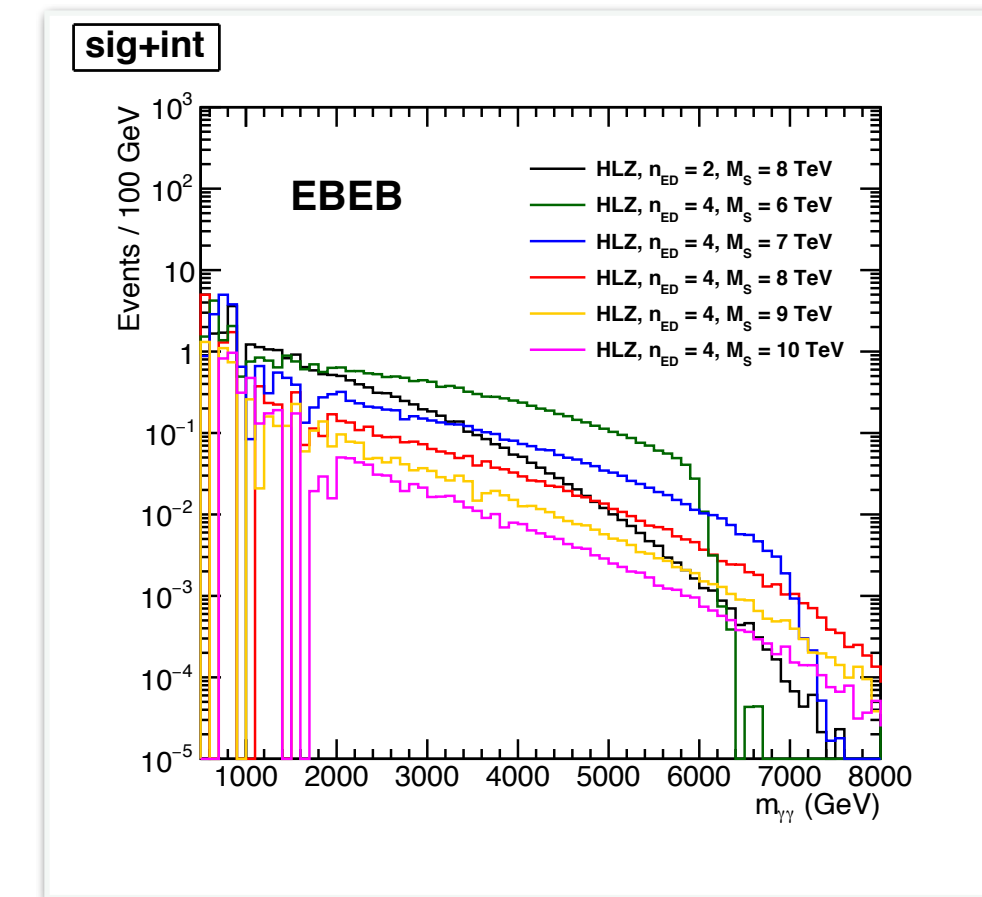
ADD convention reduction



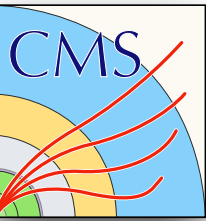
- Diphoton invariant mass distributions from different conventions are equivalent if they have the same value of η_G
 - Hewett+ with $M_S = 4000$ GeV \leftrightarrow GRW with $M_S = 4478$ GeV
- Reduction in distinct signal points
 - **GRW** (constant positive interference)
 - **HLZ assuming $n_{ED} = 2$** (positive interference with energy dependence)
 - **Hewett-** (negative interference)
- Each signal point broken into different $m_{\gamma\gamma}$ bins to improve statistics
 - 122 different samples totaling 12.2 million events



sig.+bkg.+int.

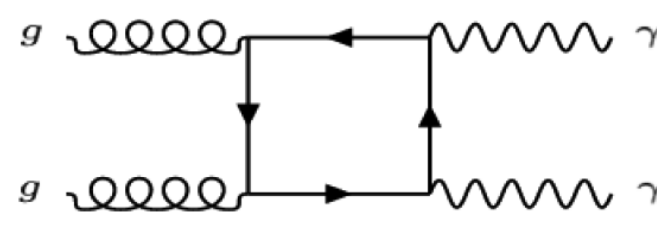


sig.+int.

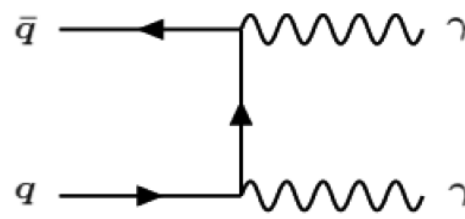


Real background

- Irreducible, prompt SM $\gamma\gamma$ background generated using Sherpa v.2.1.1 with:

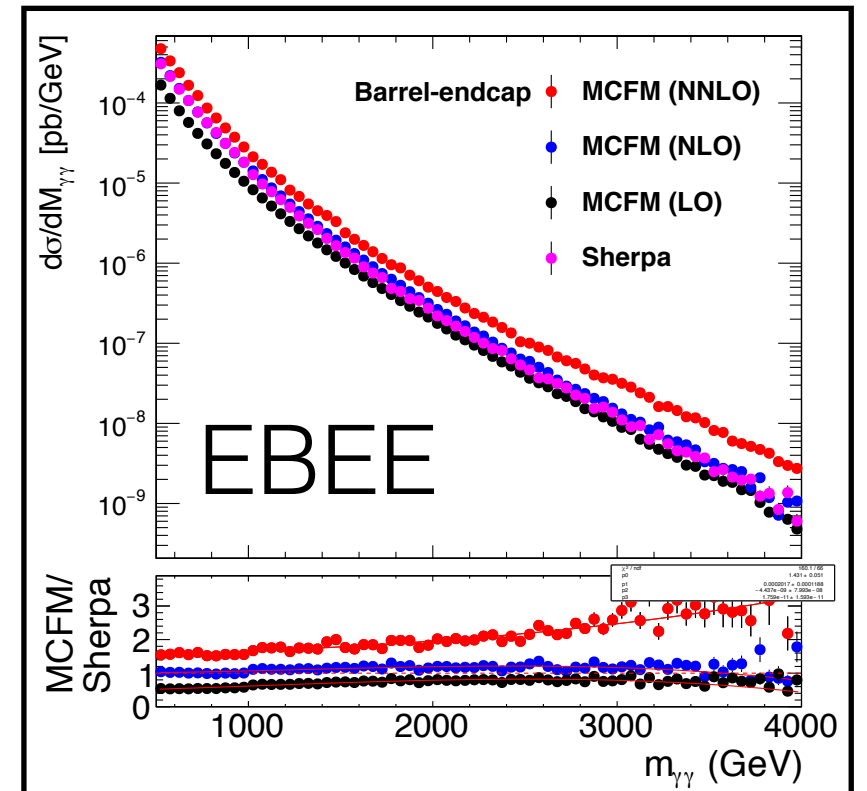
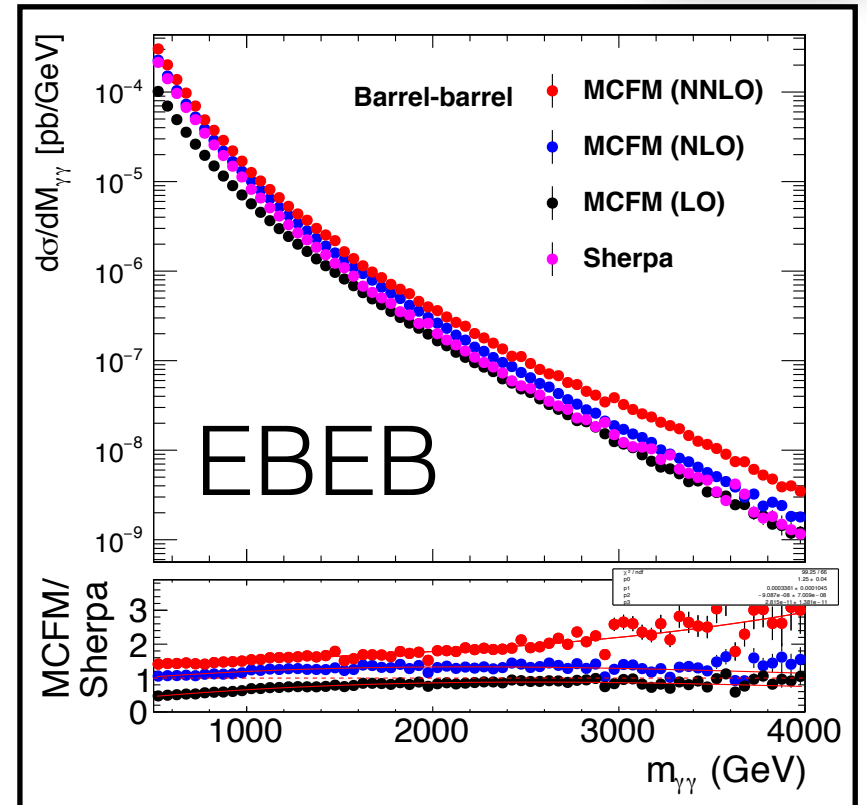


Box



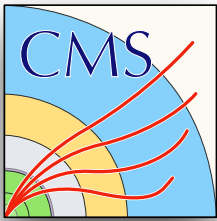
Born + 0, 1, 2, or 3 jets

- NNLO contribution to SM processes calculated using MCFM v.8.0
 - includes virtual corrections missing in Sherpa
- K factor = MCFM / GEN-level Sherpa**
 - Function of $m_{\gamma\gamma}$
 - Used to reweight fully simulated prompt diphoton events (from Sherpa) for final prediction
- K factor: 1.4-2.2(2.5) in EBEB(EBEE) for $m_{\gamma\gamma} < 3$ TeV

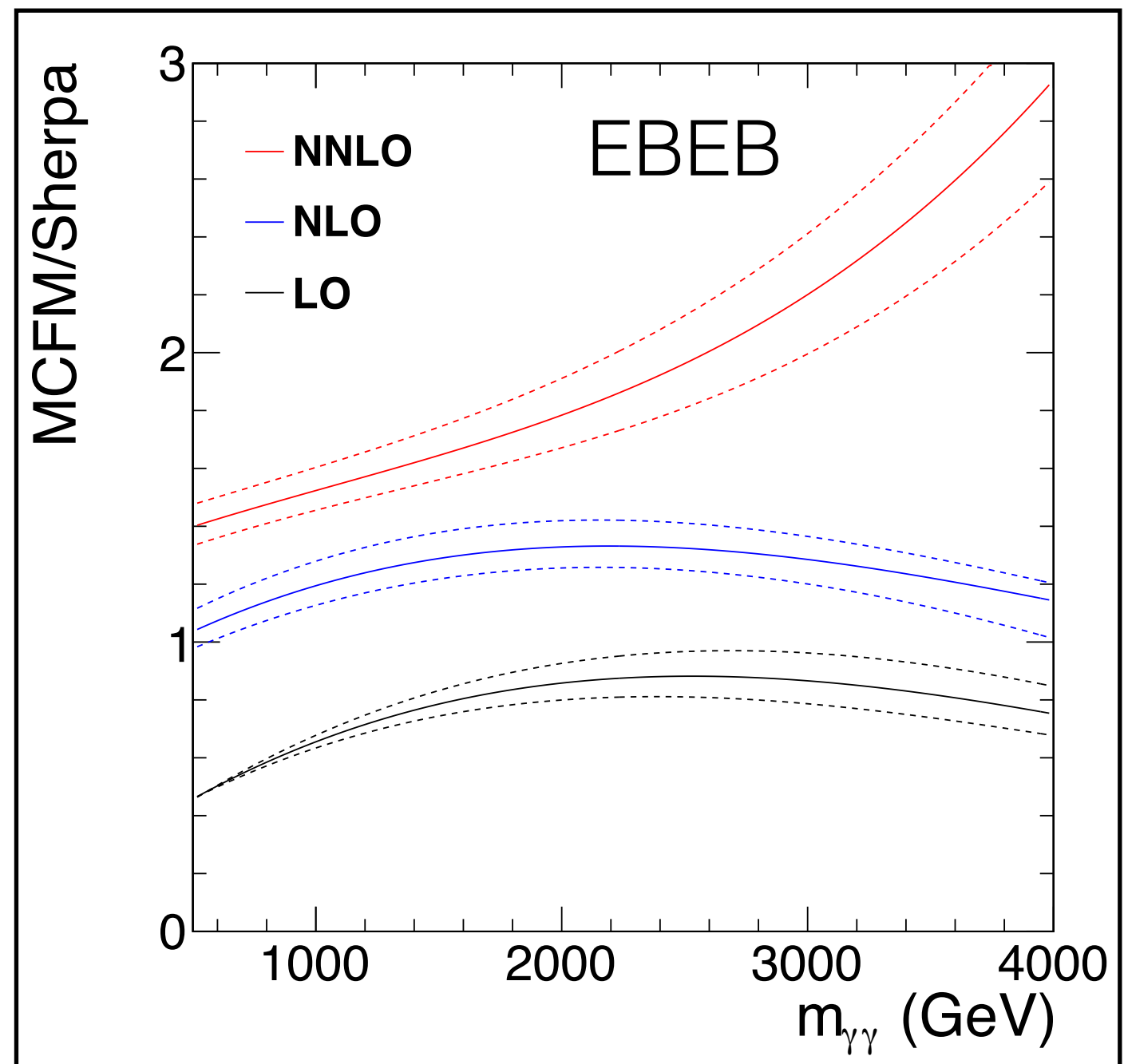




Scale variations on K factor

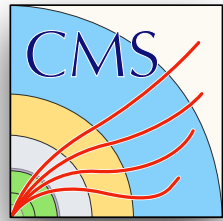


- Renormalization scale μ_r
 - sets the truncation of the perturbative calculation
- Factorization scale μ_f
 - sets the transition point between the hard calculation and the PDFs (separating long- and short-distance processes)
- Scale variations
 - $\mu_f = \mu_r = 2 m_{\gamma\gamma}$
 - $\mu_f = \mu_r = m_{\gamma\gamma}$
 - $\mu_f = \mu_r = 1/2 m_{\gamma\gamma}$
- Similar level of variation observed in EBEE
- Treated as a systematic uncertainty

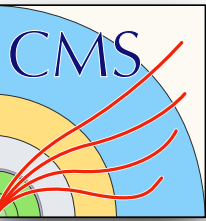




Fake background

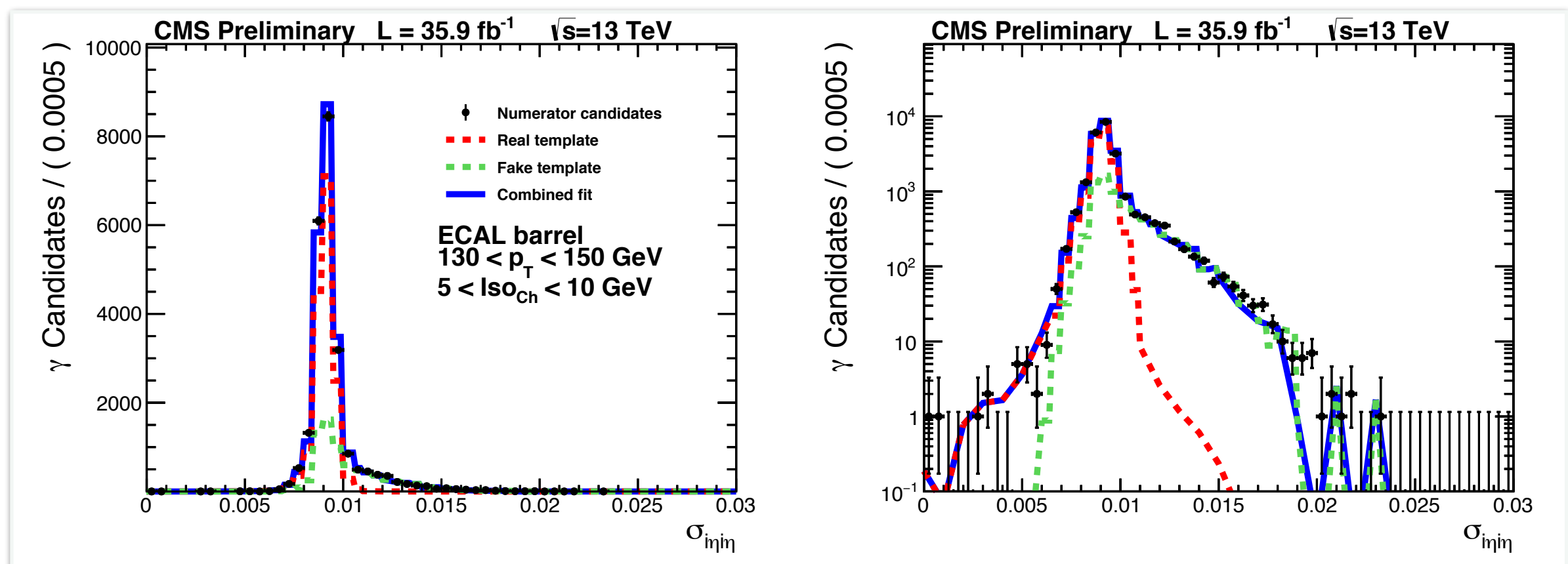


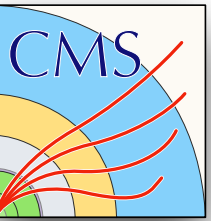
- Reducible background from SM γj or jj events where one or two jets with large EM activity fake a photon signature
 - misreconstructed as a photon in the ECAL
- Fake rate function $f(p_T)$ is measured in a jet-enriched data reference sample as a function of photon p_T in EB and EE
 - combined jet- and muon-triggered dataset
- **fake rate:** $f(p_T) = \text{numerator} / \text{denominator}$
 - **numerator:** number of jets passing photon ID
 - **denominator:** number of jets passing a looser photon-like ID
- Contamination from real photons is removed from **numerator** through a template fit



Template fit

- **Template variable** - Shower shape variable $\sigma_{i\eta i\eta}$
- **Real template** - Constructed from photon-rich MC using MC truth information to identify real photons
- **Fake template** - Constructed from reference data sample using a sideband in the isolation variable Iso_{Ch}
- **Template fit** - Performed using MLE on data with relaxed $\sigma_{i\eta i\eta}$





Fake rate

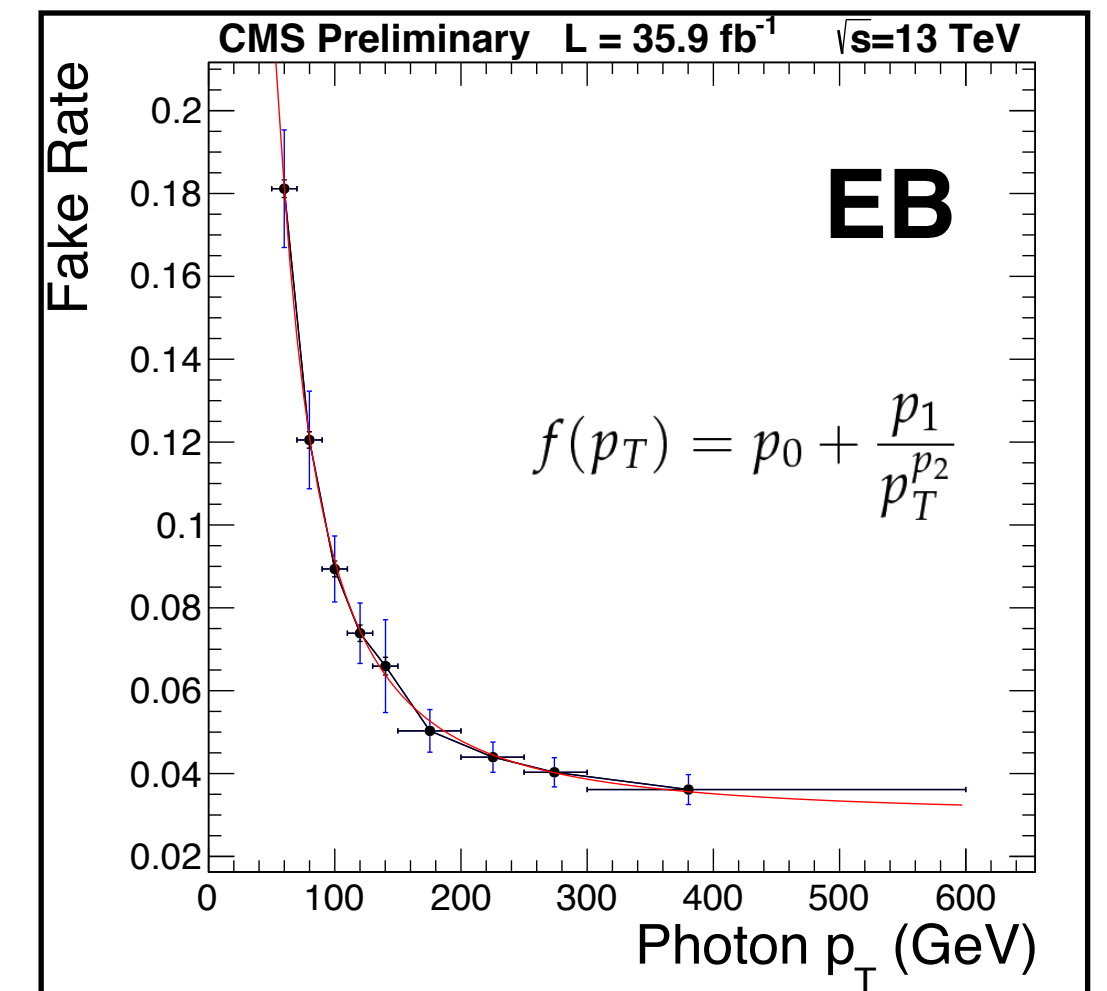
- **Denominator** objects in analysis diphoton data sample are reweighted by $f(p_T)$ to give a fake prediction

$$jj = (f_1 F_1)(f_2 F_2)$$

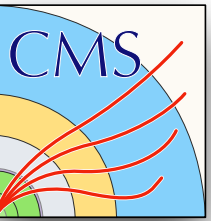
$$\gamma j = (R_1 N_2) + (N_1 R_2)$$

$$= (T_1 - f_1 F_1)(f_2 F_2) + (f_1 F_1)(T_2 - f_2 F_2)$$

$$= T_1(f_2 F_2) + (f_1 F_1)T_2 - 2(f_1 F_1)(f_2 F_2)$$



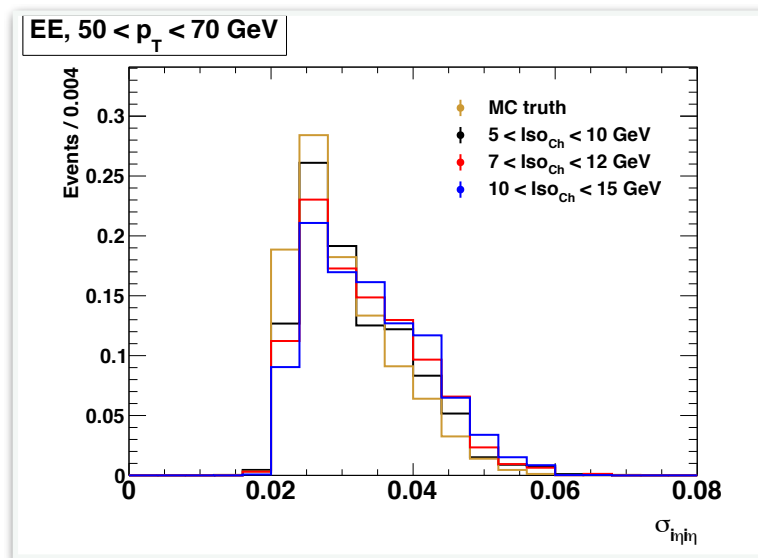
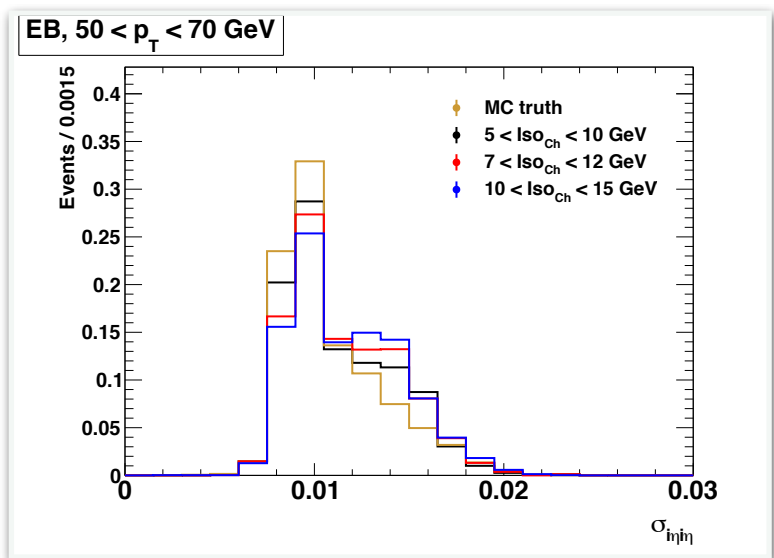
- Fake contribution is less than 4 (14)% in EBEB (EBEE) for $m_{\gamma\gamma} > 1$ TeV



Closure test to photon fake rate method

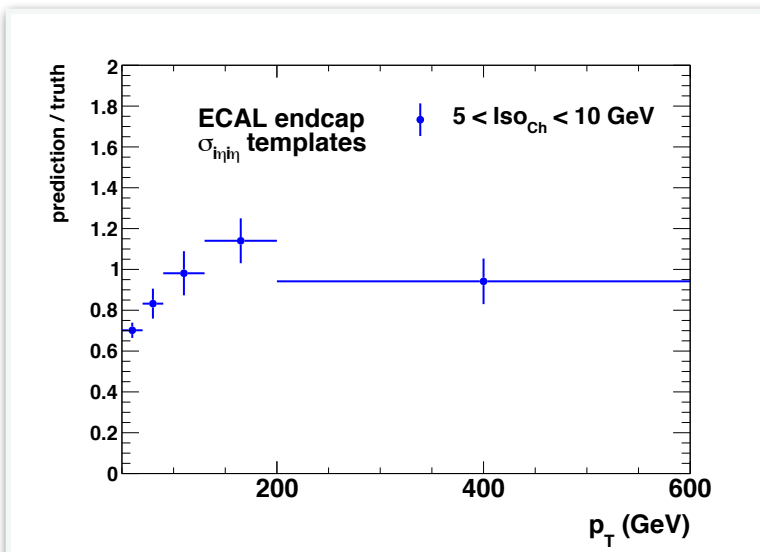
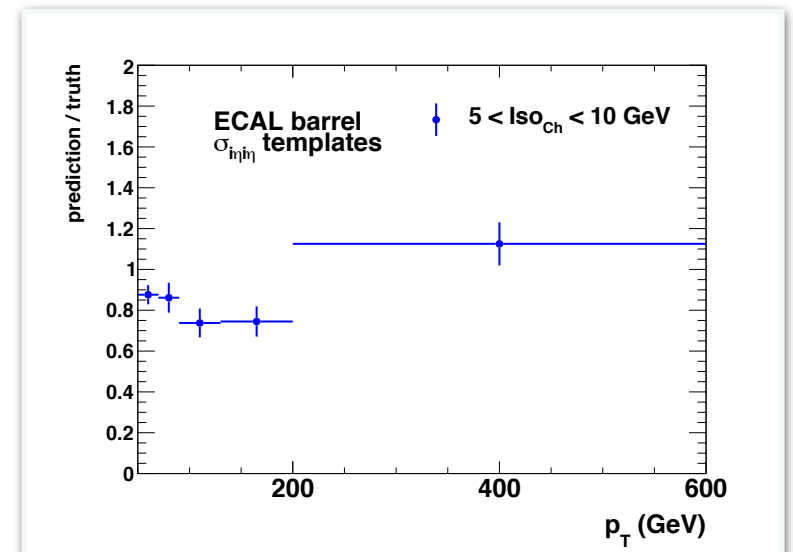
MC based closure test is performed by comparing

1. Fake rate method applied to jet-enriched MC sample (“treat MC as data”) to determine a **fake prediction** in MC sample
2. **MC truth** calculation to identify known fake photons in MC sample



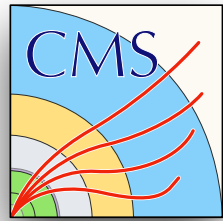
- MC fake templates to MC truth
 - choosing templates from a sideband has some bias

- Closure test predicted fake rate compared to truth fake rate
 - similar agreement for inverted relationship between template and sideband variables
 - deviation consistent with total systematic uncertainty applied to this method

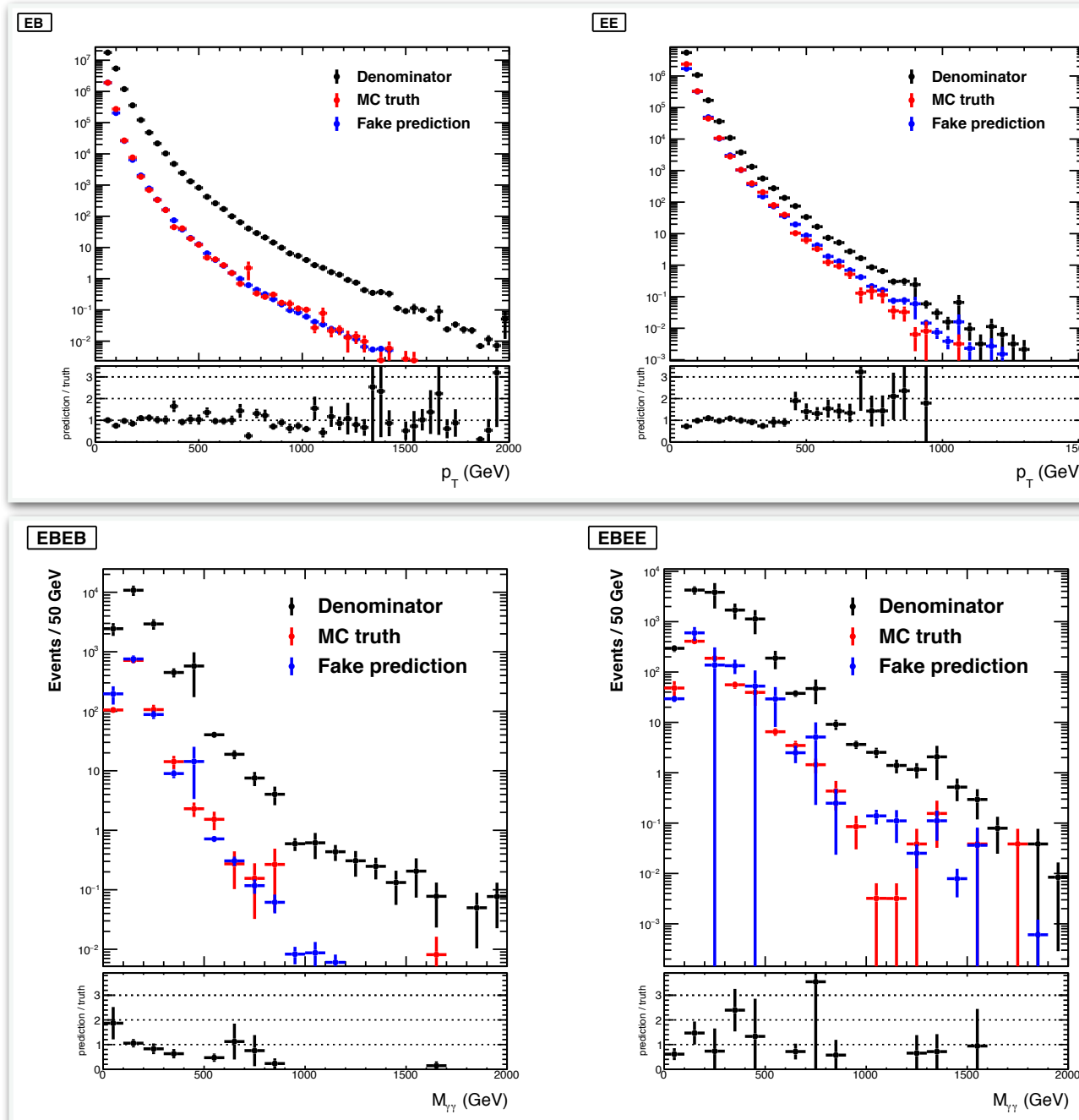




Closure test of kinematics



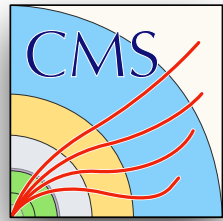
- The **re-weighted denominator objects** reflect the kinematics of known fake objects from **MC truth**



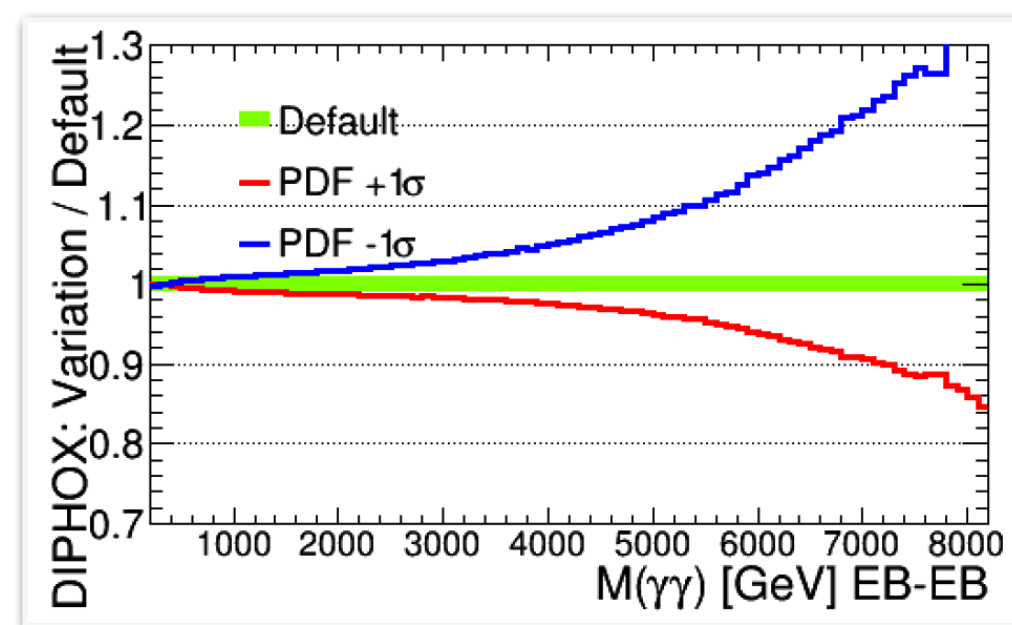
- Photon p_T in EB and EE
- Diphoton $m_{\gamma\gamma}$ γj objects in EBEB and EBEE



Systematic uncertainties

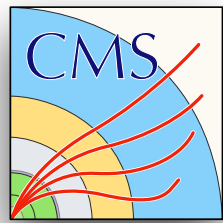


- Systematic uncertainties are considered for
 - real background prediction
 - fake background measurement
 - signal calculation
- Affecting either the shape or normalization of distribution
- CT10 PDF set is used for signal and background simulation
- PDF uncertainties are calculated using the MC calculator DIPHOX at NLO
 - 26 eigenvector pairs are varied by $\pm 1\sigma$ around nominal value
 - each eigenvector variation is considered a separate systematic





Summary of systematic uncertainties



Prompt diphoton background

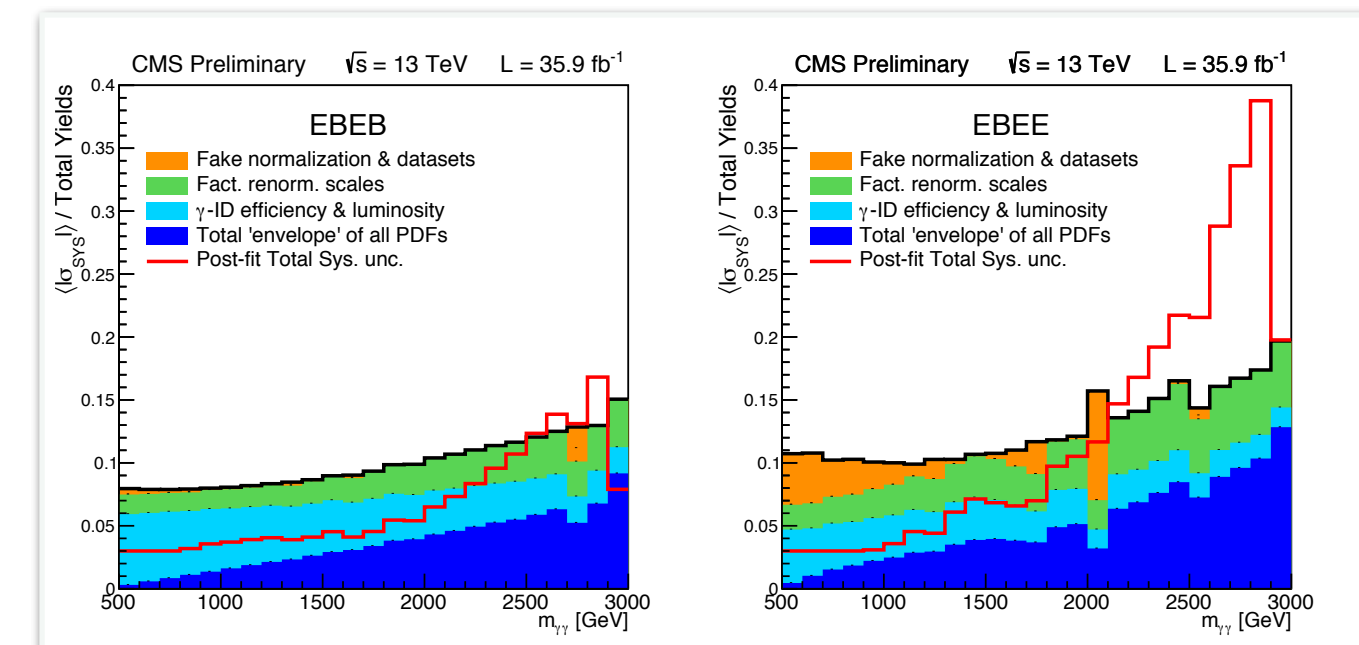
- normalization is allowed to float arbitrarily, which absorbs uncertainties in
 - higher order terms not included in our NNLO K factor
 - luminosity and photon selection efficiency
- scale variations on μ_r and μ_f for the MCFM K factor calculation (shape)
- 26 PDF eigenvector pair variations (shape)
- shape differences in NNLO MCFM and NLO MCFM and NLO DIPHOX

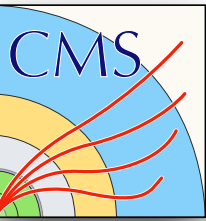
Fake background

- 30% uncertainty on fake rate normalization
 - pileup, photon η , change in sideband, change in template, non-closure, real photon contamination
- shape differences in fake rate from jet- and muon-triggered datasets

MC signal

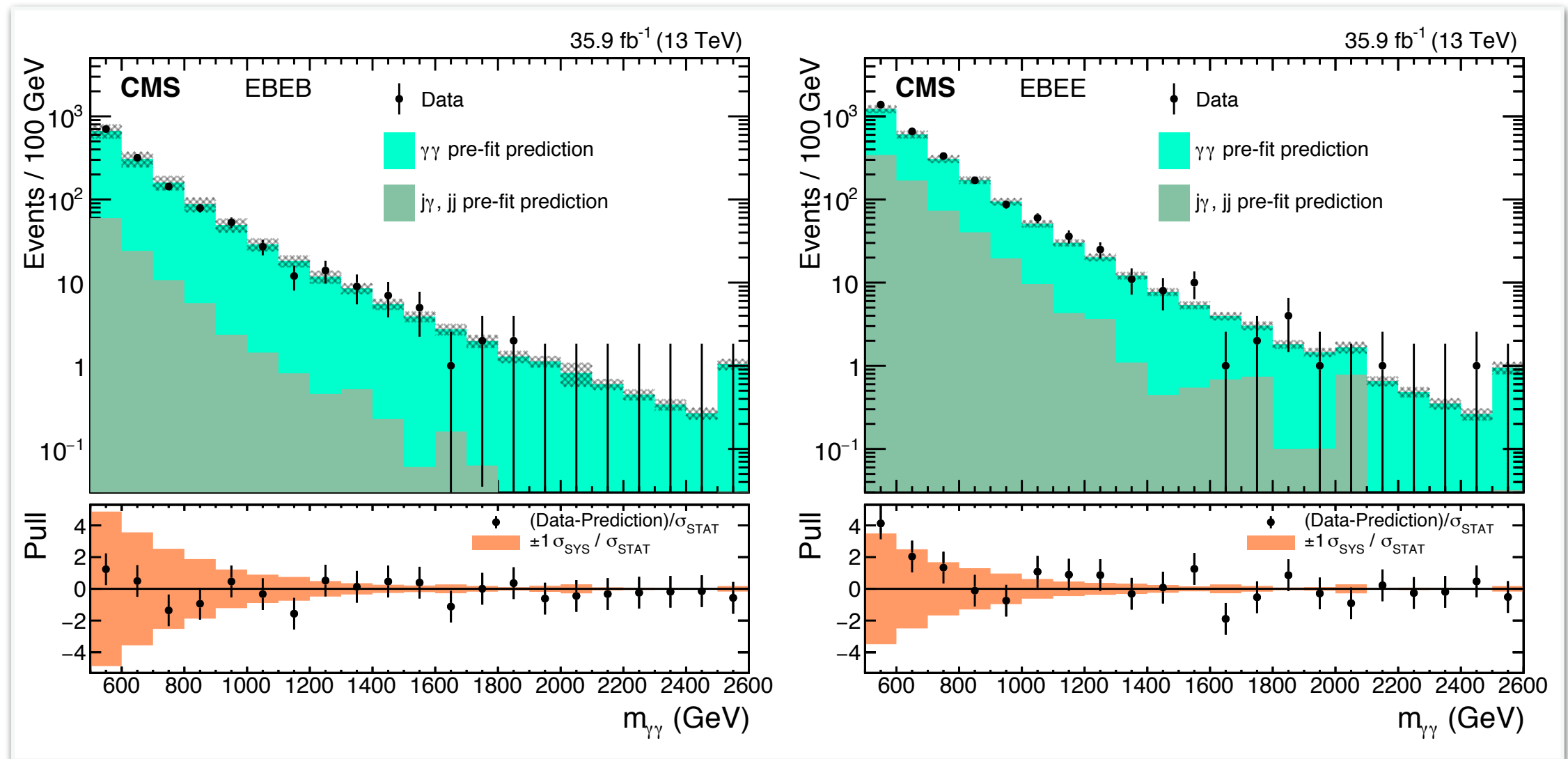
- 2.5% for integrated luminosity (normalization)
- 6% for photon selection efficiency (normalization)
- 26 eigenvector pair variations (shape)





Diphoton invariant mass spectrum

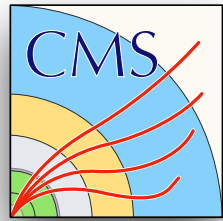
- Search region $m_{\gamma\gamma} > 500$ GeV (initially blind above 1 TeV)
- **Pre-fit** prediction of $m_{\gamma\gamma}$ spectra in excellent agreement with data



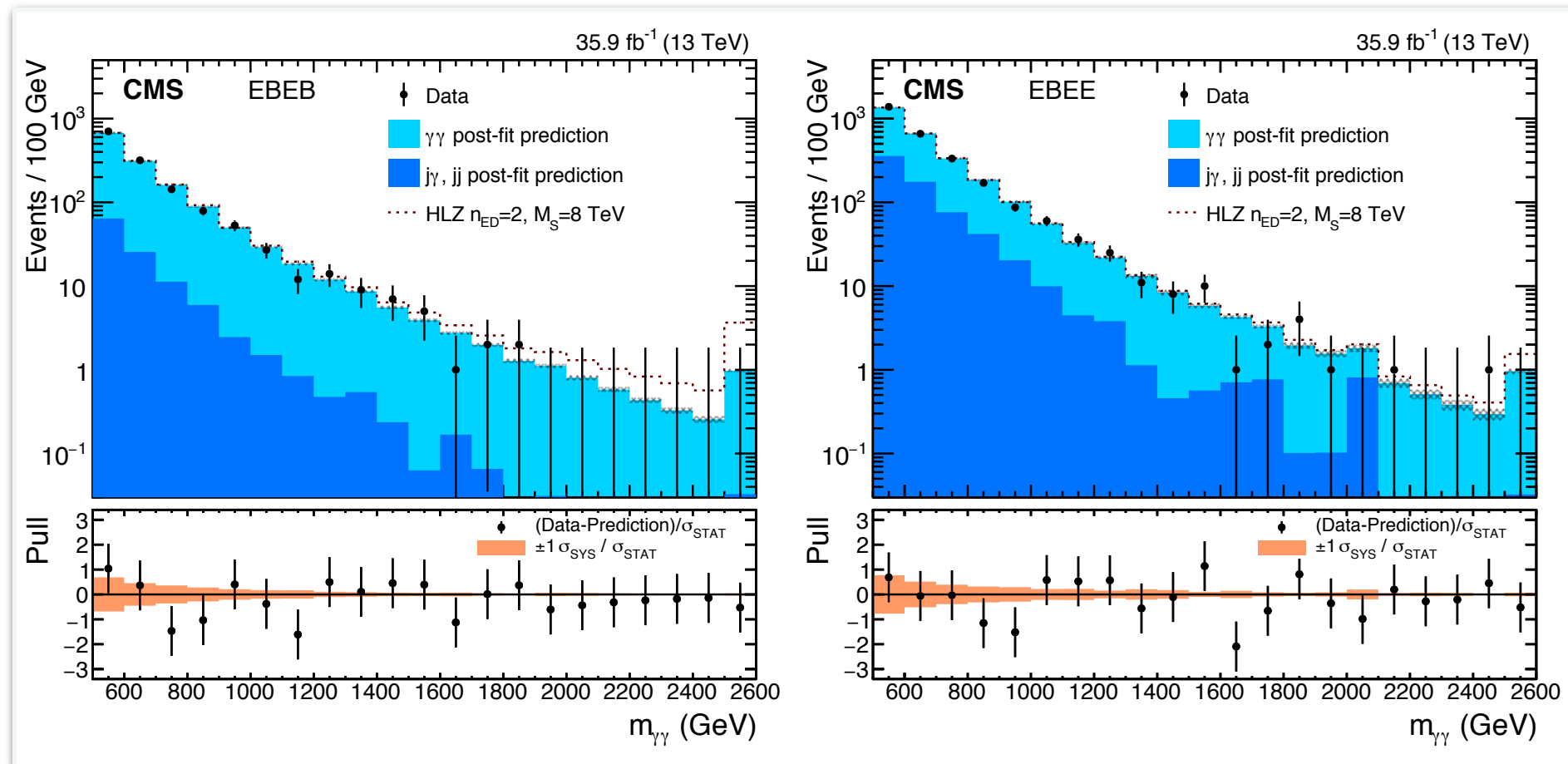
- Highest $m_{\gamma\gamma}$ events
 - 1840 GeV (EBEB)
 - 2444 GeV (EBEE)
- No significant excess of data over background



Diphoton invariant mass spectrum



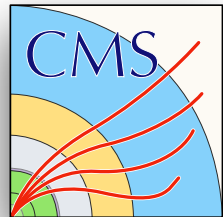
- **Post-fit** in $m_{\gamma\gamma}$ gives final prediction
 - allow real background normalization to float, constrained primarily by data at low $m_{\gamma\gamma}$
 - performed simultaneously with limit extraction
 - example signal distribution superimposed



Category	Type	0.5-1 TeV	1-1.5 TeV	1.5-2 TeV	2-13 TeV	0.5-13 TeV
EBEB	Total pre-fit background	1275.7	73.0	11.1	3.5	1363.3
	Total post-fit background	1285 ± 40	73.7 ± 2.9	11.0 ± 0.5	3.30 ± 0.22	1373.0 ± 40.1
	Data	1296	69	10	0	1375
EBEE	Total pre-fit background	2406.1	121.4	15.6	4.4	2547.5
	Total post-fit background	2645 ± 60	128 ± 6	16.1 ± 1.2	4.1 ± 0.5	2793.2 ± 60.3
	Data	2631	140	18	2	2791



Statistical methods



- Bayesian inference is used

- Bayes' theorem

- $P(A)$ prior
- $P(A|B)$ posterior
- $P(B|A)$ likelihood

$$P(A|B) = \frac{P(B|A)P(A)}{P(B)}$$

$$\mathcal{L}_i(n_i|\mu) = \frac{(\mu s_i + b_i)^{n_i} e^{-(\mu s_i + b_i)}}{n_i!}$$

- Binned (Poissonian) likelihood on number of data events \mathbf{n} given signal \mathbf{s} and background \mathbf{b}
 - signal strength μ

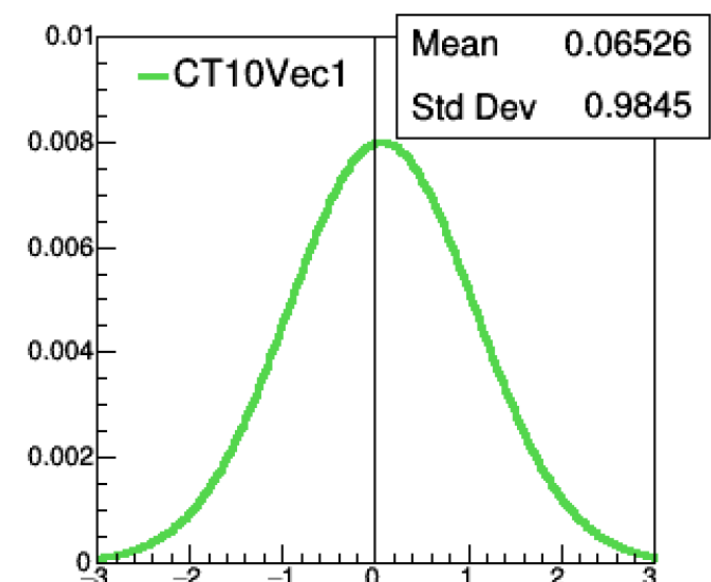
- Flat prior $\pi(\mu)$ considered on ADD signal strength

$$P(\mu|n_i) = \mathcal{L}_i(n_i|\mu)\pi(\mu)$$

- Signal and background depend on systematic uncertainties
 - nuisance parameters θ assigned to each systematic and marginalized using a choice of prior $\pi(\mu, \theta)$

$$P(\mu|n_i) = \int P(\mu, \theta|n_i)d\theta = \int \mathcal{L}_i(n_i|\mu, \theta)\pi(\mu, \theta)d\theta$$

- Maximum likelihood estimate provides
 - posterior background prediction
 - posterior signal strength prediction





Limit setting

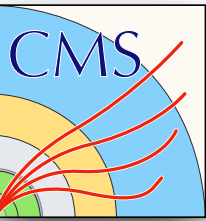


- Posterior signal strength predictions used to derive 95% CL exclusion limits on ADD model parameters

- Integrate to find μ_{up}

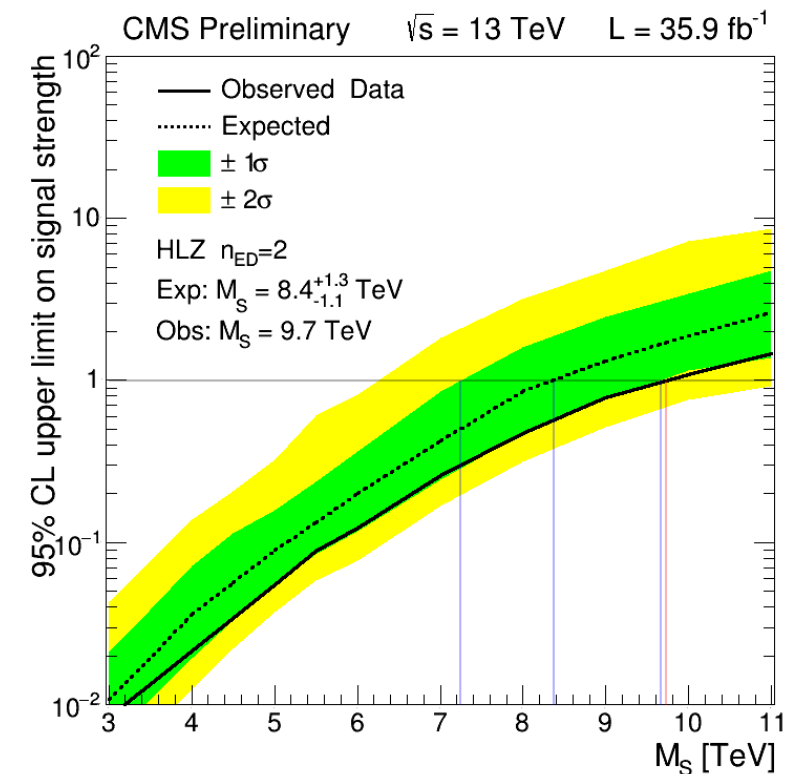
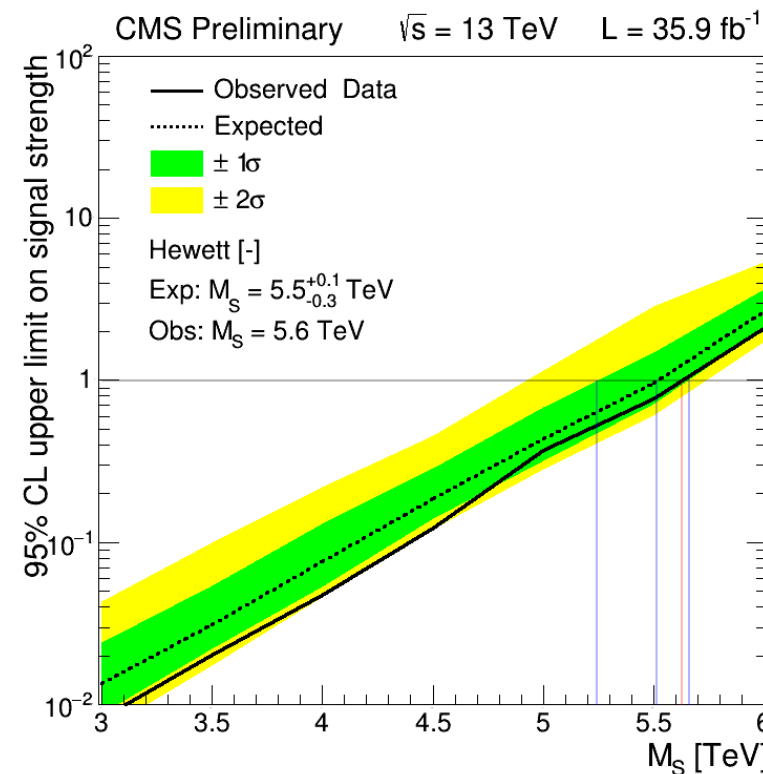
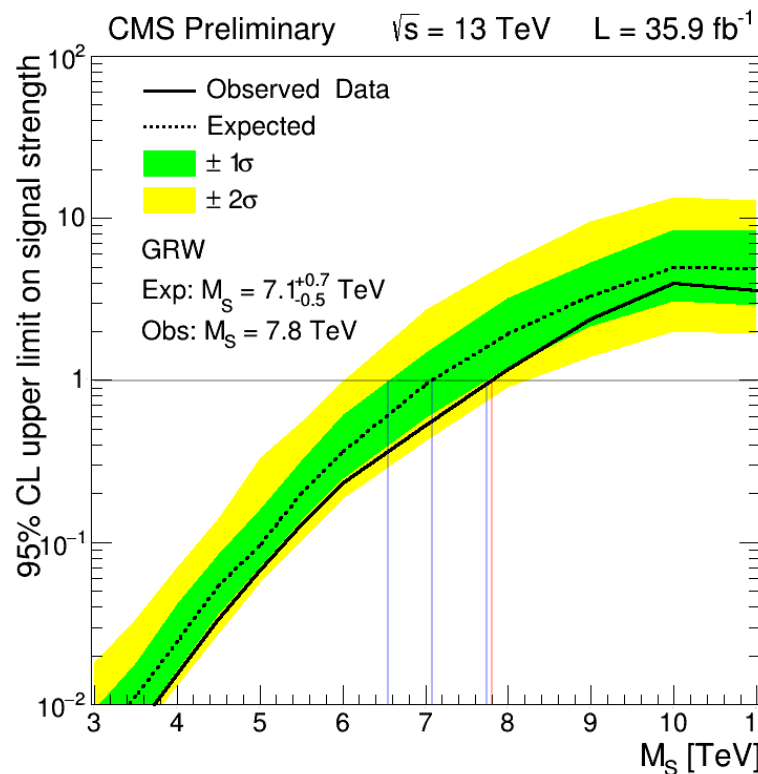
$$0.95 = \frac{\int_0^{\mu_{\text{up}}} P(\mu|n_i) d\mu}{\int_0^\infty P(\mu|n_i) d\mu} = \frac{\int_0^{\mu_{\text{up}}} \mathcal{L}_i(n_i|\mu) d\mu}{\int_0^\infty \mathcal{L}_i(n_i|\mu) d\mu}$$

- Upper limits on the ADD signal strength are translated into lower limits of M_S
 - signal strength 1.0 excluded
- Done separately for GRW, HLZ assuming $n_{ED} = 2$, and Hewett- conventions
 - limits on other conventions achieved using η_G



Limits on ADD model

- Upper limits on the ADD signal strength are translated into lower limits of M_S

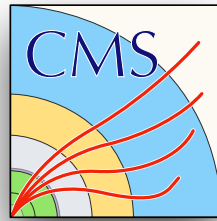


- Exclusion limits on M_S range from 5.6-9.7 TeV

Signal	GRW	Hewett	HLZ						
		negative	positive	$n_{ED} = 2$	$n_{ED} = 3$	$n_{ED} = 4$	$n_{ED} = 5$	$n_{ED} = 6$	$n_{ED} = 7$
Expected	$7.1^{+0.7}_{-0.5}$	$5.5^{+0.1}_{-0.3}$	$6.3^{+0.6}_{-0.4}$	$8.4^{+1.3}_{-1.1}$	$8.4^{+0.8}_{-0.6}$	$7.1^{+0.7}_{-0.5}$	$6.4^{+0.6}_{-0.5}$	$6.0^{+0.6}_{-0.4}$	$5.6^{+0.6}_{-0.4}$
Observed	7.8	5.6	7.0	9.7	9.3	7.8	7.0	6.6	6.2



Conclusion



- A nonresonant, high-mass diphoton search using 35.9 fb^{-1} , corresponding to the full 2016 dataset, was performed with CMS
 - NNLO prediction of the prompt SM diphoton background
 - data-driven estimate of the fake background
- Data are consistent with background-only hypothesis
- Limits set on the ADD model of large extra dimensions
 - exclusion limits on $M_S = 5.6\text{-}9.7 \text{ TeV}$ depending on the cutoff convention
 - improves current best limits by ATLAS (*arXiv: 1707.04147*)
- First CMS nonresonant, high-mass diphoton search done using LHC Run 2 data
 - previous CMS result used 2011 data with $\sqrt{s} = 7 \text{ TeV}$ pp collisions (*arXiv: 1112.0688*)
- Result has been published in PRD
- Extra dimensions are not ruled out, but their solution to the hierarchy problem has been narrowed by this effort

PHYSICAL REVIEW D 98, 092001 (2018)

Search for physics beyond the standard model in high-mass diphoton events from proton-proton collisions at $\sqrt{s}=13 \text{ TeV}$

A. M. Sirunyan *et al.**
(CMS Collaboration)

(Received 1 September 2018; published 2 November 2018)

A search for physics beyond the standard model is performed using a sample of high-mass diphoton events produced in proton-proton collisions at $\sqrt{s} = 13 \text{ TeV}$. The data sample was collected in 2016 with the CMS detector at the LHC and corresponds to an integrated luminosity of 35.9 fb^{-1} . The search is performed for both resonant and nonresonant new physics signatures. At 95% confidence level, lower limits on the mass of the first Kaluza-Klein excitation of the graviton in the Randall-Sundrum warped extra-dimensional model are determined to be in the range of 2.3 to 4.6 TeV , for values of the associated coupling parameter between 0.01 and 0.2 . Lower limits on the production of scalar resonances and model-independent cross section upper limits are also provided. For the large extra-dimensional model of Arkani-Hamed, Dimopoulos, and Dvali, lower limits are set on the string mass scale M_S ranging from 5.6 to 9.7 TeV , depending on the model parameters. The first exclusion limits are set in the two-dimensional parameter space of a continuum clockwork model.

DOI: 10.1103/PhysRevD.98.092001

I. INTRODUCTION

While the standard model (SM) of particle physics has been an enormously successful description of observed phenomena, it is still widely believed to be incomplete. In the SM, the Higgs boson mass receives quantum corrections from loops containing SM particles. Because the Higgs boson is a fundamental scalar, the magnitude of the mass corrections is set by the cutoff parameter of the loop integrals and the only natural mass scale in the SM that can act as a cutoff is the Planck scale ($M_{\text{Pl}} \sim 10^{19} \text{ GeV}$) at which quantum gravity is expected to emerge. Therefore, unless the Higgs boson mass parameter is fine-tuned to an extreme degree, there must exist some new physics beyond the SM to constrain these quantum corrections and stabilize the mass of the Higgs boson. Many models for such new physics have been proposed. We consider three such models in this paper.

Through their modification of the effective Planck scale, extra spatial dimensions have been proposed as a possible solution to this hierarchy problem [1,2], which arises from the large difference between the gravitational and electroweak scales. In the model proposed by Arkani-Hamed, Dimopoulos, and Dvali (ADD) [3–5], the existence of n_{ED}

*Full author list given at the end of the article.

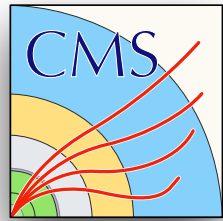
Published by the American Physical Society under the terms of the Creative Commons Attribution 4.0 International license. Further distribution of this work must maintain attribution to the author(s) and the published article's title, journal citation, and DOI. Funded by SCOAP³.

2470-0010/2018/98(9)/092001(26) 092001-1 © 2018 CERN, for the CMS Collaboration

Phys. Rev. D **98**, 092001 (2018)
arXiv:1809.00327 [hep-ex]



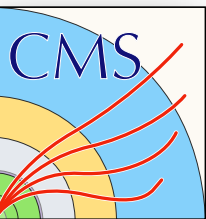
Thank you



*Thank you to the many
friends, family, teachers, mentors,
officemates, roommates, and collaborators,
all having an enormous impact during my
time as a graduate student*



Backup



LHC fill decay

LHC Page1 Fill: 5849 E: 6499 GeV t(SB): 01:06:32 20-06-17 16:34:56

PROTON PHYSICS: STABLE BEAMS

Energy: 6499 GeV I(B1): 2.20e+14 I(B2): 2.24e+14

Inst. Lumi [(ub.s)⁻¹] IP1: 11145.83 IP2: 2.51 IP5: 11087.13 IP8: 333.13

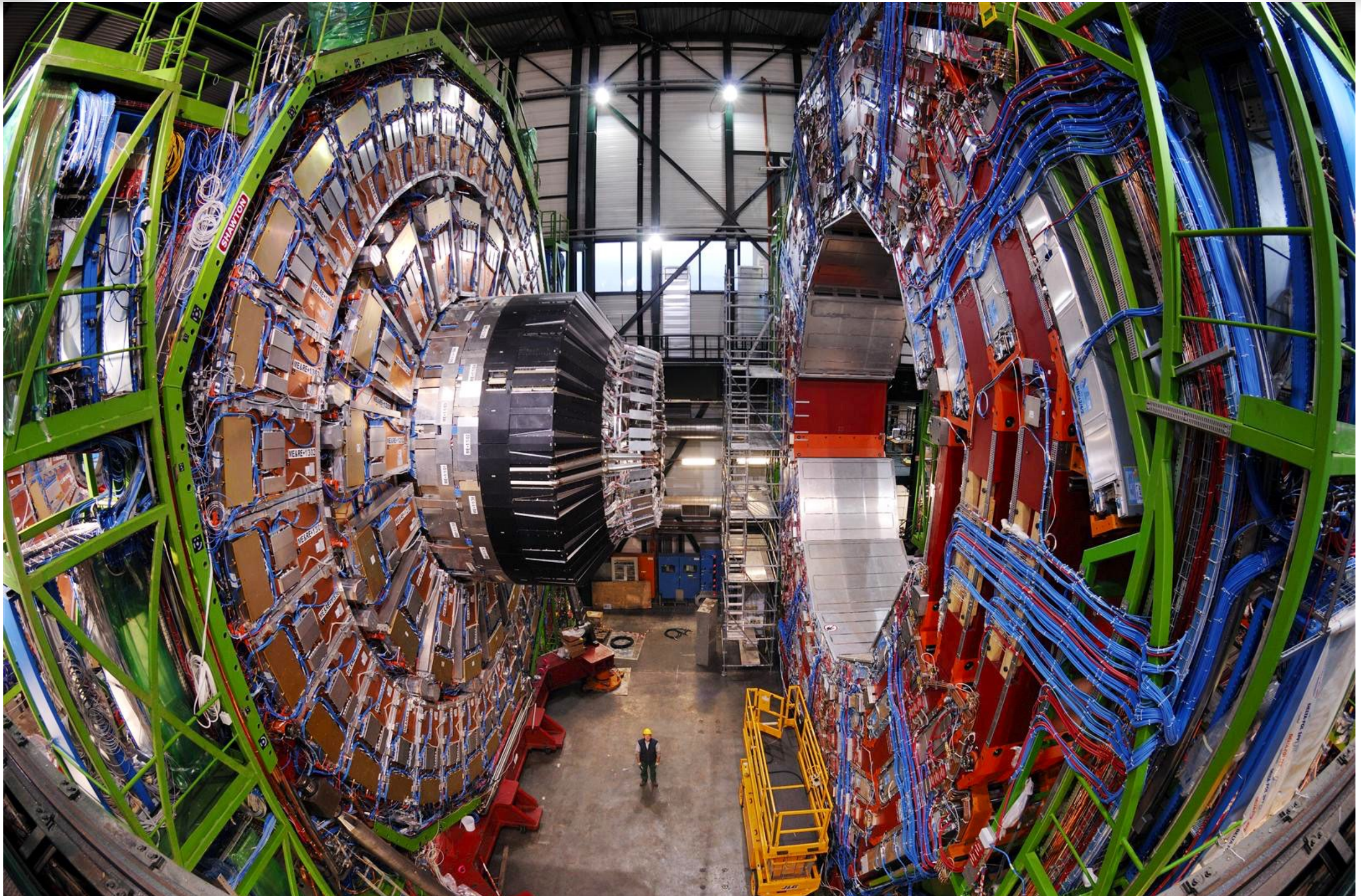
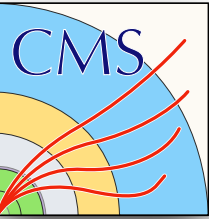
FBCT Intensity and Beam Energy Updated: 16:34:55 Instantaneous Luminosity Updated: 16:34:55

BIS status and SMP flags		B1	B2
Comments (20-Jun-2017 14:16:05)	Link Status of Beam Permits	true	true
Filling for physics with 2029b	Global Beam Permit	true	true
	Setup Beam	false	false
	Beam Presence	true	true
	Moveable Devices Allowed In	true	true
	Stable Beams	true	true

AFS: 25ns_2029b_2017_1776_1860_144bpi_17inj PM Status B1: ENABLED PM Status B2: ENABLED

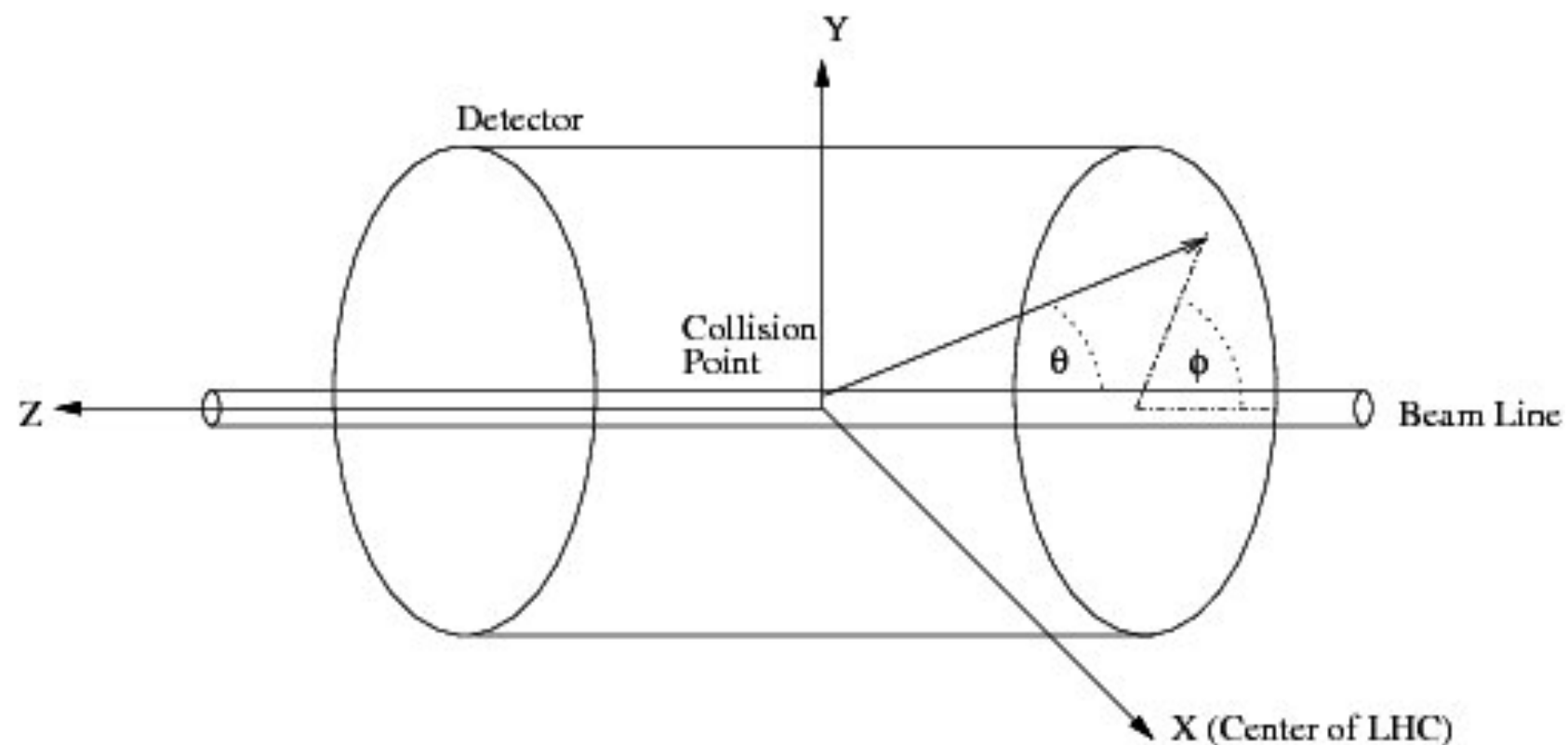
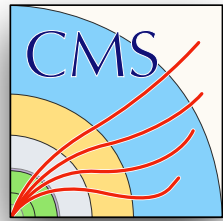


Compact Muon Solenoid



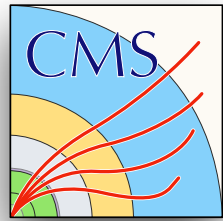


CMS coordinate system

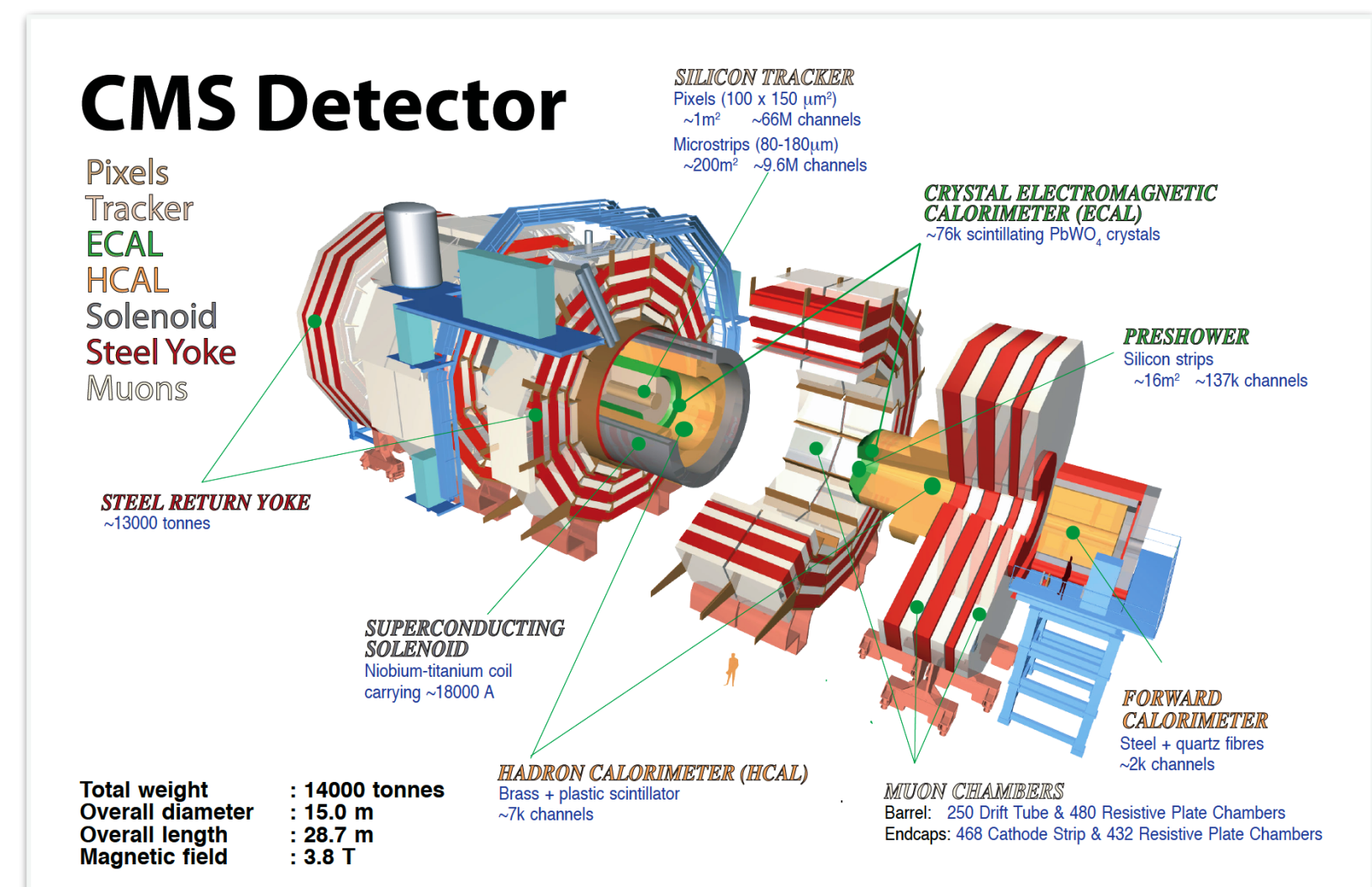




Hadron calorimeter

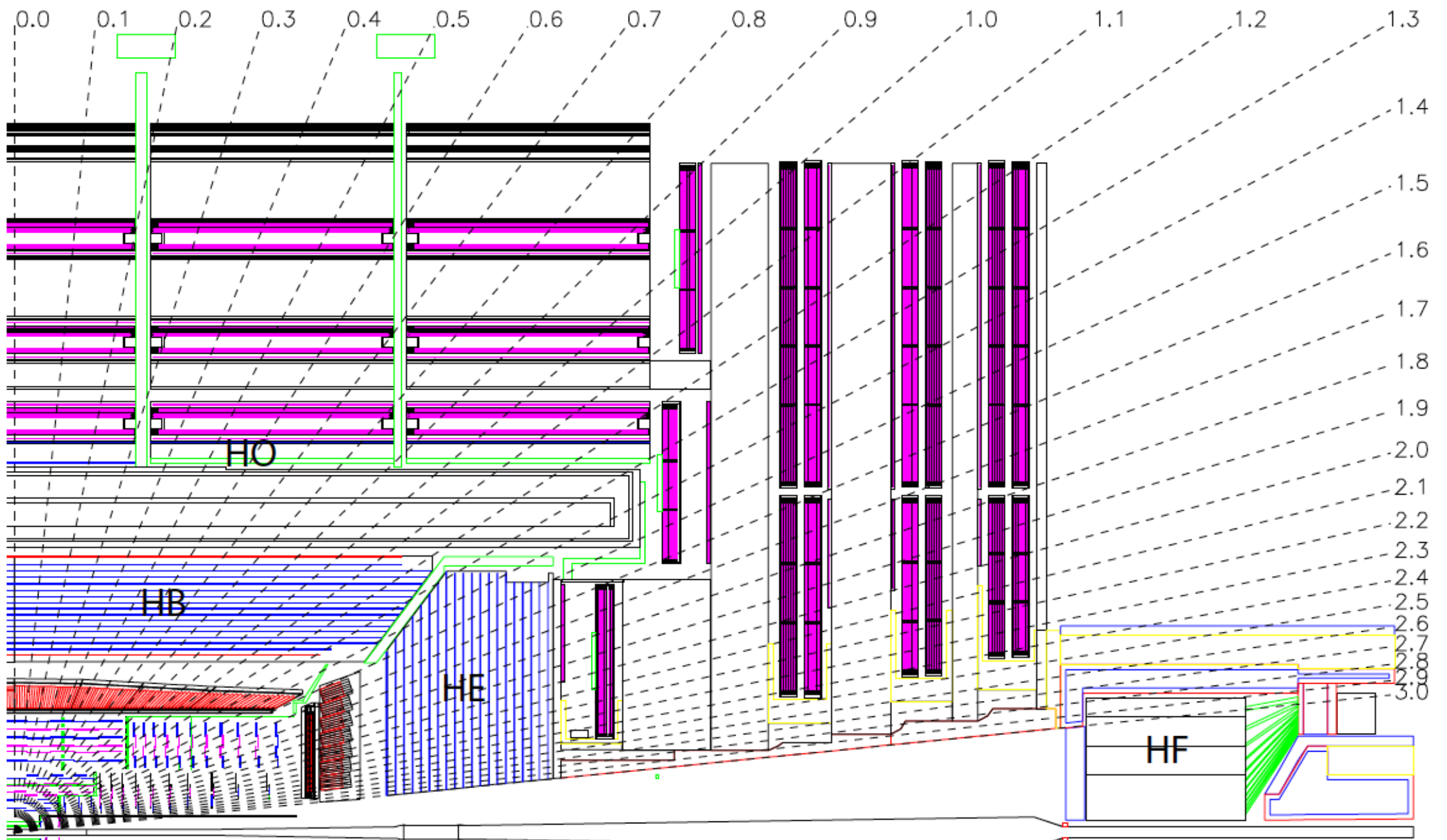


- Hadron Calorimeter (**HCAL**) detector
 - sampling calorimeter
 - barrel-endcap design located inside the CMS solenoid and outside of the tracker and Electromagnetic Calorimeter (ECAL)
 - separate outer and forward detectors
 - 4 sub-detectors
- Hadron Barrel (**HB**), Hadron Endcap (**HE**)
 - Brass absorber, plastic scintillator tiles
 - HPD photodetectors
- Hadron Outer (**HO**)
 - Outside solenoid
 - barrel section only
 - uses steel/iron absorber
 - hadron shower “tail catcher”
 - SiPM photodetectors
- Hadron Forward (**HF**)
 - Steel absorber, quartz fibers
 - high radiation
 - PMT photodetectors



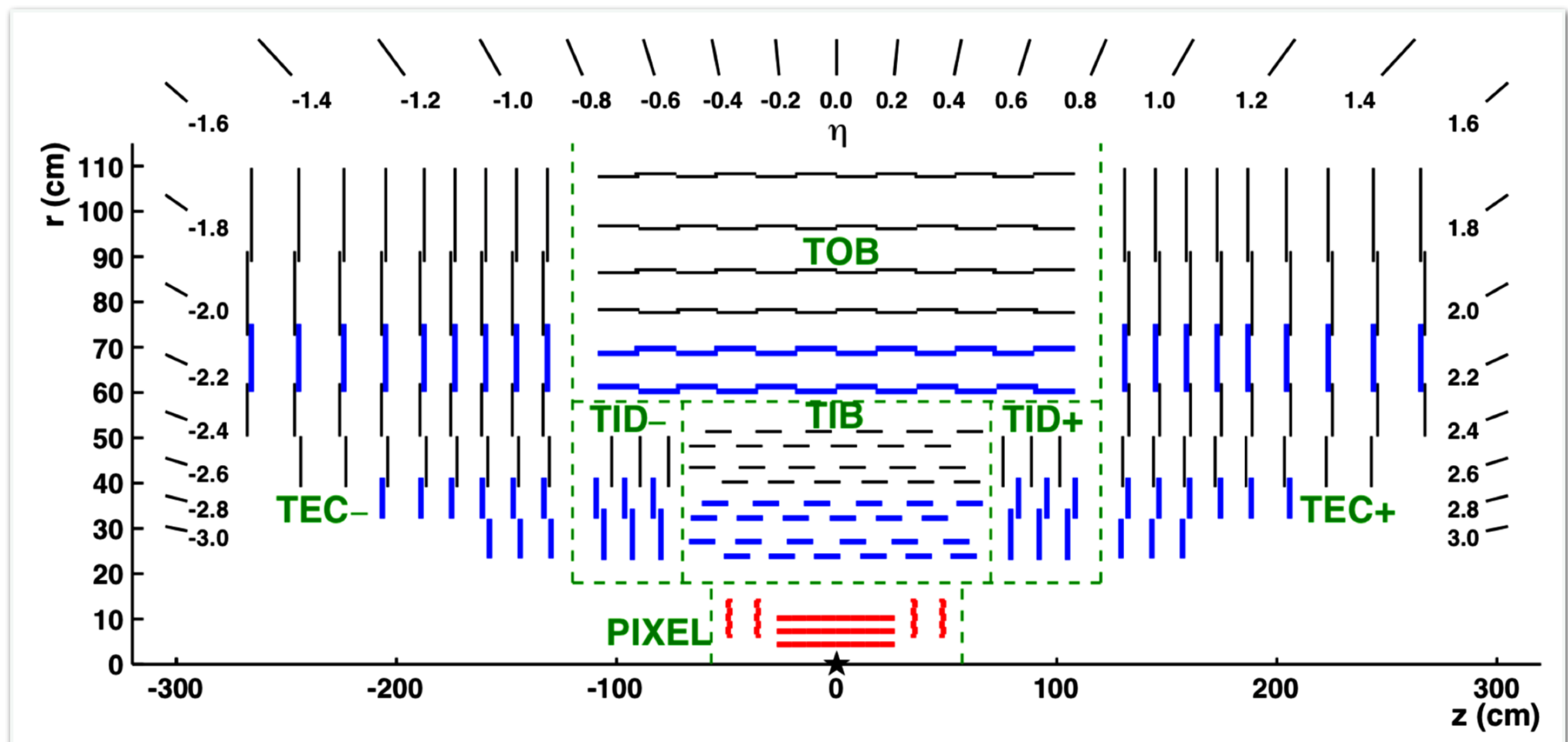
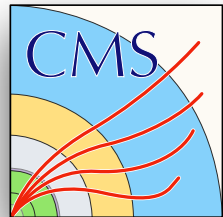


HICAL detailed view



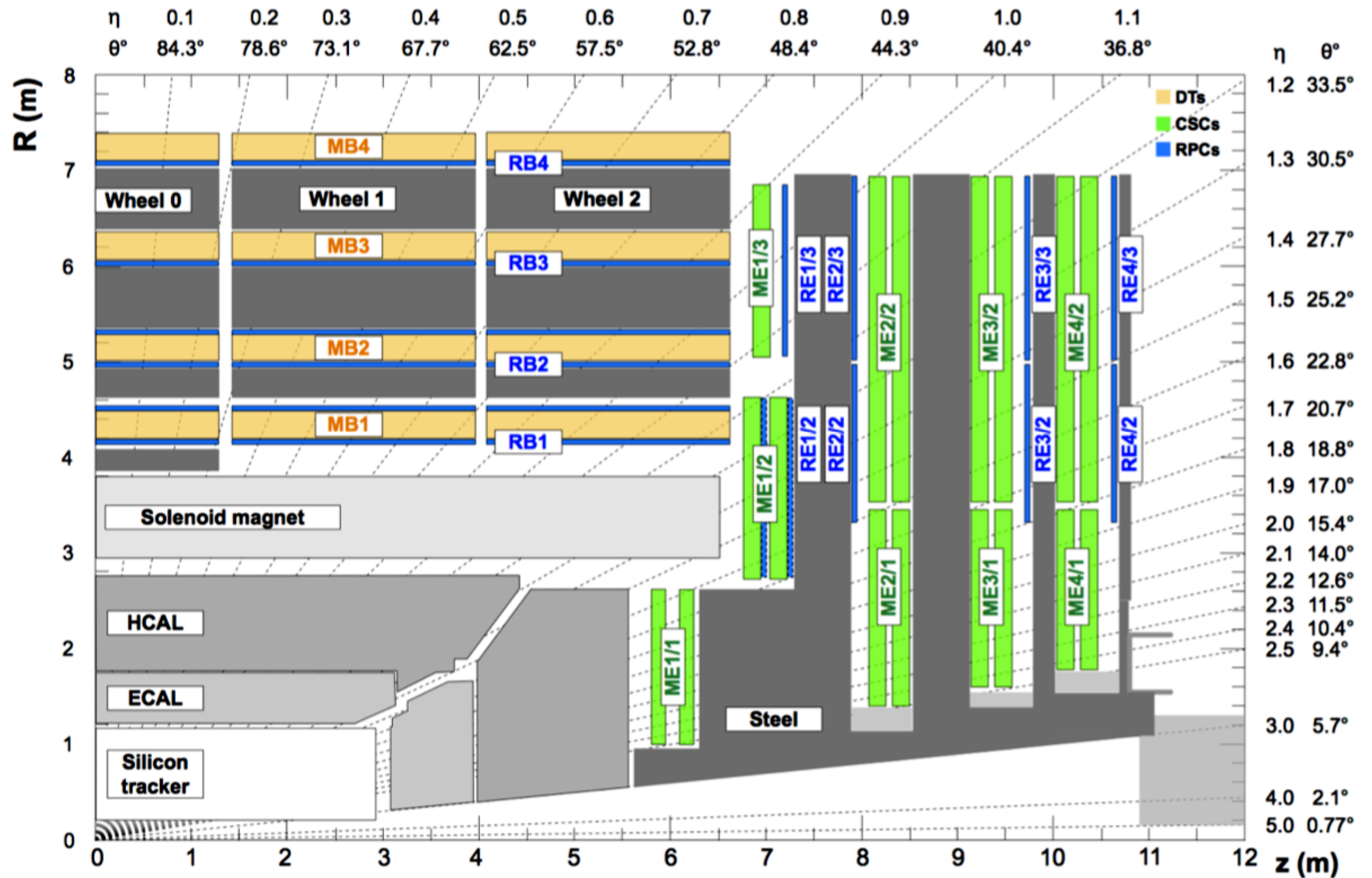


CMS tracking system



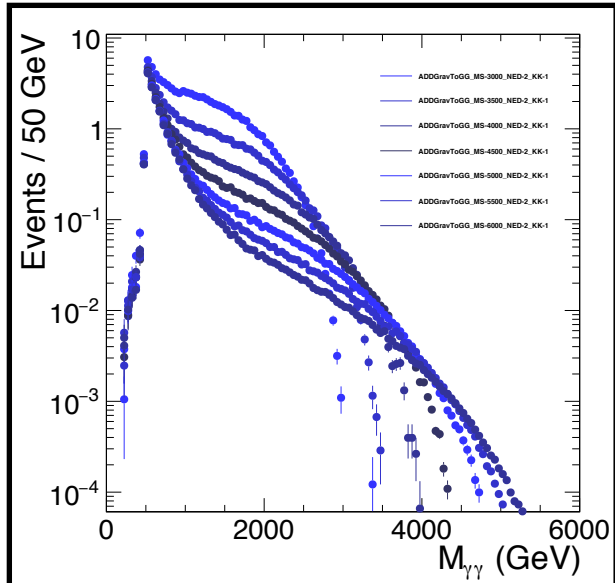
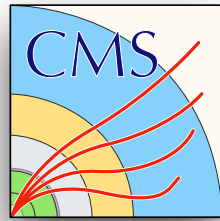


CMS muon system



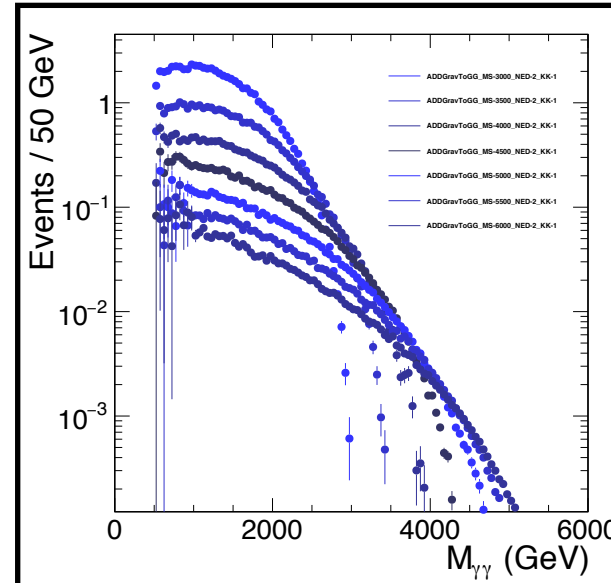


ADD signal model

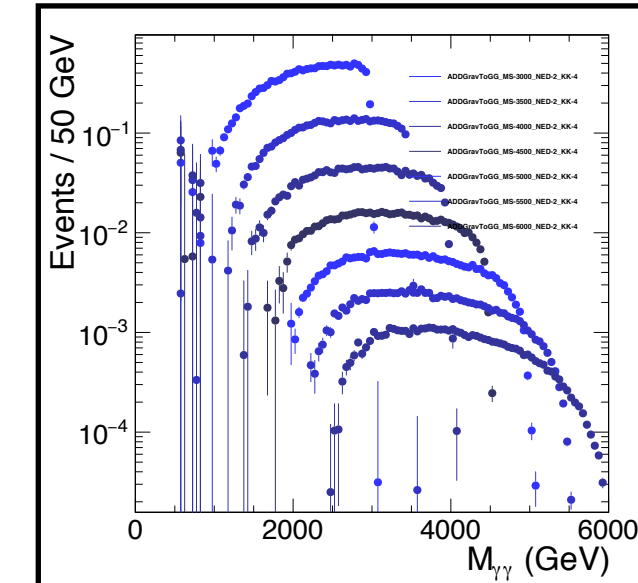


signal+background

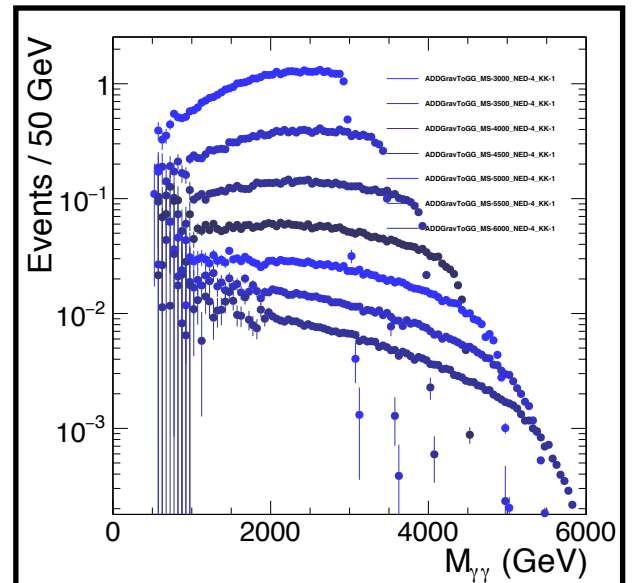
HLZ ($n_{ED} = 2$)



signal



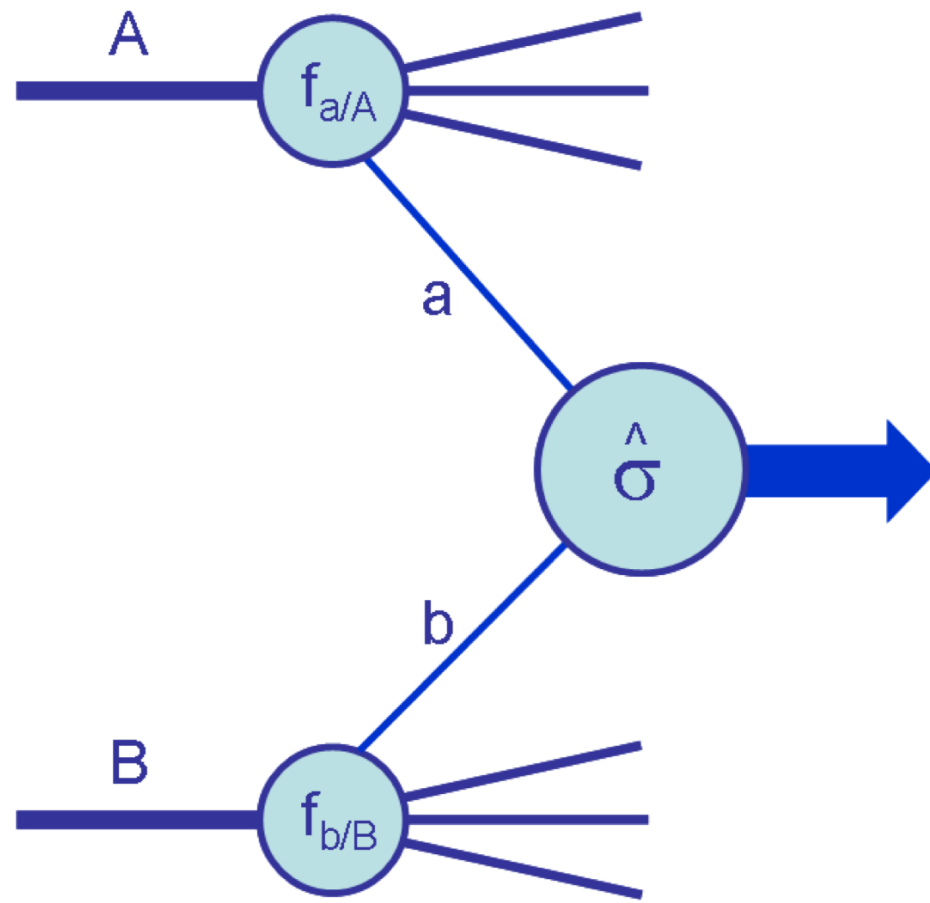
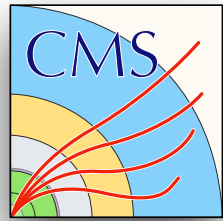
signal
Hewett-



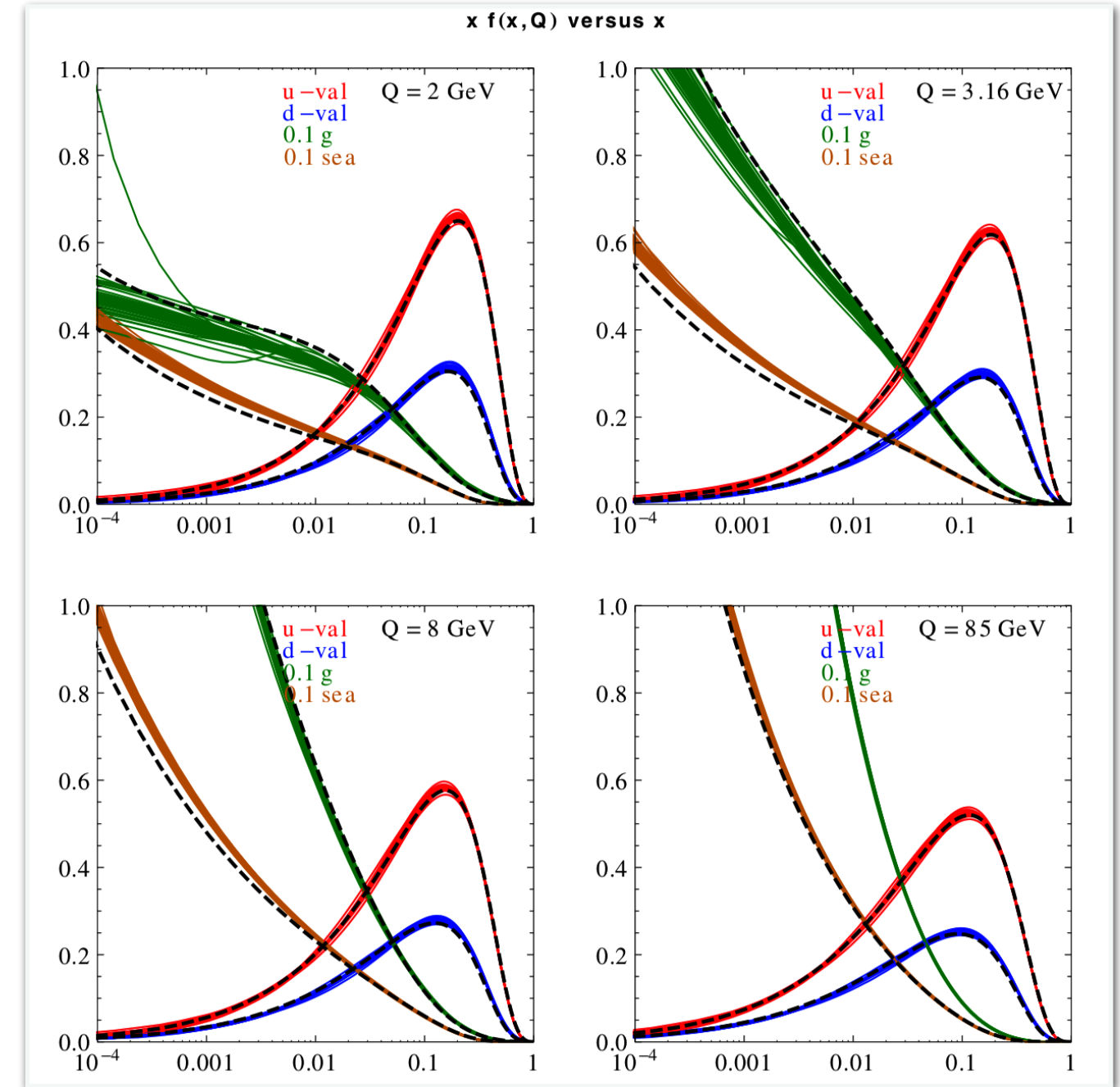
signal
GRW



PDF set

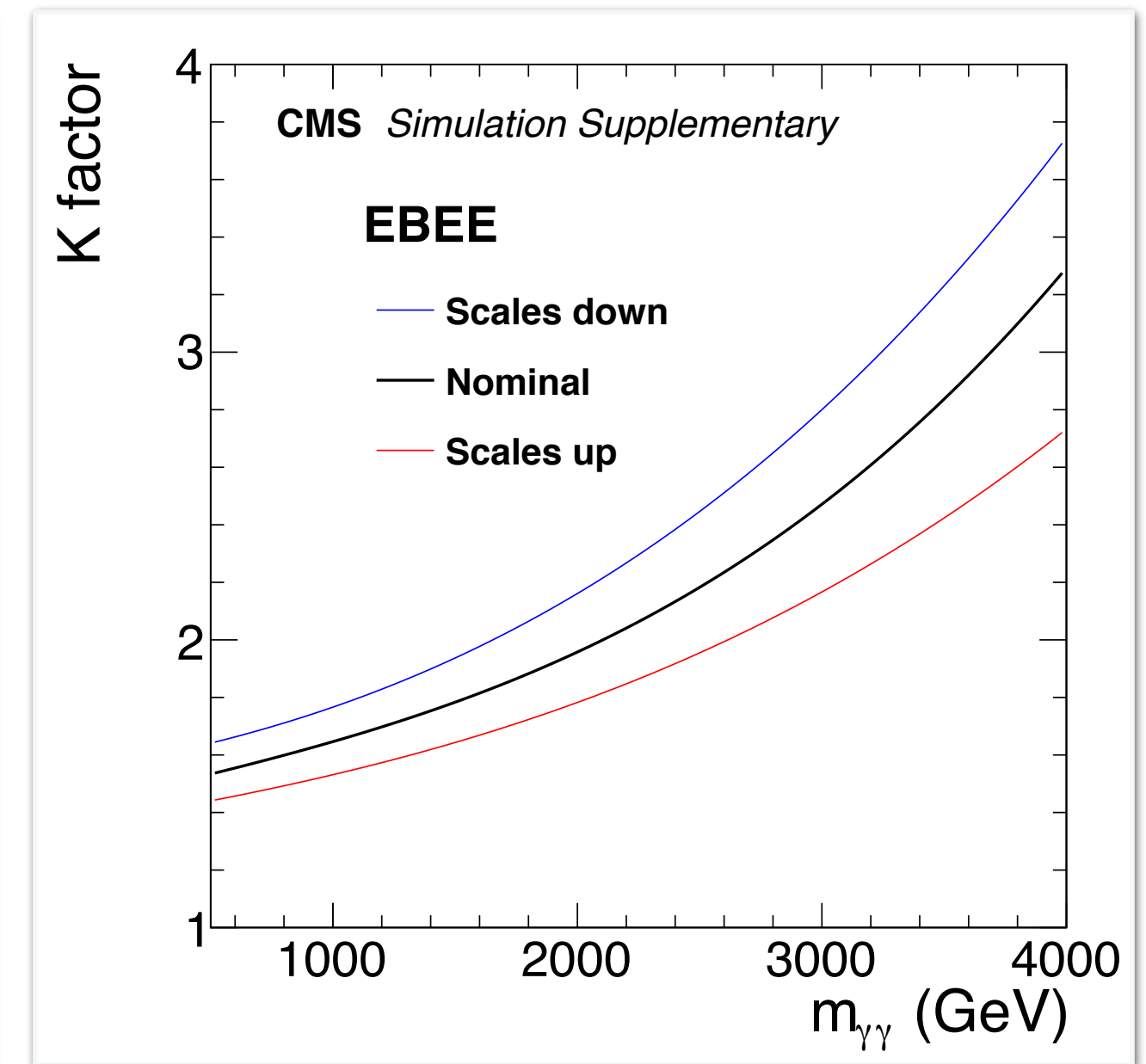
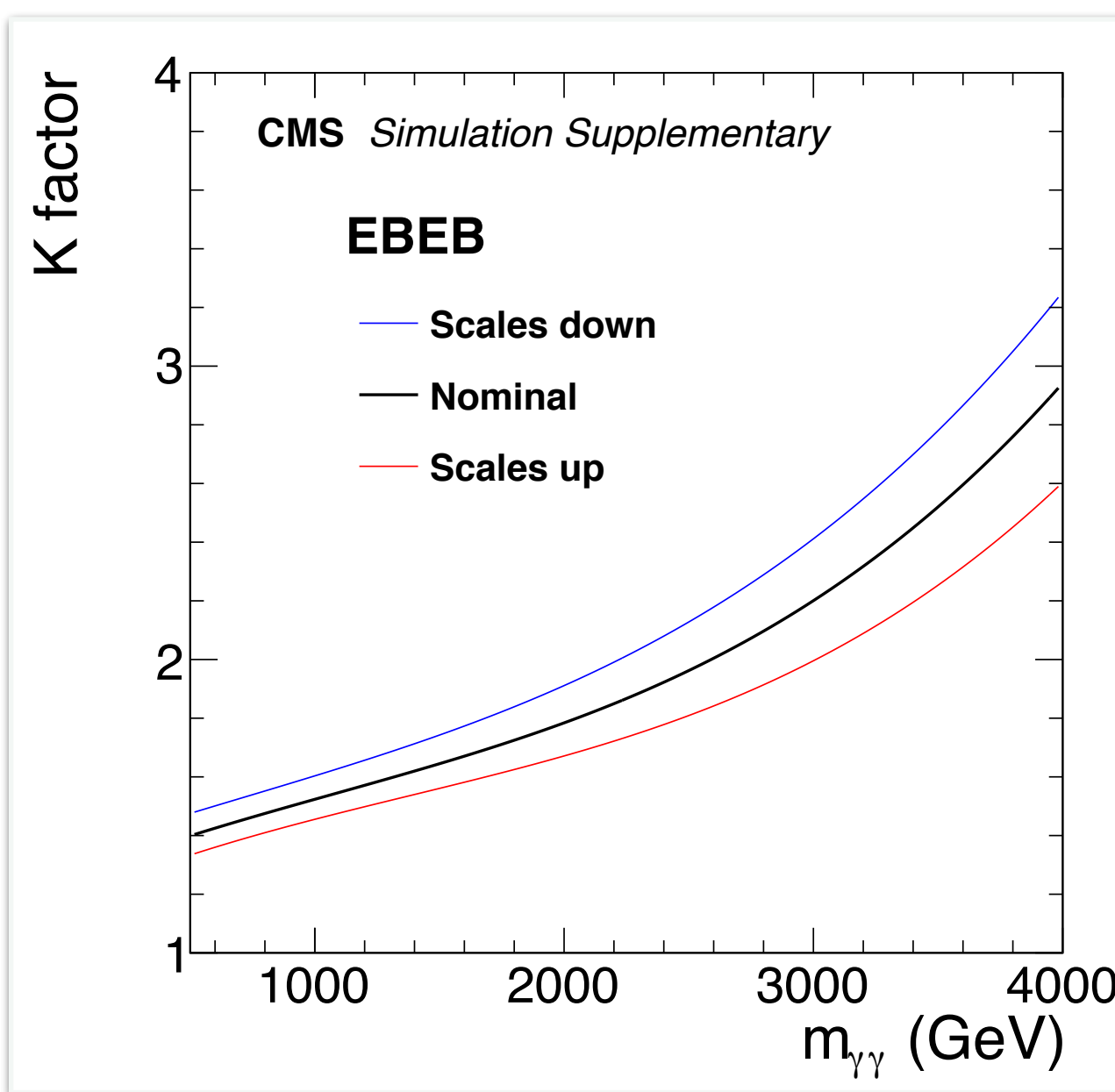
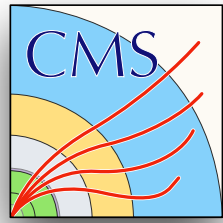


$$\sigma_{AB \rightarrow X} = \sum_{a,b} \int dx_a dx_b f_{a/A}(x_a, \mu_f^2) f_{b/B}(x_b, \mu_f^2) \hat{\sigma}_{ab \rightarrow X}$$



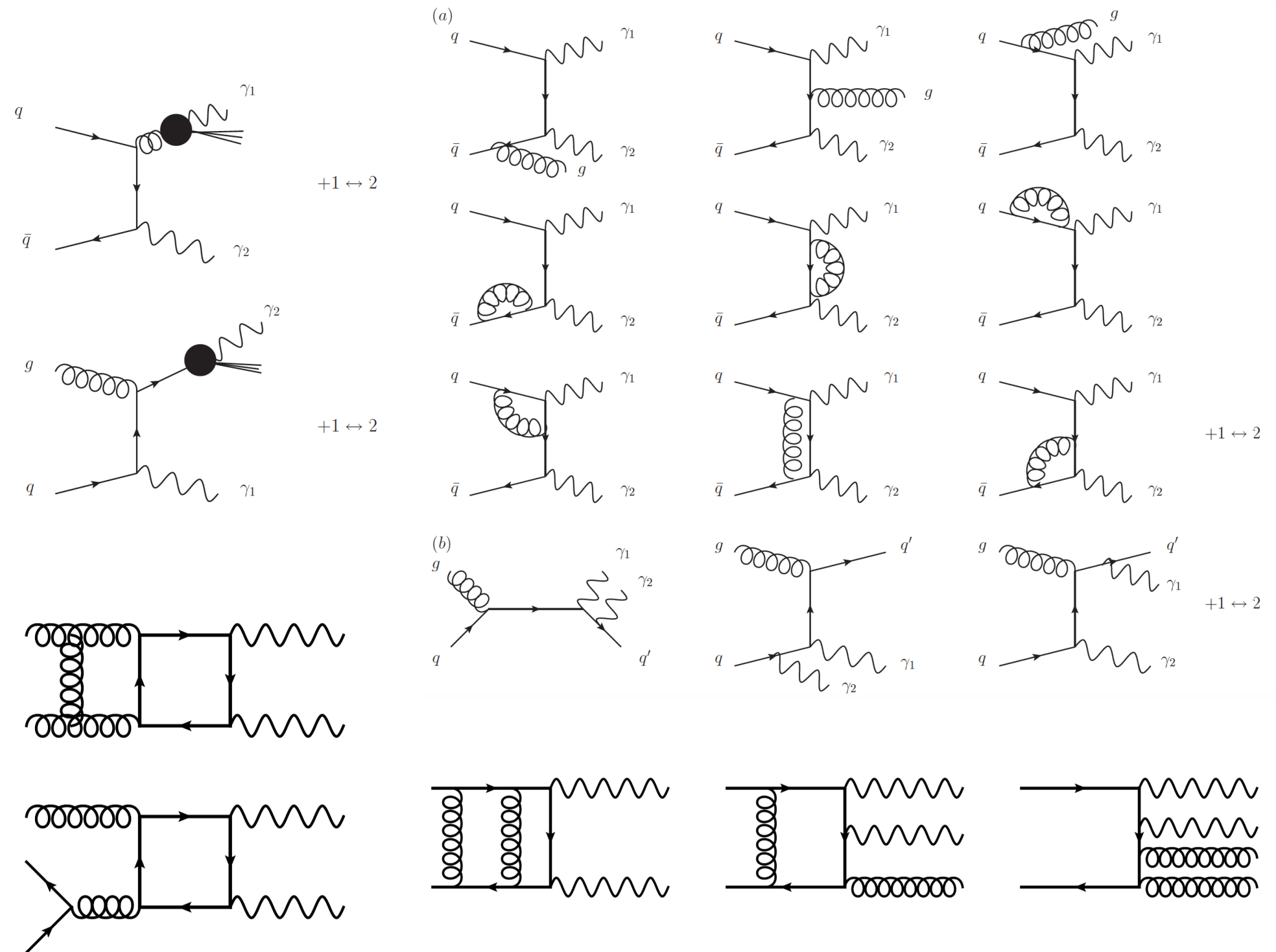
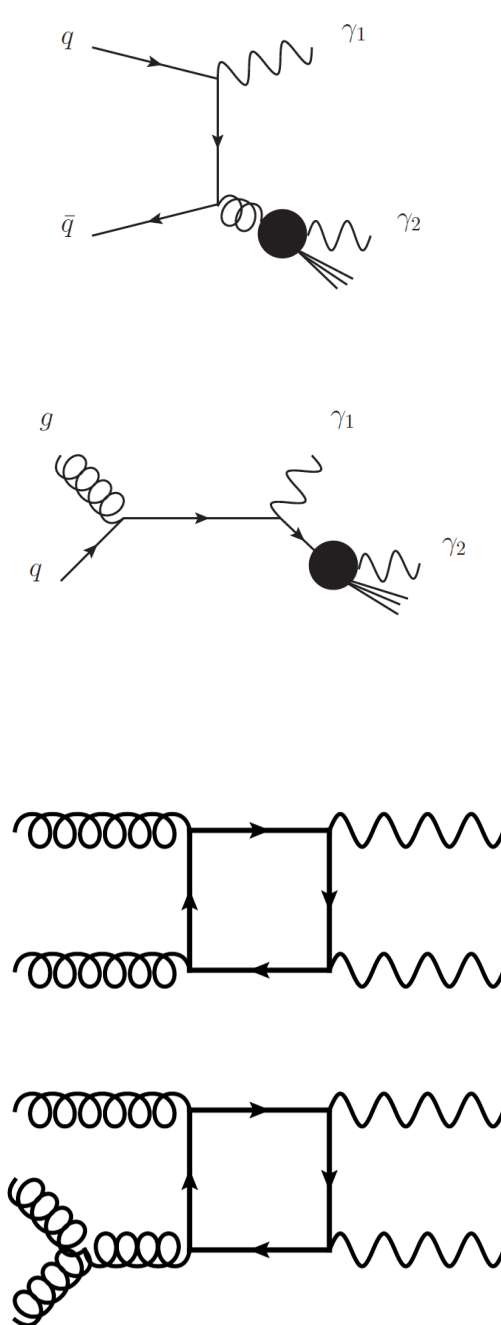
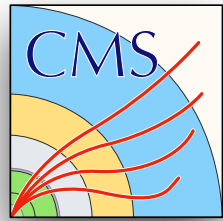


K factor variation



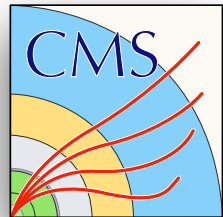


SM diphoton diagrams

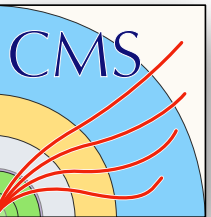




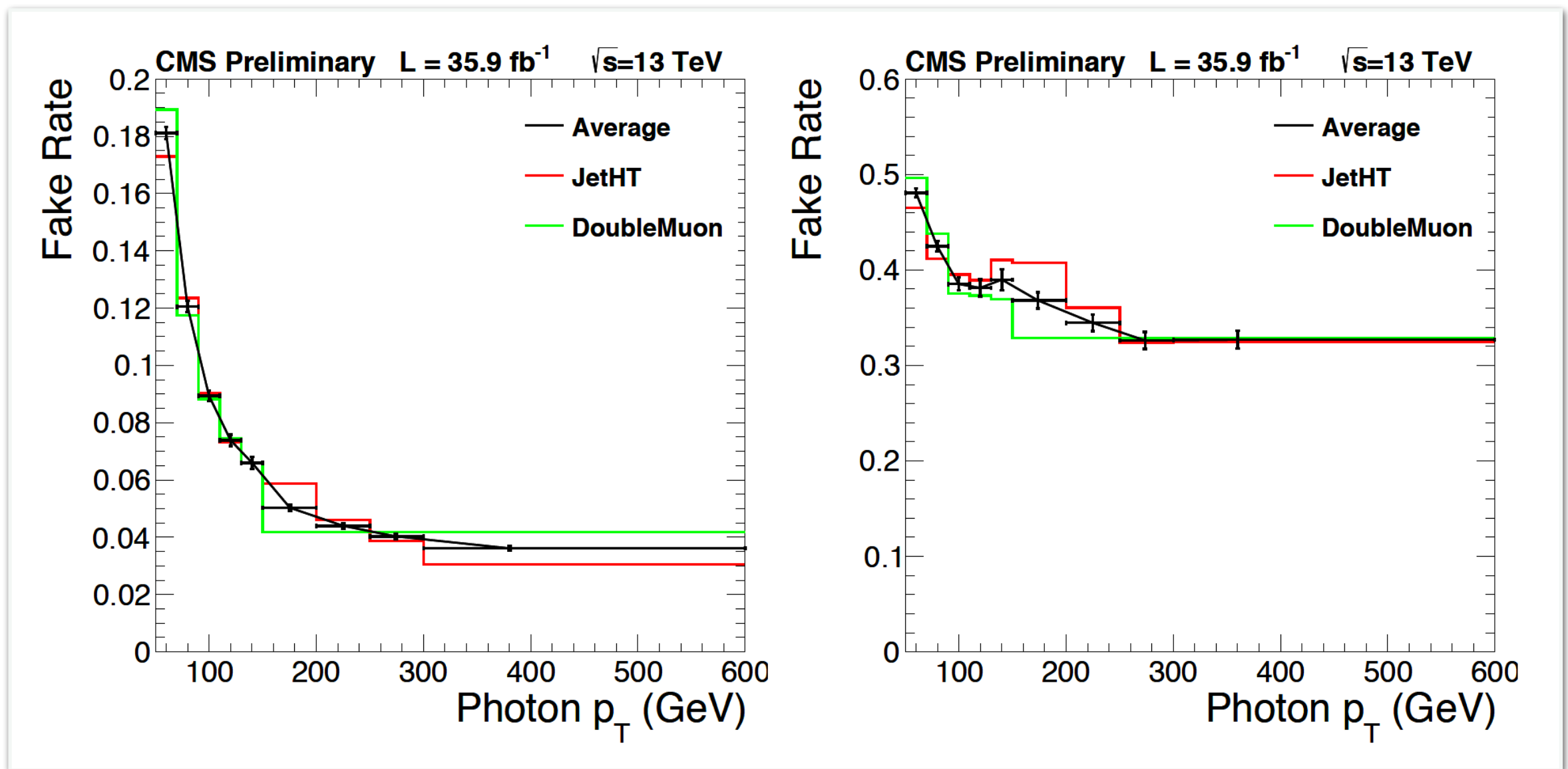
Fake rate definitions



Cut [EB {sat.} (EE {sat.})]	Photon ID	Num.	Real template	Fake template	Denom. (EB)	Denom. (EE)
Photon ID cuts						
H/E < 0.05	pass	pass	pass	pass		
$\sigma_{in\eta} < 0.0105 \{0.0112\} (0.028 \{0.030\})$	pass	template	template	template		
IsoCh < 5 GeV	pass	pass	pass	not applied	fail at least one	fail at least one
$\overline{\text{Iso}}_\gamma < 2.75 (2.00) \text{ GeV}$	pass	pass	pass	pass		pass
$R_9 > 0.8$	pass	pass	pass	pass	pass	pass
Electron veto						
CSEV	pass	pass	pass	pass	pass	pass
Additional fake rate cuts						
$\sigma_{i\phi i\phi} > 0.009$	not applied	pass	pass	pass	pass	pass
$5 < \text{IsoCh} < 10 \text{ GeV}$	not applied	not applied	not applied	pass	not applied	not applied
Hadronic/E < 0.1	not applied	not applied	not applied	not applied	pass	pass
$\text{IsoCh} < 0.2 p_T$	not applied	not applied	not applied	not applied	pass	pass
$\overline{\text{Iso}}_\gamma < 0.2 p_T$	not applied	not applied	not applied	not applied	pass	not applied

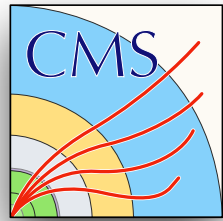


Fake rate

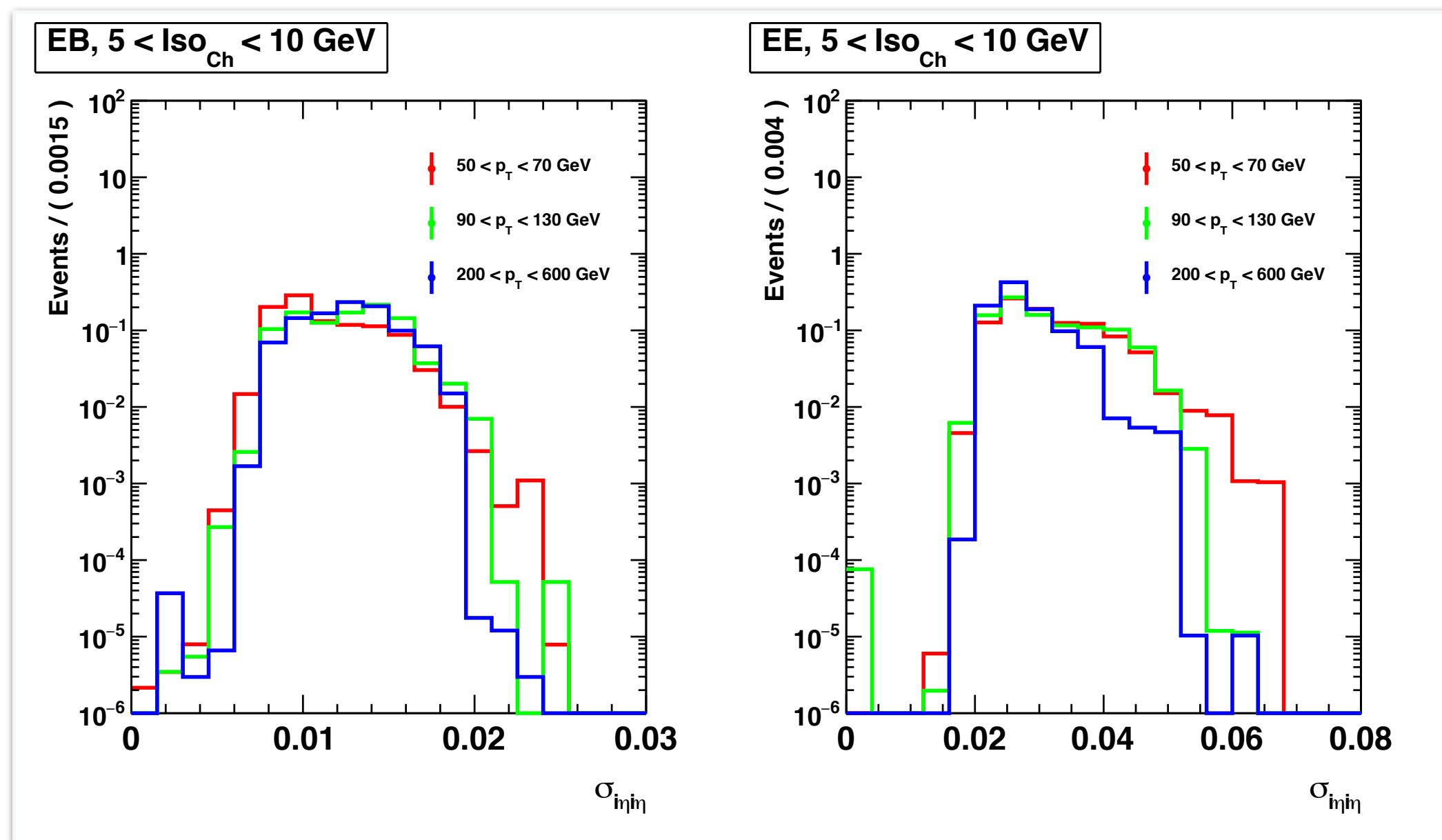


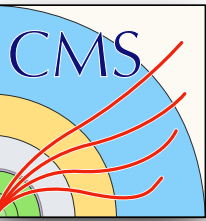


MC fake templates vs. p_T



- Fake templates have dependence on photon p_T , so we perform the method in photon p_T bins

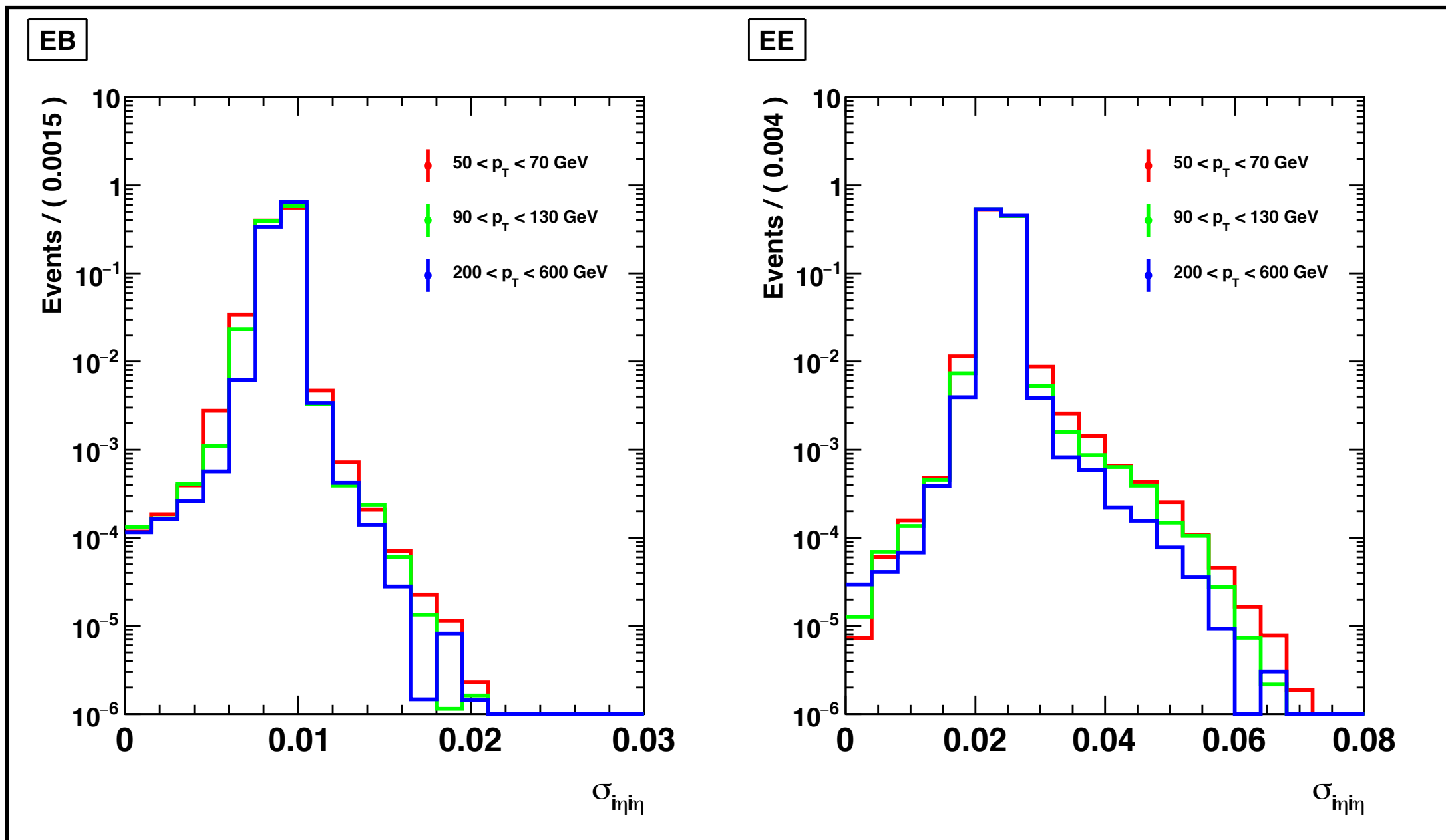


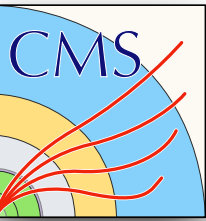


Real templates

- Real templates taking from photon rich MC
- Templates has dependence on photon p_T

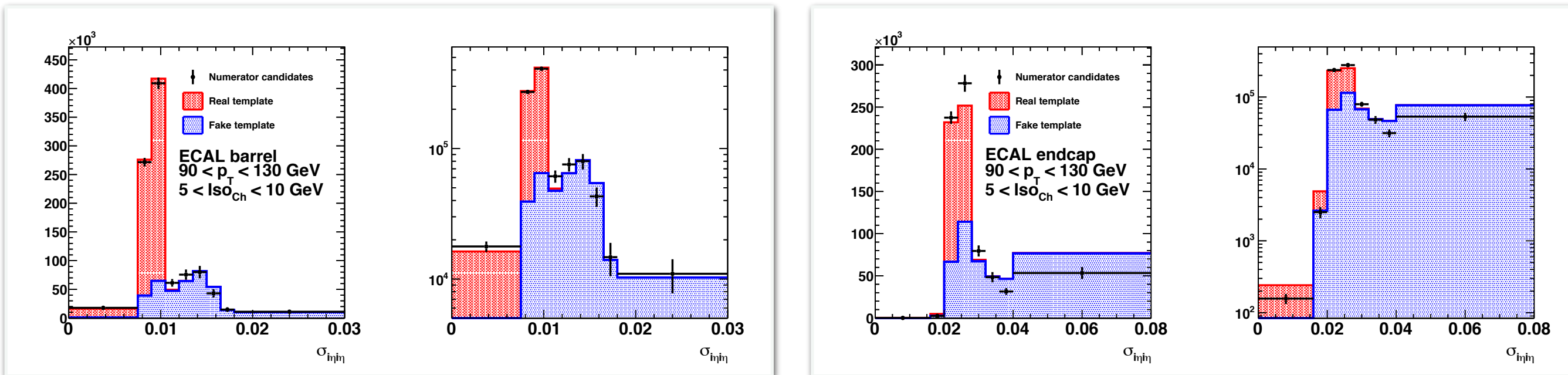
$\sigma_{i\eta i\eta}$
templates



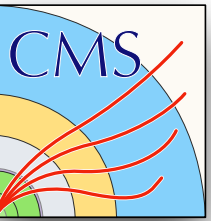


MC template fits

- Numerator obtain after integrating the post template fits in each p_T bin for EB and EE separately

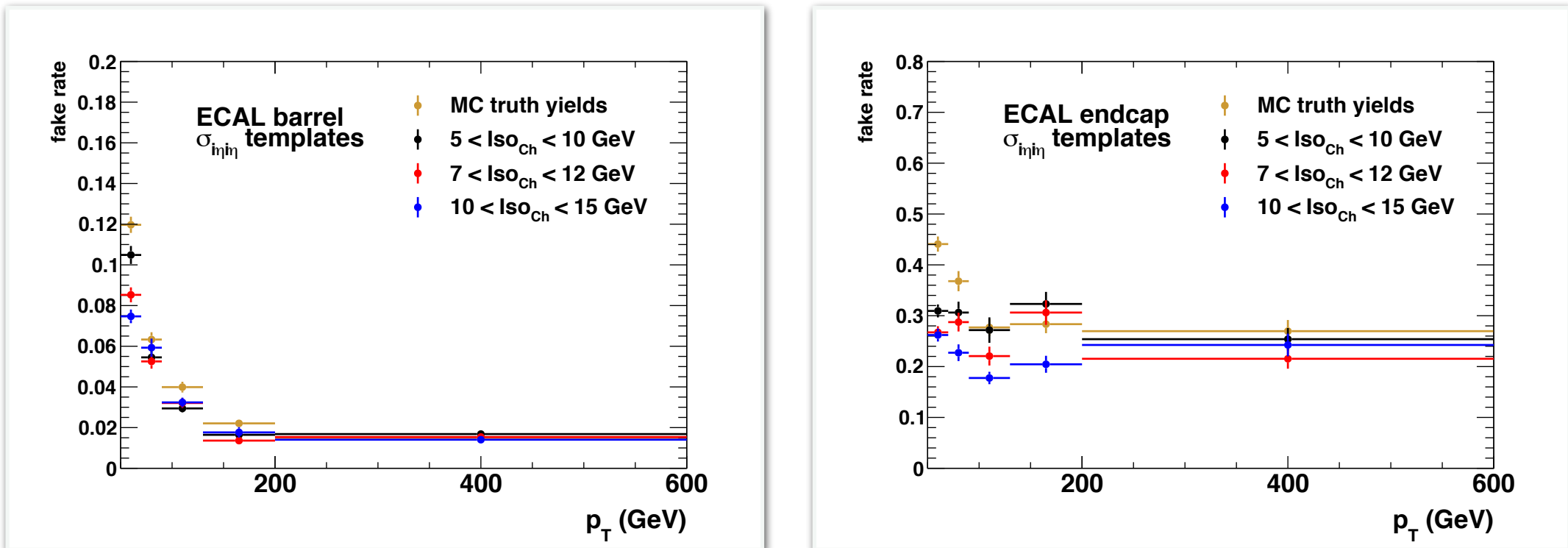


- Count number of object passing denominator definition in each p_T bin to form fake rate

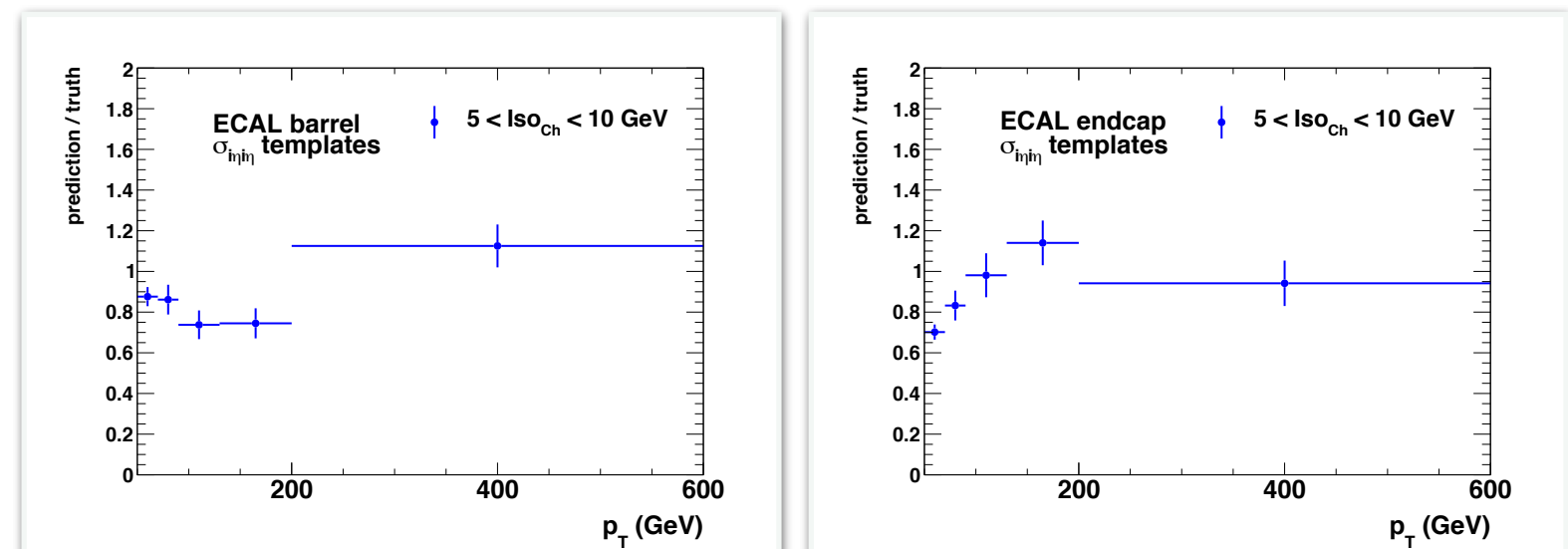


MC fake rates and closure test

- MC fake rates compared to MC truth

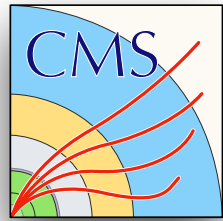


- Closure test predicted fake rate compared to truth fake rate

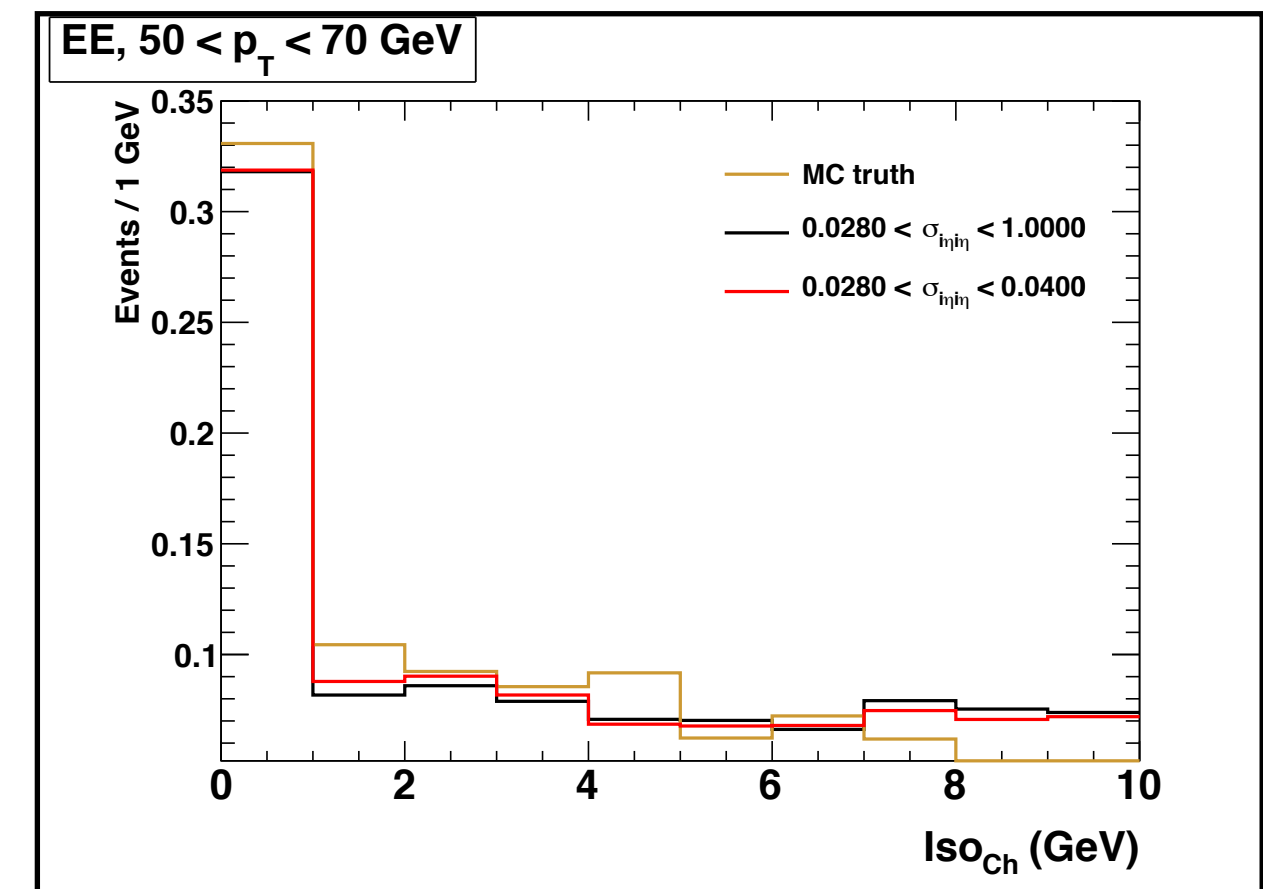
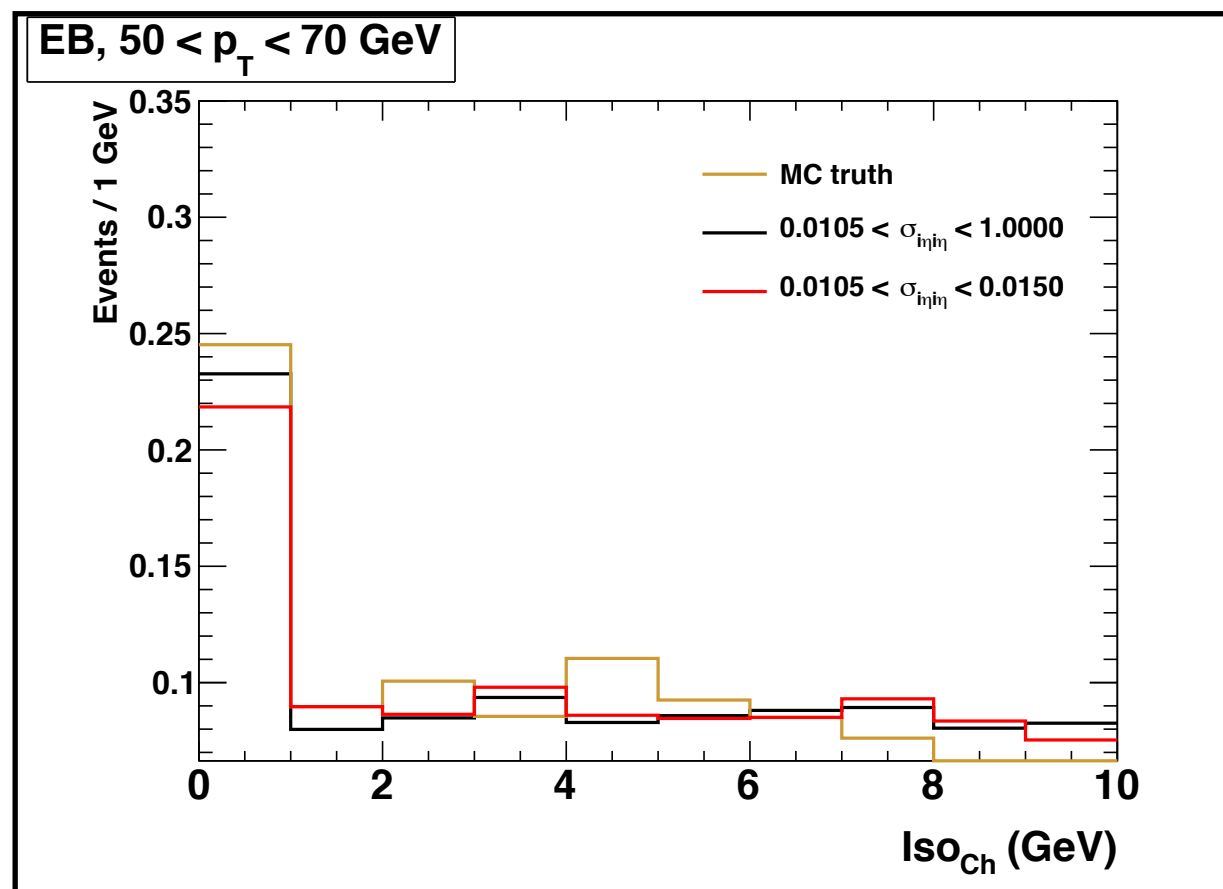




MC IsoCh fake templates

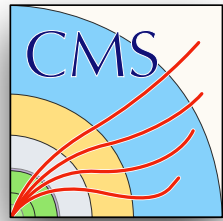


- One systematic can be studied by inverting the template and sideband variables
- Now use
 - template variable $IsoCh$
 - sideband variable $\sigma_{inj\eta}$

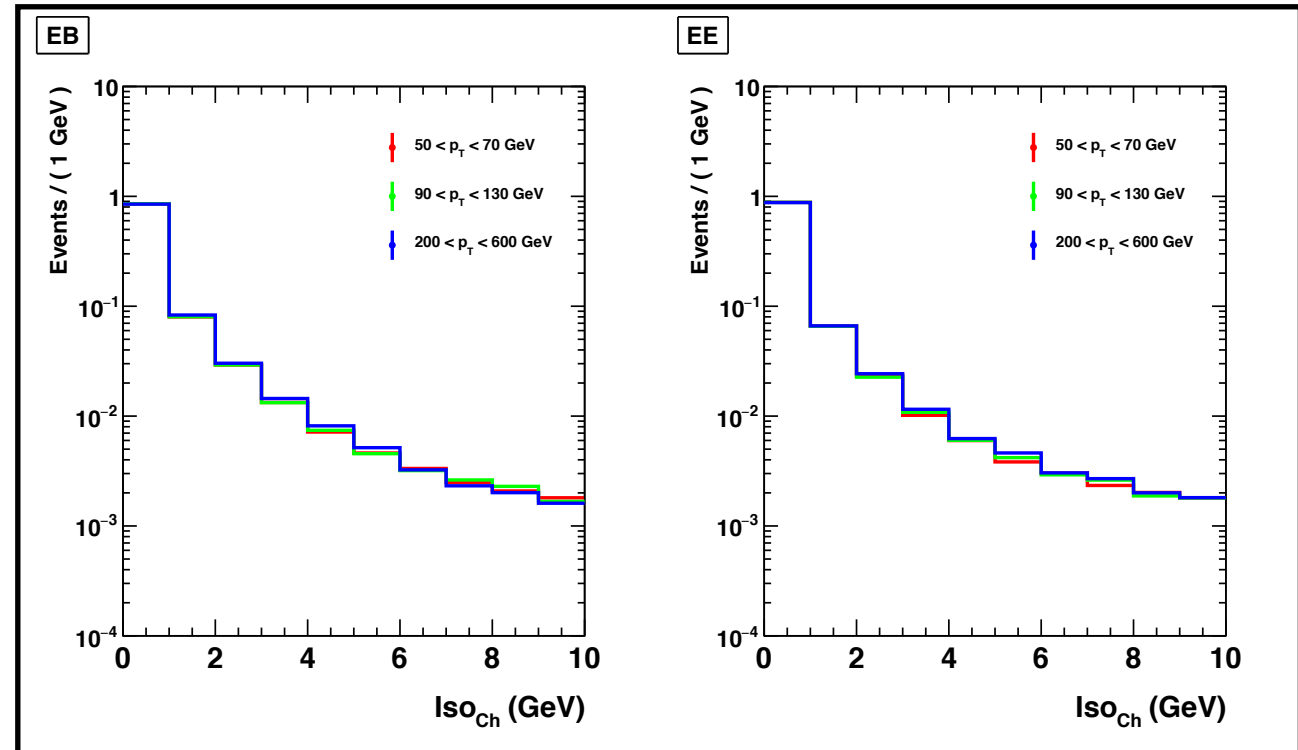




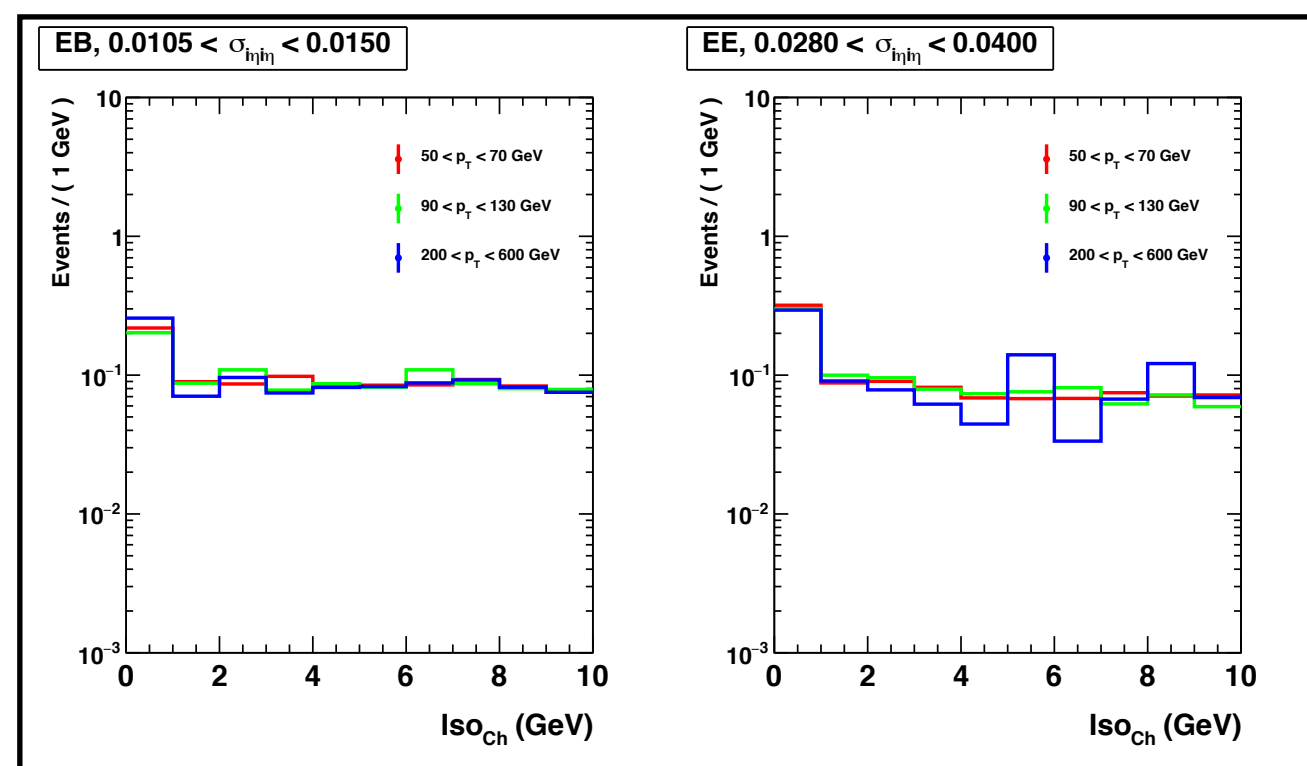
MC IsoCh templates vs. p_T



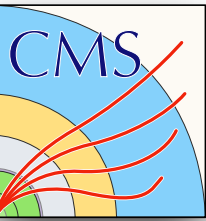
- One nice feature,
no dependence
on p_T



IsoCh
fake templates

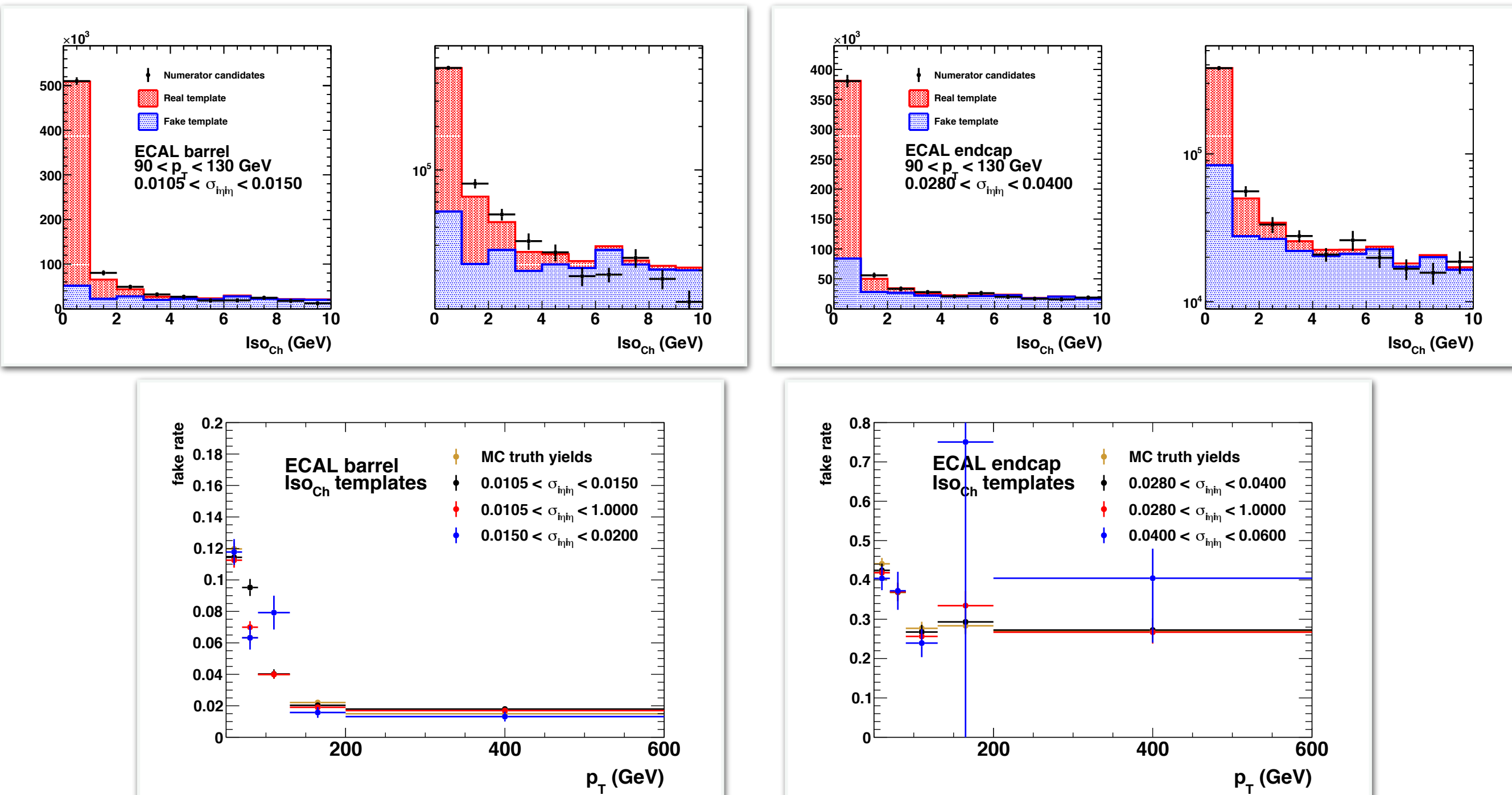


IsoCh
real templates



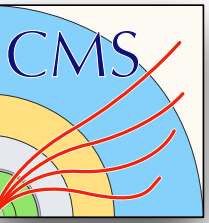
MC IsoCh template fits

- MC template fit example and MC fake rate with MC truth

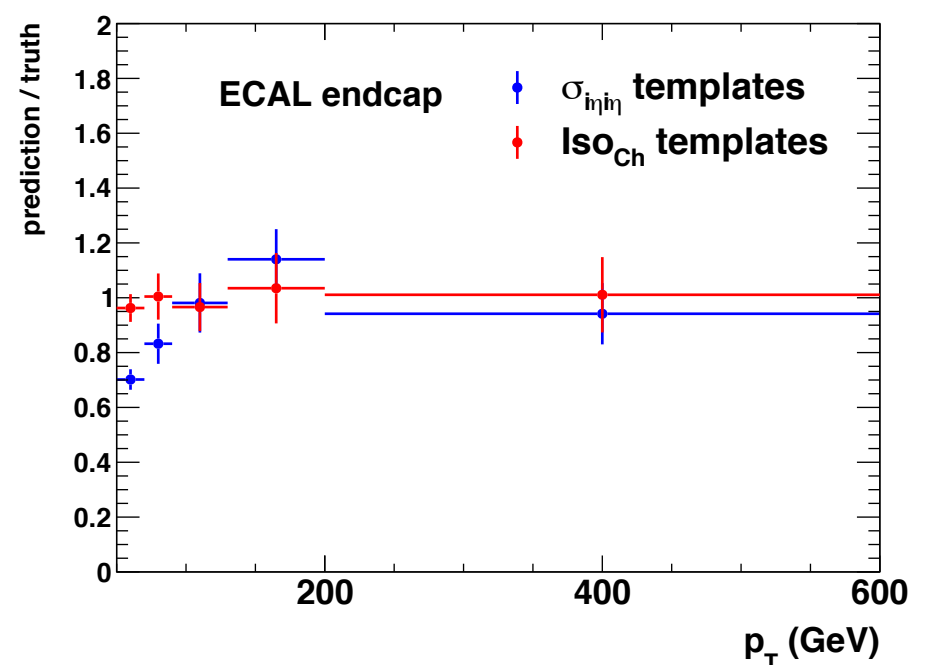
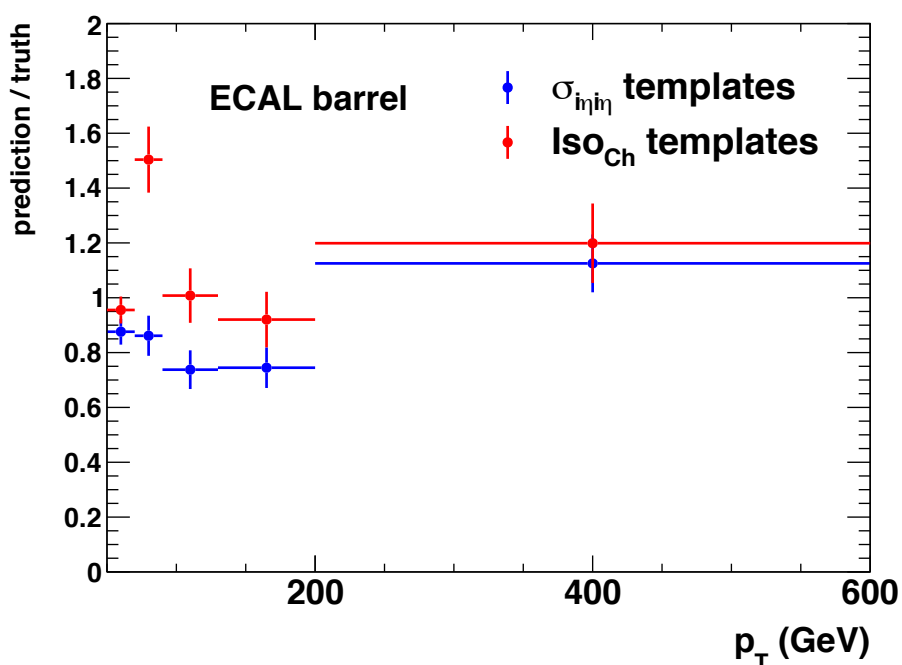
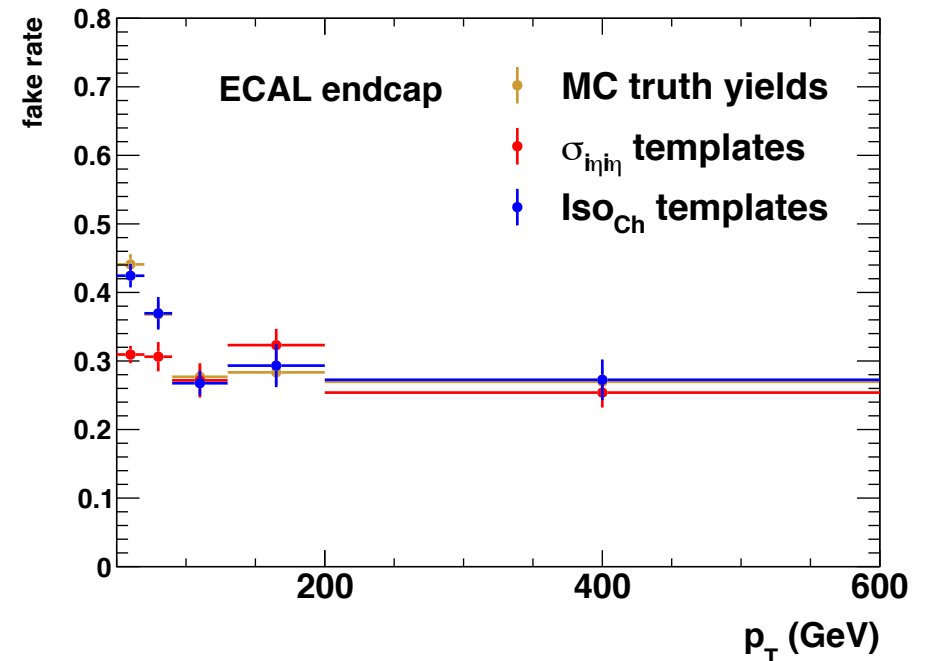
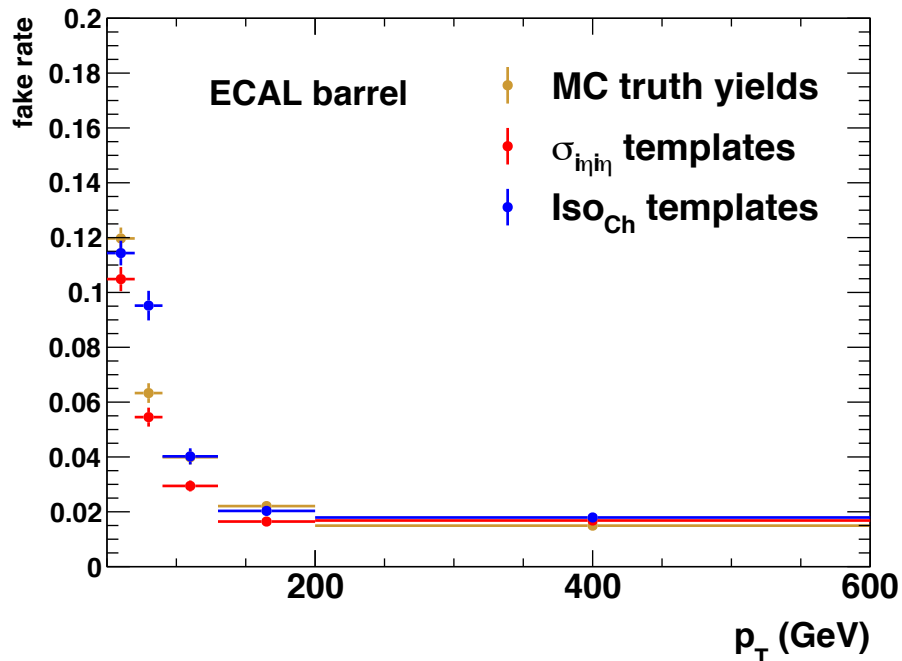




MC closure test comparison

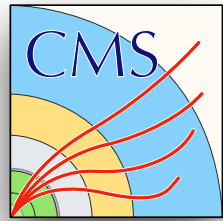


- Agreement in MC fake rate and MC closure test with both template choices

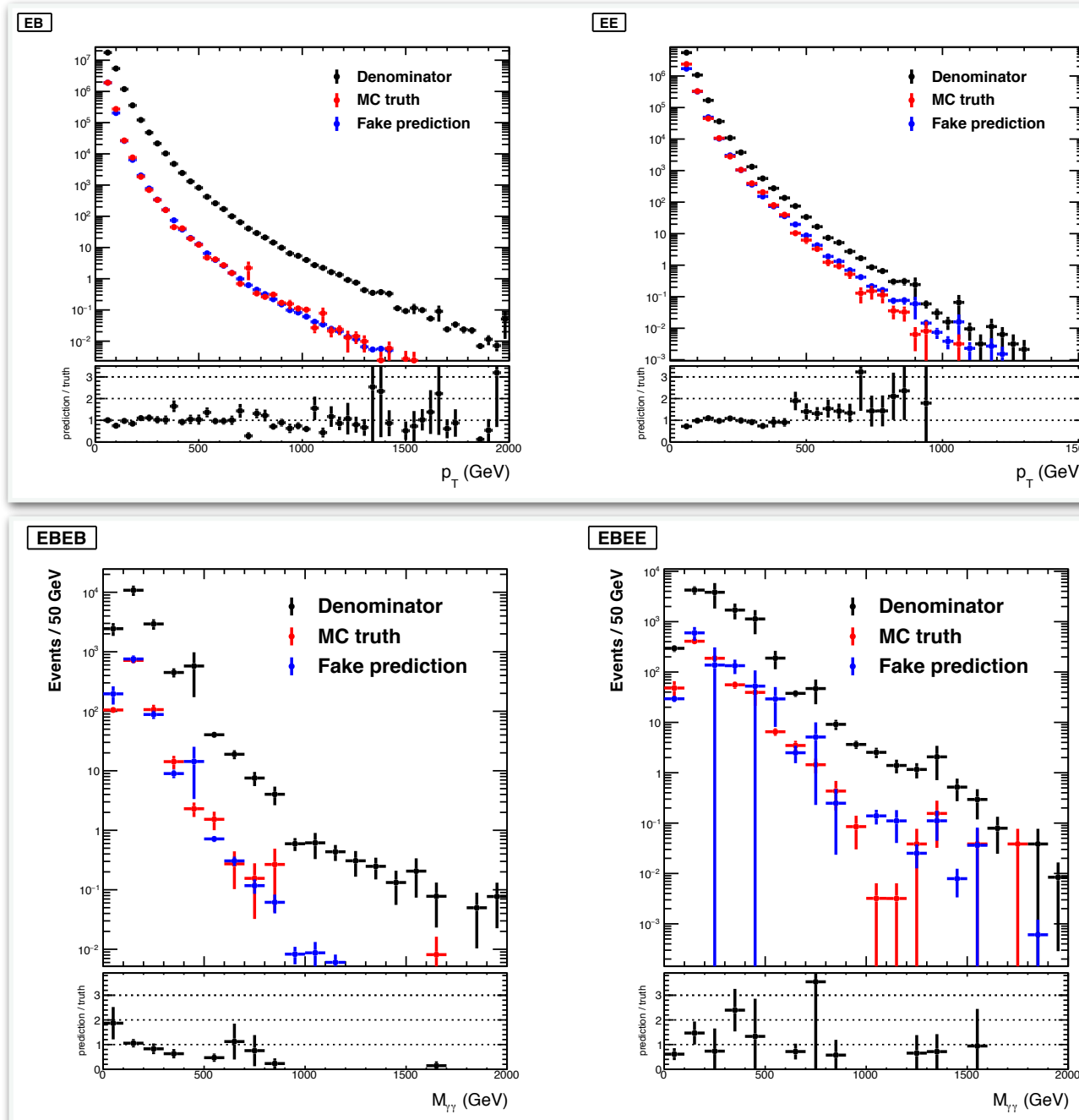




Closure test of kinematics



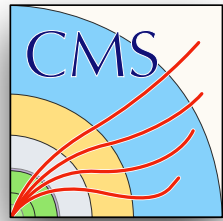
- The **re-weighted denominator objects** reflect the kinematics of known fake objects from **MC truth**



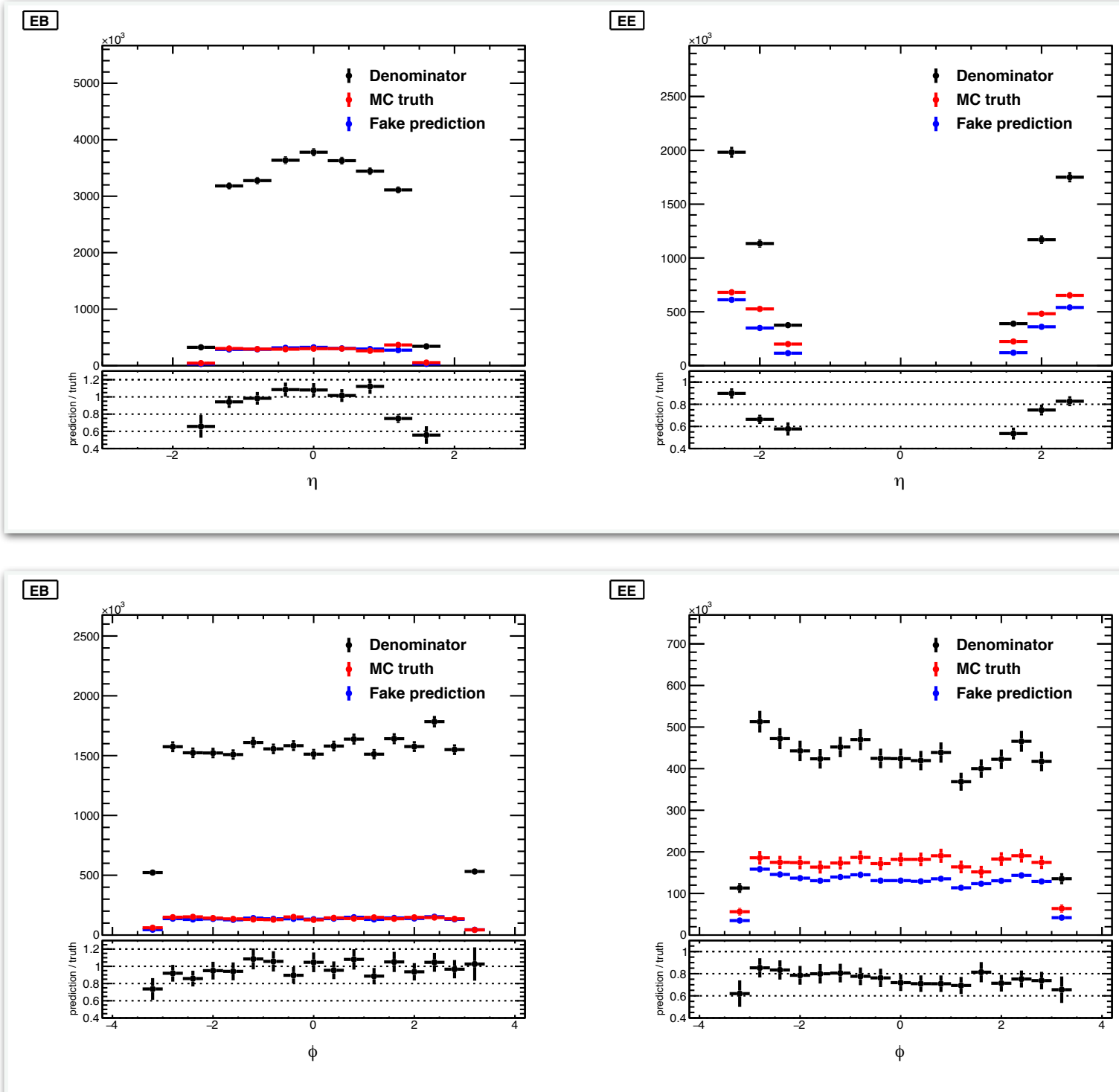
- Photon p_T in EB and EE
- Diphoton $m_{\gamma\gamma}$ $\gamma+j$ objects in EBEB and EBEE



Closure test photon kinematics

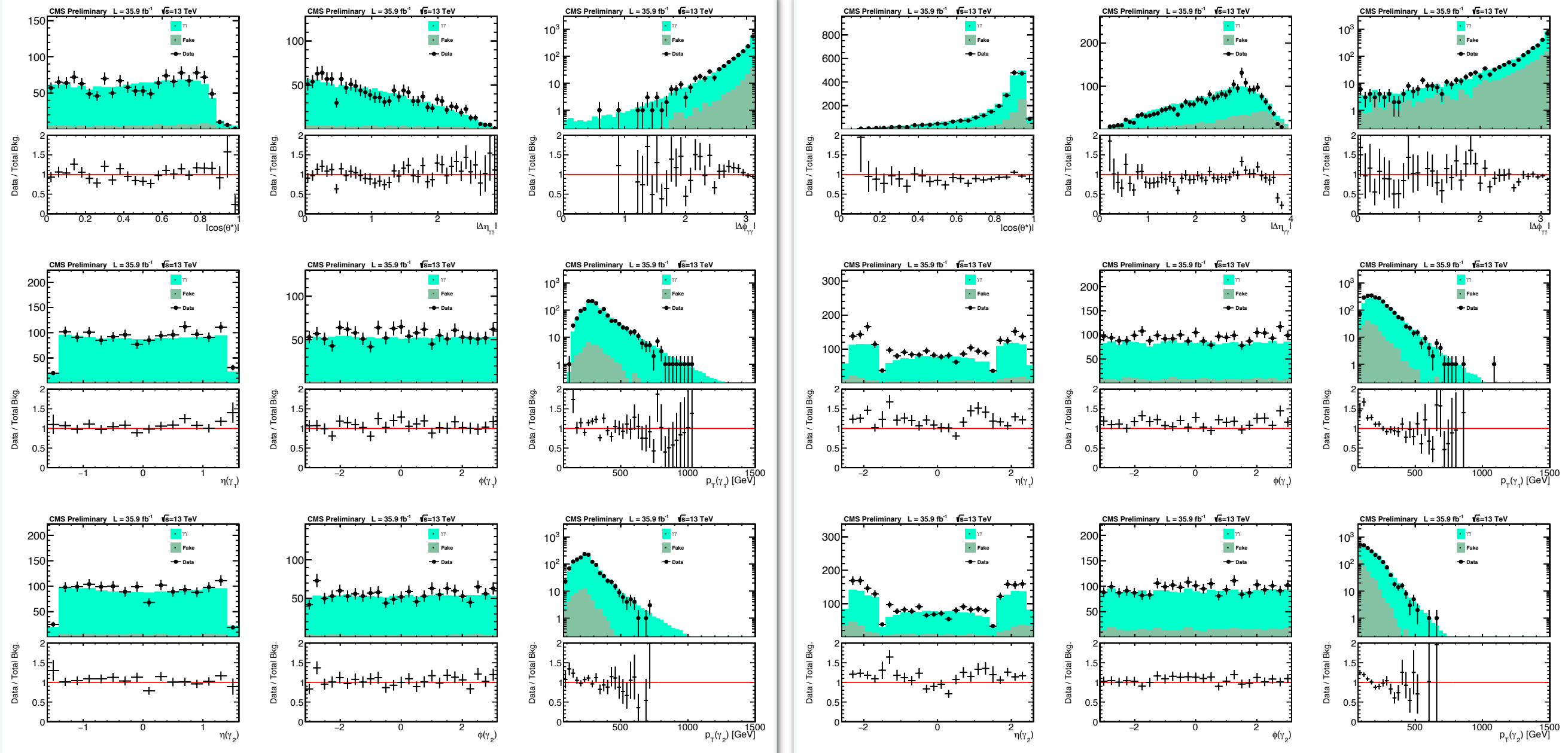


- Photon η and ϕ
 - EB, EE
- Some η dependence





Photon kinematics



EBEB

EBEE



Systematic uncertainty correlation matrix

